

Electronic offprint
for author's personal use

JSCSEN 73(5)513–595(2008)

UDC 54:66

ISSN 0352–5139

**Journal of
the Serbian
Chemical Society**

e version
electronic

VOLUME 73

NO 5

BELGRADE 2008

Available on line at



www.shd.org.yu/JSCS/

The full search of JSCS
is available through

DOAJ DIRECTORY OF
OPEN ACCESS
JOURNALS
www.doaj.org



CONTENTS

Organic Chemistry and Biochemistry

- A. D. Marinković, N. V. Valentić, D. Ž. Mijin, G. G. Ušćumlić and B. Ž. Jovanović: ^{13}C - and ^1H -NMR substituent-induced chemical shifts in *N*(1)-(4-substituted phenyl)-3-cyano-4,6-dimethyl-2-pyridones 513
- D. Gođevac, B. Pejin, G. Zdunić, K. Šavikin, D. Stešević, V. Vajs and S. Milosavljević: Flavonoids from the aerial parts of *Onobrychis montana* subsp. *scardica* 525
- Lj. P. Stanojević, M. Ž. Stanković, V. D. Nikolić and Lj. B. Nikolić: Anti-oxidative and antimicrobial activities of *Hieracium pilosella* L. extracts 531

Inorganic Chemistry

- V. V. Glodjović and S. R. Trifunović: Stereospecific ligands and their complexes. II. Synthesis and characterization of the *s-cis*- $\text{K}[\text{Ru}(\text{S},\text{S}\text{-eddp})\text{Cl}_2]\cdot 3\text{H}_2\text{O}$ (Short communication) 541

Theoretical Chemistry

- S. Stanković, J. Đurđević, I. Gutman and R. Milentjević: Partitioning of π -electrons in rings of diaza-derivatives of acenes 547

Physical Chemistry

- S. Kanagaprabha, R. R. Palanichamy and V. Sathiyabama: Franck-Condon factors and r-centroids for the diatomic fluorides of germanium and silicon 555

Electrochemistry

- L. Li, C. Wang, S. Chen, X. Hou and X. Yang: Investigation of the pitting of aluminum induced by chloride ions by holographic microphotography 561

Analytical Chemistry

- M. M. Issa, R. M. Nejem, M. Al-Kholy, N. S. El-Abadla, R. S. Helles and A. A. Saleh: An indirect atomic absorption spectrometric determination of ciprofloxacin, amoxicillin and diclofenac sodium in pharmaceutical formulations 569

Environmental Chemistry

- B. Jovančičević, M. Antić, M. Vrvic, M. Ilić, M. Novaković, R. M. Saheed and J. Schwarzbauer: Transformation of a petroleum pollutant during soil bioremediation experiments 577

Metallurgy

- D. D. Stanojević, M. B. Rajković, D. V. Tošković and M. A. Tomić: Lead and silver extraction from waste cake from hydrometallurgical zinc production 585

- Errata 595



www.shd.org.yu

J. Serb. Chem. Soc. 73 (5) 513–524 (2008)
JSCS–3732



JSCS@tmf.bg.ac.yu • www.shd.org.yu/JSCS

UDC 547.77+542.913:547.97:66.022.39–035.8

Original scientific paper

¹³C- and ¹H-NMR substituent-induced chemical shifts in *N*(1)-(4-substituted phenyl)-3-cyano-4,6-dimethyl-2-pyridones

ALEKSANDAR D. MARINKOVIĆ*[#], NATAŠA V. VALENTIĆ[#], DUŠAN Ž. MIJIN[#],
GORDANA G. UŠĆUMLIĆ[#] and BRATISLAV Ž. JOVANOVIĆ[#]

*Department of Organic Chemistry, Faculty of Technology and Metallurgy, University of
Belgrade, Karnegijeva 4, 11120 Belgrade, P. O. Box 3503, Serbia*

(Received 24 July 2007, revised 22 January 2008)

Abstract: The ¹³C- and ¹H-NMR chemical shifts of thirteen *N*(1)-(4-substituted phenyl)-3-cyano-4,6-dimethyl-2-pyridones were measured in deuterated dimethyl sulfoxide (DMSO-*d*₆). The correlation analysis for the substituent-induced chemical shifts (*SCS*) with σ_p , inductive (σ_I) and different scale of resonance (σ_R) parameters were performed using the *SSP* (single substituent parameter), *DSP* (dual substituent parameter) and *DSP*-*NLR* (dual substituent parameter–non-linear resonance) methods. The results of the calculations concerning the polar and resonance effects satisfactorily describe the substituent effects at the carbon atoms of interest. The mode of transmission of the substituent effects, both inductive and resonance, in relation to the geometry of the investigated pyridones is discussed.

Keywords: ¹³C-NMR substituent chemical shifts; linear free energy relationships; *N*(1)-(4-substituted phenyl)-3-cyano-4,6-dimethyl-2-pyridones.

INTRODUCTION

N(1)-(4-Substituted phenyl)-3-cyano-4,6-dimethyl-2-pyridones are not only important intermediates in the synthesis of dyes, pigments, fuels and oil additives, but also in the development of medicinal products having a broad spectrum of biological activities depending on the derivative. It is worth mentioning their analgesic and antihypertensive, anti-anaphylactic, diuretic and sodiodiuretic, anti-oxidant, antiviral and antimicrobial properties.¹ Biologically degradable agrochemical products, plant growth regulators, pesticides, and herbicides are also synthesized from pyridone derivatives.^{2–4}

Chemical shifts in ¹³C- and ¹H-NMR spectra are frequently used for the study of the transmission of electronic effects of substituents in organic molecu-

* Corresponding author. E-mail: marinko@tmf.bg.ac.yu

[#] Serbian Chemical Society member.

doi: 10.2298/JSC0805513M

les. Analysis of the ^{13}C - and ^1H -NMR substituent chemical shifts (*SCS*) is based on the principles of linear free energy relationships (LFER) using the Equation for single substituent parameter (*SSP*) or dual substituent parameter (*DSP*) in the forms:

$$SCS = \rho\sigma + h \quad (1)$$

$$SCS = \rho_I\sigma_I + \rho_R\sigma_R + h \quad (2)$$

where ρ is a proportionality constant reflecting the sensitivity of the ^{13}C - and ^1H -NMR chemical shifts to substituent effects, σ is the corresponding substituent constant and h is the intercept.

Eq. (1) attributes the observed substituent effects to an additive blend of polar and π -delocalization effects, given as the corresponding σ_p values. In the *DSP*, Eq. (2), the *SCS* are correlated by a linear combination of the inductive (σ_I) and various resonance scales (σ_R° , σ_R , σ_R^+ and σ_R^-), depending on the electronic demand of the atom under examination. The calculated values ρ_I and ρ_R are relative measures of the transmission of inductive and resonance effects, respectively, through the investigated system.

Dual substituent parameter–non-linear resonance (*DSP*–*NLR*) analysis⁵ is a successful method in the modeling of long-range substituent effects to the ^{13}C -NMR substituent chemical shifts (in substituted aromatic systems^{5–7}), which shows deviations from Hammett-type correlations. The requirement for different σ_R scales can be better accommodated by the use of the (*DSP*–*NLR*) method developed by Bromilow *et al.*,⁵ which allows the resonance scale to vary with the electron demand of the site. This was achieved by the use of the parameter ε , characteristic of the group attached to the site, and Eq. (3):

$$SCS = \rho_I\sigma_I + \rho_R\sigma_R^\circ/(1 - \varepsilon\sigma_R^\circ) + h \quad (3)$$

This gave the best correlation of *para*-*SCS* in *p*-disubstituted benzenes,⁵ as well as in eight β -substituted styrenes,⁶ 3-phenyl and 3-thienyl-2-cyanoacrylamides⁷ and *N*-1-*p*-substituted phenyl-5-methyl-4-carboxy uracils.⁸

In this study, linear free energy relationships (LFER) were applied to the ^{13}C - and ^1H -NMR chemical shifts in *N*(1)-(4-substituted phenyl)-3-cyano-4,6-dimethyl-2-pyridones, with the aim of obtaining insight into the factors determining the chemical shifts in the investigated compounds. The transmission of polar and resonance electronic effects in the investigated compounds (Fig. 1), from the substituent (*X*) in the phenyl group to the carbon atoms of the pyridone and phenyl ring, as well as to the 5-H hydrogen, were studied using Eqs. (1), (2) and (3).

EXPERIMENTAL

All the *N*(1)-(4-substituted phenyl)-3-cyano-4,6-dimethyl-2-pyridone derivatives were synthesized as described in the literature.⁹

The structures of the studied compounds were determined using UV, IR, ^{13}C - and ^1H -NMR and MS data. The IR spectra were recorded on a Bomem MB 100 FTIR spectrophotometer in

the form of KBr pellets.⁹ The ¹³C- and ¹H-NMR spectral measurements were performed on a Bruker AC 250 spectrometer at 200 MHz. The spectra were recorded at room temperature in deuterated dimethyl sulfoxide (DMSO-*d*₆). The chemical shifts are expressed in ppm, referenced to the residual solvent signal at 39.5 ppm. The chemical shifts were assigned by the complementary use of DEPT, two-dimensional ¹H-¹³C correlation HETCOR and by selective INEPT long-range experiments. All mass spectra were recorded on a Thermo Finnigan Polaris Q ion trap mass spectrometer, including a TraceGC 2000 (ThermoFinnigan Corp., Austin, TX, USA) integrated GC-MS/MS system.

Geometry optimization

The reported conformation of the molecular forms were obtained by the semi-empirical MO PM6 method,^{10a,b} with implicit DMSO solvation (COSMO) (Keywords: EF, GNORM = 0.01, EPS = 48) using the MOPAC 2007 program package. A VEGA ZZ 2.2.0 was used as the graphical user interface (GUI).¹¹

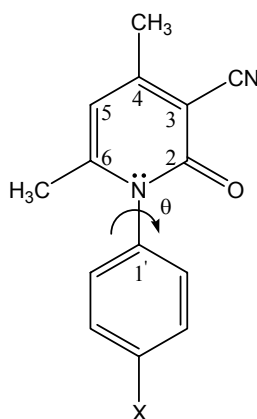


Fig. 1. General formula of the *N*(1)-(4-substituted phenyl)-3-cyano-4,6-dimethyl-2-pyridones, where (X) is H, NMe₂, OH, OMe, Me, Et, F, Cl, Br, I, NO₂, COCH₃ and COOH.

RESULTS AND DISCUSSION

The chemical shifts of the corresponding pyridone ring carbon atoms and the hydrogen at 5-position of the pyridone ring, as well as the *para*-carbon in the phenyl ring (C(1'-Ph)) for investigated compounds are given in Table I in terms of the substituent chemical shifts (*SCS*) relative to the parent compound.

The values of the *SCS* in Table I indicate that the substituent at the phenyl ring has a relatively small influence on the electron density at all the pyridone ring carbon atoms but is considerable for the C(1'-Ph) carbon of the phenyl ring. The chemical shifts of the C(4-Pyr), having small differences in the chemical shifts, are of no statistical values for analysis.

The aromatic ring electron-donor substituents cause a decrease of the electron density at the C(6-Pyr) carbon atom (downfield shift, including the F substituent), indicating that a reverse substituent effect operates at the C(6-Pyr) carbon. The opposite is true for electron-acceptor substituents. Electron-donor substituents increase the electron density at the other carbon atoms and H(5-Pyr) (upfield shifts), including halogens for C(5-Pyr) and C(1'-Ph) carbons. From the

comparison of the *SCS* values for the pyridone carbon atoms, it could be concluded that the C(5-Pyr) and C(3-Pyr) atoms are better shielded than the others, which probably could be attributed to their position in the conjugated system of the pyridone ring. According to the data in Table I, it could be proposed that the geometry of the investigated pyridones plays an important role, probably arising from the out-of-plane rotation of the phenyl rings for a certain torsion angle θ (Fig. 1). Thus, a definite molecular geometry is created, which is a consequence of the transmission modes of the substituent electronic effects (n,π - or π,π -conjugation).^{12,13} An aromaticity study by the NMR technique indicated that 2-pyridones have approx. 35 % of the aromatic character of benzene,¹⁴ as defined by the ability to sustain an induced ring current. This fact also indicates to the possibility of a definite non-planarity of the 2-pyridone moiety.

TABLE I. *SCS* values of H(5-Pyr), C(1'-Ph) and pyridone carbon atoms of *N*(1)-(4-substituted phenyl)-3-cyano- 4,6-dimethyl-2-pyridones in DMSO-*d*₆^a

X	H(5-Pyr)	C(2-Pyr)	C(6-Pyr)	C(3-Pyr)	C(5-Pyr)	C(1'-Ph)
H ^b	6.459	159.845	152.434	109.085	100.164	137.614
NMe ₂	-0.051	-0.41	1.852	-0.195	-0.214	-9.351
OH	-0.05	-0.31	0.747	-0.164	-0.164	-9.012
OMe	-0.018	-0.137	0.628	-0.068	-0.105	-7.494
Me	-0.011	-0.082	0.246	-0.031	-0.164	-2.577
Et	-0.011	-0.082	0.246	-0.031	-0.068	-2.395
F	0.003	0.155	0.191	0.115	-0.032	-3.834
Cl	0.008	0.182	-0.217	0.109	-0.022	-1.183
Br	0.006	0.182	-0.218	0.109	-0.020	-0.728
I	0.002	0.191	-0.227	0.133	-0.014	-0.247
NO ₂	0.058	0.646	-0.701	0.424	0.150	5.616
COCH ₃	0.042	0.355	-0.428	0.224	0.106	3.959
COOH	0.022	0.327	-0.455	0.237	0.091	3.769

^a¹³C-Chemical shifts (in ppm) expressed relative to the unsubstituted compound; ^bchemical shifts of the unsubstituted compound relative to TMS (1H) and residual solvent signal at 39.5 ppm (¹³C)

To explain this observation, LFER analysis was applied using the *SSP* equation (Eq. (1)) and σ_p values from literature.¹⁵ The obtained results are given in Table II.

TABLE II. Correlations of the *SCS* values for the investigated compounds with the *SSP* equation

<i>SCS</i> type	ρ	h	r^a	s^b	F^c	n^d
<i>SCS</i> _{H(5-Pyr)}	0.070 (± 0.006)	-0.004 (± 0.002)	0.959	0.009	127	13
<i>SCS</i> _{C(2-Pyr)}	0.671 (± 0.040)	0.045 (± 0.016)	0.981	0.059	278	13
<i>SCS</i> _{C(6-Pyr)}	-1.53 (± 0.132)	0.203 (± 0.054)	0.961	0.193	133	13
<i>SCS</i> _{C(3-Pyr)}	0.395 (± 0.032)	0.047 (± 0.013)	0.966	0.046	155	13
<i>SCS</i> _{C(5-Pyr)}	0.247 (± 0.024)	-0.047 (± 0.010)	0.950	0.036	102	13
<i>SCS</i> _{C(1'-Ph)}	10.57 (± 1.243)	-2.33 (± 0.506)	0.932	1.810	72	13

^aCorrelation coefficient; ^bstandard error of estimate; ^cF-test for the significance of the regression; ^dnumber of points

Based on the sign of the constants ρ in correlations from Table II, it can be concluded that the effect of substituents on the phenyl ring have the same direction at all the carbon atoms, with the exception of C(6-Pyr), where it was the opposite. Much better results of the correlation coefficients (r), standard deviation (s) and F for H(5-Pyr) atom were obtained if the hydroxy group was assigned the σ_p^+ value, while the almost unchanged value of ρ is 0.062 ($r = 0.978$; $s = 0.006$; $F = 243$; $n = 6$). Separate correlations were performed for the C(3-Pyr) carbon: $\rho = 0.239$ ($r = 0.997$; $s = 0.006$; $F = 713$; $n = 5$) for the electron-donors (OH excluded) and $\rho = 0.517$ ($r = 0.984$; $s = 0.026$; $F = 155$; $n = 7$) for the electron-acceptors (F excluded). Electron-acceptor substituents exert larger electronic effects at the C(3-Pyr) carbon due to the opposing electron accepting effect of the cyano group and for these substituents, the value of ρ is significantly higher. The correlation for the C(6-Pyr) carbon is also significantly improved if σ_p^+ values are assigned to N(Me)₂, OH, OCH₃ and F ($\rho = -0.981$; $r = 0.990$; $s = 0.101$; $F = 509$; $n = 13$), thus showing that electron-donor substituents achieved better resonance interactions with this carbon. The substituent showed the highest influence at the C(1'-Ph) carbon but the correlation coefficients were only moderate. Two separate correlations, first for NMe₂, Me, Et, H, COOH and COCH₃, the gave the results: $\rho = 10.130$; $r = 0.997$; $s = 0.434$; $F = 646$; $n = 6$ and second for OH, OCH₃, F, Cl, Br and NO₂, which gave: $\rho = 12.860$; $r = 0.990$; $s = 0.745$; $F = 256$; $n = 7$, show well the complex influence of substituents and the pyridone ring on the chemical shifts of this carbon.

Although the *SSP* analysis uses an additive blend of inductive and resonance parameters of substituents given as σ_p values, it presented a satisfactory description of the transmission of substituent effects through the investigated systems.

To measure the separate contributions of the inductive and resonance effects of a substituent (X), regression analyses according to the *DSP* equation (Eq. (2)) with σ_R° , σ_R , σ_R^+ substituent constants^{16,17} were carried out, and results of the best fit are given in Table III.

The results of the correlation analysis from Table III indicate that the *SCS* values of the C(6-Pyr) carbon correlate better with the σ_R^+ and the *SCS* values of H(5-Pyr) with the σ_R substituent constants, while for the other carbon atoms acceptable results were obtained with the σ_R° values. The better correlation of the *SCS* values for the C(6-Pyr) with the σ_R^+ values indicates a somewhat higher contribution of extended resonance interaction for this carbon. Reversely, the better correlations of the *SCS* of the other carbons with the σ_R° values indicate a definite attenuation effect of the transmission of electronic substituent effects to these carbons. The ρ_I values in Table III show the dependence of the inductive effects on the molecular geometry of the investigated compounds. The ρ_R values depend on the σ scale used, which proves that the demand of the carbon atoms of investigated compounds for electrons is significantly different.

TABLE III. Correlation of the SCS values for investigated compounds with DSP equation

	Scale ^a	ρ_I	ρ_R	h	r	s	F	n	f^b
$SCS_{H(5-Pyr)}$	σ_R°	0.066 (± 0.016)	0.093 (± 0.014)	-0.004 (± 0.006)	0.931	0.012	33	13	-
	σ_R	0.061 (± 0.013)	0.076 (± 0.009)	-0.004 (± 0.005)	0.957	0.009	55	13	-
	σ_R^+	0.055 (± 0.017)	0.042 (± 0.006)	0.002 (± 0.006)	0.926	0.012	31	13	-
$SCS_{C(2-Pyr)}$	σ_R°	0.803 (± 0.030)	0.827 (± 0.032)	0.057 (± 0.012)	0.997	0.022	780	11 ^c	0.078
	σ_R	0.770 (± 0.049)	0.594 (± 0.038)	0.011 (± 0.020)	0.993	0.036	292	11 ^c	0.128
	σ_R^+	0.712 (± 0.110)	0.352 (± 0.043)	0.027 (± 0.044)	0.966	0.081	70	13	0.282
$SCS_{C(6-Pyr)}$	σ_R°	-1.300 (± 0.416)	-2.000 (± 0.365)	0.193 (± 0.157)	0.904	0.311	23	13	0.475
	σ_R	-1.171 (± 0.254)	-1.740 (± 0.175)	0.058 (± 0.100)	0.966	0.189	70	13	0.289
	σ_R^+	-1.016 (± 0.122)	-1.052 (± 0.048)	-0.022 (± 0.046)	0.995	0.083	361	11 ^d	0.122
$SCS_{C(3-Pyr)}$	σ_R°	0.482 (± 0.026)	0.478 (± 0.028)	0.017 (± 0.011)	0.994	0.020	352	11 ^c	0.113
	σ_R	0.464 (± 0.048)	0.335 (± 0.037)	0.018 (± 0.020)	0.981	0.036	103	11 ^c	0.208
	σ_R^+	0.439 (± 0.073)	0.174 (± 0.031)	0.022 (± 0.030)	0.957	0.053	44	11 ^c	0.312
$SCS_{C(5-Pyr)}$	σ_R°	0.225 (± 0.044)	0.332 (± 0.031)	-0.046 (± 0.018)	0.979	0.025	92	11 ^e	0.231
	σ_R	0.164 (± 0.047)	0.276 (± 0.027)	-0.010 (± 0.020)	0.978	0.026	87	11 ^e	0.236
	σ_R^+	0.131 (± 0.073)	0.155 (± 0.024)	0.020 (± 0.033)	0.950	0.040	37	11 ^e	0.354
$SCS_{C(1'-Ph)}$	σ_R°	5.890 (± 0.692)	17.932 (± 0.750)	-0.362 (± 0.283)	0.994	0.518	349	11 ^c	0.116
	σ_R	5.142 (± 0.957)	12.927 (± 0.748)	-0.228 (± 0.393)	0.989	0.717	183	11 ^c	0.159
	σ_R^+	4.125 (± 2.179)	6.788 (± 0.934)	-0.049 (± 0.910)	0.944	1.559	33	11 ^c	0.357

^a σ_I , σ_R° , σ_R and σ_R^+ are from Ref. 13 and 14; ^bTaft f value, $f = s/r.m.s.$; ^cwithout COOH and OH; ^dwithout OCH₃ and F; ^ewithout CH₃ and H

The correlations of the SCS values for the pyridone derivatives was performed according to a literature method of reference⁵ to determine the electronic demand of the carbon atoms, applying DSP-NLR analysis. The results are given in Table IV.

The results given in Table IV show the correlations of the SCS of all carbon atoms obtained using the DSP-NLR Equation (Eq. (3)) were as good, or much

better. Generally, based on the above results, it can be concluded that two opposing effects, *i.e.*, substituent electronic effects in the phenyl ring and electronic interactions in the pyridone part of the molecules are balanced, giving an overall effect on the chemical shifts of all the carbon atoms. The two separate π -polarizable systems, *i.e.*, the substituted phenyl and the pyridone rings, are defined by MO PM6 calculations. The optimized structures show the unambiguous perpendicular orientation of these rings for all the investigated compounds, except for the NO₂ substituted molecule, which is twisted by 72° from the plane of the pyridone ring. Transmission of the resonance effect from the substituted phenyl ring is efficiently suppressed in this way and the optimized structure is presented in Fig. 2 for the parent compound.

TABLE IV. Correlations of the SCS values for the investigated compounds with the DSP-NLR equation

	ρ_I	ρ_R	h	ε	r	s	F	n	f
$SCS_{C(2-Pyr)}$	0.805 (± 0.027)	0.775 (± 0.028)	0.007 (± 0.01)	-0.18	0.998	0.020	935	11 ^a	0.071
$SCS_{C(6-Pyr)}$	-1.134 (± 0.080)	-0.802 (± 0.024)	0.065 (± 0.030)	-1.50	0.998	0.056	819	11 ^b	0.081
$SCS_{C(3-Pyr)}$	0.480 (± 0.025)	0.510 (± 0.029)	0.016 (± 0.010)	0.20	0.995	0.018	384	11 ^a	0.108
$SCS_{C(5-Pyr)}$	0.215 (± 0.040)	0.312 (± 0.027)	-0.038 (± 0.017)	-0.24	0.982	0.023	110	11 ^c	0.213
$SCS_{C(1'-Ph)}$	5.942 (± 0.573)	16.133 (± 0.558)	-0.313 (± 0.235)	-0.28	0.996	0.430	510	11 ^a	0.095

^aWithout OH and COOH; ^bwithout OCH₃ and F; ^cwithout CH₃ and H

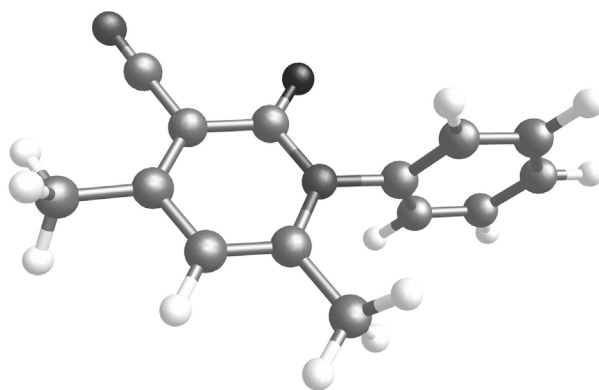


Fig. 2. Conformation of N(1)-phenyl-3-cyano-4,6-dimethyl-2-pyridine optimized by the MO semi-empirical PM6 method and implicit DMSO solvation (COSMO) using MOPAC 2007.

The calculated ρ_I and ρ_R values from Table IV indicate a prevalent polar (inductive/field) effect on the C(2-Pyr) and C(6-Pyr) carbon atoms of the pyridone ring. It can be noted that ρ_I and ρ_R are negative for the C(6-Pyr) carbon atom, while those for the other carbon atoms are positive. A negative sign of ρ_I is indicative of a reverse SCS effect, *i.e.*, inductive electron-acceptor substituents cause

an upfield shift, which is considered to be due to π -polarization.¹⁸ A similar effect has been observed in other systems, *i.e.*, in 3-aryl-2-cyanoacrylamides,⁷ *N*-benzylideneanilines,¹⁹ 2-substituted-5-(dimethylamino)phenyl dimethylcarbamates,²⁰ and in other systems containing a conjugated side chain.

As is cited in the literature, π -polarization of a distant π -system by a substituent dipole need not be transmitted *via* an intervening π -system,¹⁸ and theoretical results have demonstrated that a substituent dipole acts mainly in polarizing each of the π -units individually.²¹ This is defined as localized polarization. On the other hand, the terminal atoms of a conjugated π -system show some additional polarization of the whole π -network. This component is termed extended polarization.

Transmission of substituent electronic effects could be presented by mesomeric structures of the investigated pyridones and the contribution of π -polarization (Fig. 3).

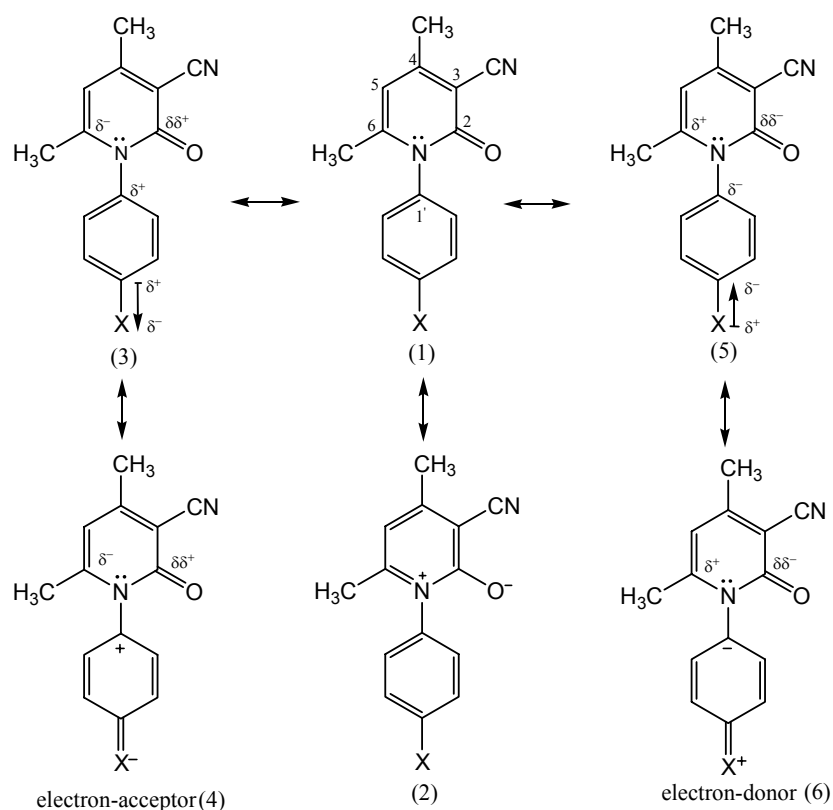


Fig. 3. Mesomeric structures with the contribution of π -polarization.

In structure (1), if X is an electron-acceptor substituent, a dipole on X (or near the C–X bond) is induced (structure (3)) and interaction of this dipole through

the space of the molecule results in polarization of the individual π -units (localized polarization). The reverse is true for electron-donor substituted compounds (structure (5)). The polarization mechanism of small localized π -units, presented by structures (3) and (5), is very important as well as polarization of the entire conjugated system of the investigated compounds (extended polarization). Resonance interaction in the extended conjugated system of the pyridone ring (structure (2)) has an opposing effect to the polarization caused by an electron-acceptor substituent (structure (4)). The net result is that the electron-acceptor substituents increase the electron density about the C(6-Pyr) carbon, hence, the increased shielding caused an upfield shift. Reversely, electron-donor substituents support the resonance interaction in the pyridone unit, which could be attributed to a potential delocalization of the electron lone pair at the N(1) nitrogen.

The correlation between the *SCS* values of the C(1'-Ph) atom and the substituent parameters using the *DSP-NLR* method ($r = 0.996$ and $f = 0.095$) shows that the demand for electrons of this atom is $\varepsilon = -0.28$. Sign and value of the parameter ε show that the pyridone ring, according to literature data for the COOEt group of -0.48 ,⁵ attached to the C(1'-Ph) atom has a moderate electron-acceptor character. This fact probably could be explained by a small contribution of the mesomeric structure (2), which has a higher electron-accepting power.

A somewhat lower demand for electrons ($\varepsilon = -0.18$) was observed for the C(2-Pyr) atom of the pyridone ring. The low polarizability of the π -carbonyl electrons is influenced by the vicinity of an electron-accepting oxygen, which contributes to a lower sensitivity.

The C(6-Pyr) carbon has the highest demand for an electron ($\varepsilon = -1.50$). Electron-acceptors cause an increased electron density at this carbon (structures (3) and (4)), opposing the conjugation present in the pyridone unit, while electron donors have the opposite effect (structures (5) and (6)). The C(3-Pyr) carbon has an ε value of 0.20, the higher electron density being the result of the neighboring cyano group, which increases the electron density at this carbon. A similar literature value⁵ of ε for an NMe₂ group (0.25) proves that the electron density of the pyridone ring is shifted to the carbonyl group. The electron demand for the C(5-Pyr) carbon is -0.24 , which indicates a significantly lower deficiency of electron density than the C(6-Pyr) carbon.

The contribution of the individual electronic effects of substituents on the phenyl ring to the carbon atoms of the pyridone ring and the C(1'-Ph) of the phenyl ring can be analyzed based on the ratio $\lambda = \rho_R/\rho_I$. Using the values of ρ_R and ρ_I from Table IV, the calculated values λ for the C(2-Pyr), C(6-Pyr), C(3-Pyr), C(5-Pyr) and C(1'-Ph) atoms are: 0.96, 0.71, 1.06, 1.45 and 2.72, respectively. *DSP* analysis and calculation of the λ parameter (for the same set of carbon atoms) gave the following results: 1.03, 1.04, 0.99, 1.48 and 3.04, respectively. Comparison of the values of λ from *DSP* (Eq. (2)) with those from *DSP-NLR* (Eq. (3))

indicates a significant decrease only for the C(6-Pyr) carbon atom, which has the highest electron demand ($\varepsilon = -1.50$), which probably suggests that the localized π -polarization effect is dominant in this part of the molecule.

The contributions of resonance and inductive substituent effects at the C(3-Pyr) and C(2-Pyr) atoms are balanced, while the resonance effect is dominant at the C(5-Pyr) atom. According to their position in the pyridone conjugated system and the influence of substituent electronic effects, the C(5-Pyr) carbon atom is more susceptible to the net π electron shifts caused by a substituent.

The electronic substituent effects are transmitted through the phenyl ring by resonance and inductive/field interaction toward the C(1'-Ph) carbon by developing different charges at the phenyl carbon atoms. The electron density, according to MO calculation, is localized at the C(2'-Ph)-C(3'-Ph) and C(5'-Ph)-C(6'-Ph) carbons for all compounds investigated. The large attenuation effect of the electronic substituent effects transmission to N(1) atom is influenced by the geometry of two perpendicular rings. Electron-donor substituents develop a negative charge at the C(1'-Ph) carbon (Fig. 3, structure (6)), while the opposite is true for electron-acceptors (Fig. 3, structure (4)). Only in the compound with the NO₂ group, which has strong negative inductive and resonance effects, did a decrease in the torsion angle occur and thus, the n,π -conjugation was increased.

The net electronic effect from substituents to the π -electron of pyridone system is transmitted mainly by inductive/field effects. Repulsion between π -electrons of the carbonyl group and the electron rich phenyl ring in electron-donor substituted compounds cause a somewhat higher interaction with the electron of the C(6-Pyr)-C(5-Pyr) double bond through space, thus the deshielding of the C(6-Pyr) carbon is higher. The opposite is true for electron-acceptor substituted compounds. According to the MO calculation, the electron density of the π -pyridone system is localized at the C(6-Pyr)-C(5-Pyr) and C(3-Pyr)-C(2-Pyr) carbons for all the investigated compounds. Thus, the substituent electronic effects are mainly reflected in the polarization of small π -polarizable units of the pyridone ring.

CONCLUSIONS

In summary, it can be concluded that the *DSP*-NLR analysis of the obtained results revealed that the applied method was successful for the correlation of the *SCS* values of the investigated compounds. All correlations were of good precision, indicating that the substituent effects on the ¹³C-NMR chemical shifts in this series are due to electron transfer. The inductive/field effect is the dominant factor for some of the observed carbon atoms of the pyridone ring. The resonance effect is the most prominent on the C(1'-Ph) carbon, while the reverse substituent effect was observed at the C(6-Pyr) atom, as a consequence of π -polarization.

Acknowledgements. The authors acknowledge the financial support of the Ministry of Science of the Republic of Serbia (Project 142063).

ИЗВОД

СУПСТИТУЕНТИМА ИЗАЗВАНА ^{13}C - И ^1H -NMR ХЕМИЈСКА ПОМЕРАЊА
N(1)-(4-СУПСТИТУИСАНИ ФЕНИЛ)-3-ЦИЈАНО-4,6-ДИМЕТИЛ-2-ПИРИДОНААЛЕКСАНДАР Д. МАРИНКОВИЋ, НАТАША В. ВАЛЕНТИЋ, ДУШАН Ж. МИЈИЋ,
ГОРДАНА Г. УШЋУМЛИЋ И БРАТИСЛАВ Ж. ЈОВАНОВИЋКаџедра за орџанску хемију, Технолошкометалурџику факултетџи, Универзитетџи у Беоџраду,
џ. џр. 3503, Карнеџијева 4, 1120 Беоџрад

^{13}C - и ^1H -NMR хемијска померања тринаест N(1)-(4-супституисани фенил)-3-цијано-4,6-диметил-2-пиридона су одређена у деутерисаном диметилсулфоксиду (DMSO- d_6). Корелациона анализа хемијских померања појединих угљеникових атома испитиваних једињења изазвана присутним супституентима (SCS) са σ_p , индуктивним (σ_I) и различитим резонанционим (σ_R) константама је извршена коришћењем SSP (монопараметарска), DSP (двопараметарска) и DSP-NLR (двопараметарска нелинеарна) метода. Резултати корелационих анализа на задовољавајући начин описују ефекте супституената за посматране угљеникове атоме. Дискутован је начин преношења ефеката супституената, индуктивних и резонанционих, у односу на геометрију испитиваних молекула.

(Примљено 24. јула 2007, ревидирано 22. јануара 2008)

REFERENCES

1. V. P. Litvinov, S. G. Krivokolysko, V. D. Dyachenko, *Chem. Heterocycl. Compd.* **35** (1999) 509
2. M. C. Seidel, K. L. Viste, R. Y. Yih, US 3.503.986 (1970)
3. M. C. Seidel, K. L. Viste, R. Y. Yih, US 3.576.814 (1971)
4. M. C. Seidel, K. L. Viste, R. Y. Yih, US 3.761.240 (1973)
5. J. Bromilow, R. T. C. Brownlee, D. J. Craik, M. Sadek, R. W. Taft, *J. Org. Chem.* **45** (1980) 2429
6. S. Datta, A. De, S. P. Bhattacharyya, C. Medhi, A. K. Chakravarty, J. S. A. Brunskill, S. Fadoujou, K. Fish, *J. Chem. Soc., Perkin Trans.* **2** (1988) 1599
7. S. P. Bhattacharyya, A. De, A. K. Chakravarty, J. S. A. Brunskill, D. F. Ewing, *J. Chem. Soc., Perkin Trans.* **2** (1985) 473
8. F. H. Assaleh, A. D. Marinković, B. Ž. Jovanović, J. Csanádi, *J. Mol. Struct.* **833** (2007) 53
9. D. Mijin, A. Marinković, *Synth. Commun.* **36** (2006) 193.
10. a) J. J. P. Stewart, *J. Comput.-Aided Mol. Des.* **4** (1990) 1; b) J. J. P. Stewart, *J. Mol. Model.* **13** (2007) 1173; MOPAC 2007 (<http://openmopac.net/>)
11. A. Pedretti, L. Villa, G. Vistoli, *J. Comput.-Aided Mol. Des.* **18** (2004) 167; VEGA ZZ 2.1.0. (<http://www.ddl.unimi.it>)
12. B. Ž. Jovanović, M. Mišić-Vuković, A. D. Marinković, V. Vajs, *J. Mol. Struct.* **482–483** (1999) 375
13. B. Ž. Jovanović, M. Mišić-Vuković, A. D. Marinković, V. Vajs, *J. Mol. Struct.* **642** (2002) 113
14. J. A. Elvidge, L. M. Jackman, *J. Chem. Soc.* (1961) 859
15. C. Hansch, A. Leo, R. W. Taft, *Chem. Rev.* **91** (1991) 165
16. A. S. Ehrenson, R. T. C. Brownlee, R. W. Taft, *Prog. Phys. Org. Chem.* **10** (1973) 1
17. N. B. Chapman, J. Shorter, Eds., *Correlation Analysis in Chemistry*, Ch. 10, Plenum Press, New York, 1978

18. J. Bromilow, R. T. C. Brownlee, D. J. Craik, P. R. Fiske, J. E. Rowe, M. Sadek, *J. Chem. Soc., Perkin Trans. 2* (1981) 753
19. R. Akaba, H. Sakuragi, K. Tokumaru, *Bull. Chem. Soc. Jpn.* **58** (1985) 1186
20. R. Rittner, J. E. Barbarini, N. F. Höehr, *Can. J. Anal. Sci. Spectrosc.* **44** (1999) 180
21. R. T. C. Brownlee, D. J. Craik, *J. Chem. Soc., Perkin Trans. 2* (1981) 760.



www.shd.org.yu

J. Serb. Chem. Soc. 73 (5) 525–529 (2008)
JSCS–3733

JSCS@tmf.bg.ac.yu • www.shd.org.yu/JSCS

UDC **Onobrychis scardica*:543.422.25:
:577.164.3:547.918

Original scientific paper

Flavonoids from the aerial parts of *Onobrychis montana* subsp. *scardica*

DEJAN GOĐEVAC^{1#}, BORIS PEJIN^{2#}, GORDANA ZDUNIĆ³, KATARINA ŠAVIKIN³,
DANIJELA STEŠEVIĆ⁴, VLATKA VAJS^{1#} and SLOBODAN MILOSAVLJEVIĆ^{2*#}

¹Institute of Chemistry, Technology and Metallurgy, Njegoševa 12, 11000 Belgrade, ²Faculty of Chemistry, Studentski trg 16, 11000 Belgrade, ³Institute for Medicinal Plant Research “Dr. Josif Pančić”, Tadeuša Košćuška, 11000 Belgrade, Serbia and ⁴Biology Department, Faculty of Science, University of Montenegro, 81000 Podgorica, Montenegro

(Received 26 September, revised 27 December 2007)

Abstract: Rutin (**1**, main constituent) and two flavone C-glycosides, vitexin (**2**) and vitexin 2"-O- α -rhamnopyranoside (**3**) were isolated from the aerial parts of *Onobrychis montana* subsp. *scardica*. They were identified by ¹H-NMR, ¹³C-NMR and UV–Vis spectroscopy (procedure with shift reagents), and high resolution ESI-MS. A relatively high content of **1** (5.27 mg/g of dry plant material), measured by HPLC, indicated *O. montana* subsp. *scardica* as a new natural source of this biologically active compound. The isolated flavonoid compounds might be of value as chemotaxonomic markers.

Keywords: *Onobrychis scardica*; Fabaceae; flavonoids.

INTRODUCTION

The Fabaceae family comprises about 12,000 species, divided into three sub-families and 500 genera, widespread throughout the world. *Onobrychis montana* DC. subsp. *scardica* (Griseb) P. W. Ball (Synonym *Onobrychis scardica* (Griseb) Halácsy) is an endemic species growing in mountainous regions of the Balkan Peninsula.¹

No previous phytochemical studies on any subspecies of *O. montana* have been reported. Chemical investigations of *Onobrychis* species revealed the presence of flavones, isoflavonoids,^{2,3} flavonoid glycosides,^{4–7} tannins,^{8,9} cinnamic acid derivatives¹⁰ and arylobenzofurans.^{11,12}

The isolation, identification and quantification (HPLC) of three flavonoid glycosides as constituents of *O. montana* subsp. *scardica* are reported in this paper. The chemotaxonomic significance of the isolated compounds is also discussed.

Serbian Chemical Society member.

* Corresponding author. E-mail: smilo@chem.bg.ac.yu

doi: 10.2298/JSC0805525G

EXPERIMENTAL

General

The ^1H - (200 MHz) and ^{13}C -NMR (50 MHz) spectra were recorded on a Varian Gemini 2000 spectrometer in $\text{DMSO-}d_6$. The UV spectra were measured on a Cintra 40 UV-Vis spectrometer. The high-resolution MS spectra were recorded on an Agilent 6210 LC ESI-MS TOF spectrometer.

Silica gel, 0.008 mm (Merck, Darmstadt, Germany), and Sephadex LH-20 (Pharmacia Fine Chemicals, Uppsala, Sweden) were used for preparative column chromatography (CC). Silica gel F-254 (Merck, Darmstadt, Germany) was used for analytical thin layer chromatography (TLC).

The HPLC separations were performed on a Hewlett-Packard Series 1100 equipped with a DAD model G1315B, bin pump model G1312A, autosampler model G1313A, and LiChrospher 100 RP-18e column ($5\ \mu\text{m}$, $250\times 4\ \text{mm}^2$).

The HPLC standard of rutin was purchased from Roth, Germany. Acetonitrile and water were of HPLC grade and all other employed solvents were of analytical grade.

Plant material

The plant material was collected in July, 2006 on the mountain Bjelasica, Montenegro. A voucher specimen (144/06) was deposited in the Herbarium of the Biology Department, Faculty of Science, University of Montenegro, Podgorica.

Extraction and isolation

The air-dried, aerial parts of *O. montana* subsp. *scardica* (240 g) were extracted with 90 % methanol, twice (700 ml + 400 ml) at room temperature and 23 g of a crude extract was obtained after evaporation of the solvent. The extract was then partitioned between 300 ml H_2O and 200 ml chloroform. The aqueous layer was re-extracted with *n*-butanol to yield 5.5 g of residue after removal of the solvent. A part of the *n*-butanol extract (3 g) was subjected to isocratic silica gel flash chromatography (FC) with $\text{EtOAc/MeOH/H}_2\text{O/HCOOH}$ 10/2/1/0.1, affording 51 fractions. The combined fractions 40–50 gave 950 mg of compound **1**, after evaporation of the solvent. Further purification of the combined fractions 18–19 on a Sephadex LH-20 column eluting with methanol yielded 2.0 mg of compound **2**. The combined fractions 25–30 after chromatography on a Sephadex LH-20 column with methanol yielded 3.0 mg of compound **3**.

HPLC analysis

HPLC analysis of the crude extract (90 % methanol) was realized using a linear gradient with two solvents (0.10 % H_3PO_4 in water as solvent A and acetonitrile as solvent B). The injection volume was 7 μl , and the elution at $1.0\ \text{ml}\ \text{min}^{-1}$ with a gradient program (0–12 min: 8.0–10 % B, 12–14 min: 10–16 % B, 14–30 min: 16 % B, 30–36 min 16–36 % B, 36–42 min: 36–60 % B, 42–46 min: 60–100 % B). UV-Vis detection was performed at 254 and 320 nm. The extracts were dissolved in methanol and the quantification was based on the measured integration area, using the calibration equation of the corresponding standard. The concentrations used for the calibration were in range 0.2–2.0 $\text{mg}\ \text{ml}^{-1}$.

RESULTS AND DISCUSSION

The structures of the isolated compounds were established by spectrometric and chromatographic methods: UV with shift reagents (NaOMe , NaOAc , H_3BO_3 , AlCl_3 and HCl), the NMR and HR-ESI-MS techniques; HPLC co-injection with

authentic samples and confirmed by comparison of the spectral data with those previously reported.^{13,14} Compound **1** was identified as *O*-glycoside rutin, and compounds **2** and **3** as *C*-glycosides vitexin and vitexin 2''-*O*- α -rhamnopyranoside and vitexin, respectively.

The HPLC analysis, carried out immediately after the extraction, revealed **1** as the dominant compound, and **2** and **3** as minor constituents (Fig. 1). According to quantitative HPLC, the content of **1** was estimated to be 55 mg/g of extract, or 5.27 mg/g of dry plant material. Thus, *O. montana* subsp. *scardica* could be regarded as a new source of **1**, known for a variety of biological activities, such as prevention of diabetes and anti-oxidant properties.¹⁵

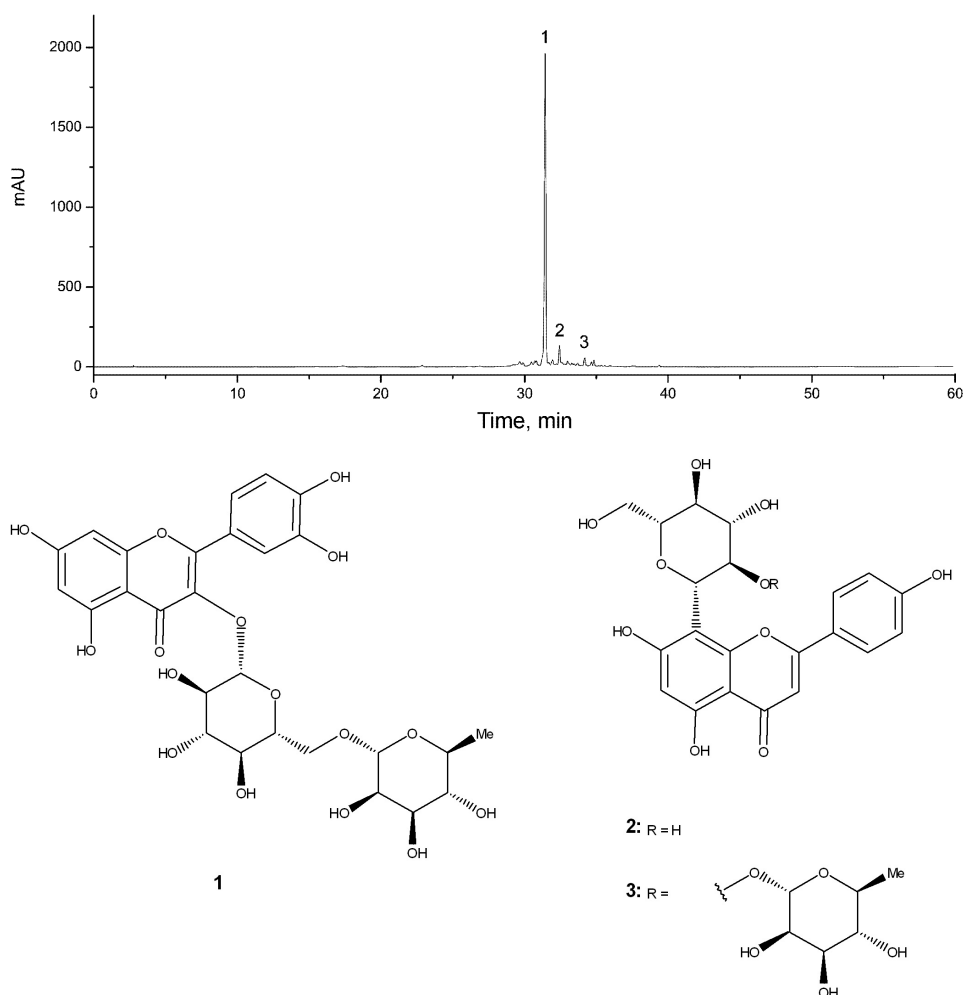


Fig. 1. HPLC profile of MeOH extract of *Onobrychis montana* subsp. *scardica*. Compounds: **1** rutin, **2** vitexin, **3** vitexin 2''-*O*- α -rhamnopyranoside.

The isolation of rutin from *O. montana* subsp. *scardica* conforms to the pattern of flavonoid distribution in several species of the *Onobrychis* genus, such as *O. viciifolia*,⁹ *O. cornuta*, *O. echidna*, *O. ferganica*, *O. grandis*, *O. amoena*, *O. chorassanica*, *O. seravschanica*,⁷ *O. biebersteinii*,⁶ *O. bobrovi*,⁵ *O. tanaitica*¹⁶ and *O. pulchella*.⁴ The minor constituent, C-glycoside vitexin, was detected previously in only one member of the genus, *i.e.*, *O. adans* from Georgia.¹⁷ This is the first report of vitexin 2"-O- α -rhamnopyranoside in this family.

Acknowledgements. The authors acknowledge their gratitude to the Ministry of Science of Serbia for financial support, project number 142053.

ИЗВОД

ФЛАВОНОИДИ ИЗ НАДЗЕМНИХ ДЕЛОВА *Onobrychis montana* subsp. *scardica*

ДЕЈАН ГОЂЕВАЦ¹, БОРИС ПЕЈИН², ГОРДАНА ЗДУНИЋ³, КАТАРИНА ШАВИКИН³, ДАНИЈЕЛА СТЕШЕВИЋ⁴,
ВЛАТКА ВАЈС¹ И СЛОБОДАН МИЛОСАВЉЕВИЋ²

¹Институт за хемију, технологију и металургију, Њеџошева 12, Београд, ²Хемијски факултет, Студентски брз 16, 11000 Београд, ³Институт за проучавање лековитог биља "Јосиф Панчић", Тадеуша Кошћука 1, 11000 Београд и ⁴Biology Department, Faculty of Science, University of Montenegro, 81000 Podgorica, Montenegro

Из надземних делова *Onobrychis montana* subsp. *scardica* изоловани су рутин (1, главни састојак) и два флавоноидна С-гликозида, витексин (2) и његов 2"-О- α -рамнопиранозид (3). Њихова структура је одређена применом ¹H-NMR, ¹³C-NMR и UV спектроскопије (процедура са реагенсима UV-померања) и масене спектрометрије високог разлагања (HR-ESI-MS). Релативно висок садржај рутина (5.27 mg/g сувог материјала) одређен помоћу течне хроматографије (HPLC), указује на *O. montana* subsp. *scardica* као нов природни извор овог биолошки активног једињења. Изолована једињења могу бити и од вредности као хемотаксономски маркери.

(Примљено 26. септембра, ревидирано 27. децембра 2007)

REFERENCES

1. N. Diklić, T. Cincović, M. Kojić, in *Flore de la Republique Socialiste de Serbie*, M. Josifović, Ed., SANU, Belgrade, 1972, vol IV, p. 254 (in French)
2. L. J. Ingham, *Z. Naturforsch. C.* **33C** (1978) 146
3. M. Halabalaki, X. Alexi, N. Aligiannis, G. Lambrinidis, H. Pratsinis, I. Florentin, S. Mitakou, E. Mikros, A. L. Skaltsounis, M. N. Alexis, *Planta Med.* **72** (2006) 488
4. A. L. Kazakov, S. F. Dzhumyrko, V. A. Kompantsev, *Khim. Prir. Soed.* **2** (1981) 245 (in Russian)
5. M. S. Luk'yanchikov, *Khim. Prir. Soed.* **2** (1982) 256 (in Russian)
6. M. S. Luk'yanchikov, A. L. Kazakov, *Khim. Prir. Soed.* **6** (1982) 784 (in Russian)
7. M. S. Luk'yanchikov, A. L. Kazakov, S. F. Dzhumyrko, *Khim. Prir. Soed.* **4** (1985) 564 (in Russian)
8. M. R. Koupai-Abyazani, A. D. Muri, B. A. Bohm, G. H. N. Towers, M. Y. Gruber, *Phytochemistry* **34** (1993) 113
9. J. P. J. Marais, I. Mueller-Harvey, E. V. Brandt, D. Ferreira, *J. Agric. Food Chem.* **48** (2000) 3440

10. Y. Lu, Y. Sun, L. Y. Foo, W. C. McNabb, A. L. Molan, *Phytochemistry* **55** (2000) 67
11. G. B. Russell, G. J. Shaw, P. E. Christmas, M. B. Yates, O. R. W. Sutherland, *Phytochemistry* **23** (1984) 1417
12. M. Halabalaki, N. Aligiannis, Z. Papoutsi, S. Mitakou, P. Moutsatsou, C. Sekeris, A. L. Skaltsounis, *J. Nat. Prod.* **63** (2000) 1672
13. P. K. Agrawal, *Carbon-13 NMR of flavonoids*, Elsevier, Amsterdam, 1989
14. S. Rayyan, T. Fossen, N. H. Solheim, Ø. M. Andersen, *Phytochem. Anal.* **16** (2005) 334
15. S. Asgary, G. Naderi, *Pharm. Acta Helv.* **73** (1999) 223
16. M. S. Luk'yanchikov, A. L. Kazakov, *Khim. Prir. Soed.* **2** (1982) 256 (in Russian)
17. I. I. Moniava, E. P. Kemertelidze, *Izvestiya Akademii Nauk Gruzinskoj SSR, Seriya Khimicheskaya* **2** (1976) 119 (in Russian).



www.shd.org.yu

J. Serb. Chem. Soc. 73 (5) 531–540 (2008)
JSCS–3734

JSCS@tmf.bg.ac.yu • www.shd.org.yu/JSCS

UDC **Hieracium pilosella* L.:633.879.6:
:665.7.038.5:615.28

Original scientific paper

Anti-oxidative and antimicrobial activities of *Hieracium pilosella* L. extracts

LJILJANA P. STANOJEVIĆ*, MIHAJLO Z. STANKOVIĆ,
VESNA D. NIKOLIĆ and LJUBIŠA B. NIKOLIĆ

Faculty of Technology, Bulevar Oslobođenja 124, 16000 Leskovac, Serbia

(Received 28 June, revised 22 October 2007)

Abstract: The anti-oxidative and antimicrobial activities of different extracts from *Hieracium pilosella* L. (Asteraceae) whole plant were investigated. The total dry extracts were determined for all the investigated solvents: methanol, dichloromethane, ethyl acetate and dichloromethane:methanol (9:1). It was found that the highest yield was obtained by extraction with methanol (12.9 g/100 g of dry plant material). Qualitative and quantitative analysis were performed by the HPLC method, using external standards. Chlorogenic acid, apigenin-7-O-glucoside and umbelliferone were detected in the highest quantity in the extracts. The qualitative and quantitative composition of the extracts depends on the solvent used. The 1,1-diphenyl-2-picrylhydrazyl (DPPH) radical scavenging effect of the extracts was determined spectrophotometrically. The highest radical scavenging effect was observed in the methanolic extract, both with and without incubation, $EC_{50} = 0.012$ and $EC_{50} = 0.015$ mg ml⁻¹, respectively. The antimicrobial activities of the extracts towards the bacteria (*Escherichia coli*, *Pseudomonas aeruginosa*, *Staphylococcus aureus*, *Bacillus subtilis*, *Salmonella enteritidis* and *Klebsiella pneumoniae*) and the fungi (*Aspergillus niger* and *Candida albicans*) were determined by the disc diffusion method. The minimal inhibitory concentrations were determined for all the investigated extracts against all the mentioned microorganisms.

Keywords: *Hieracium pilosella* L.; anti-oxidant activity; antimicrobial activity; HPLC determination.

INTRODUCTION

Hieracium pilosella L. (family Asteraceae) is a perennial herbaceous plant. It is widely spread in mountains and foothill pastures, in the areas of oak woods and undergrowth. It is mainly used as a traditional medicine for bronchitis, bronchial asthma, edema and as an ointment for wound healing. It is especially recommended for intensifying urination and eliminating slime, sand and small stones from the urinary tract and the kidneys.¹

* Corresponding author. E-mail: ljiljas76@yahoo.com
doi: 10.2298/JSC0805531S

Hieracium pilosella is used in traditional European medicine for its diuretic and anti-inflammatory effects.² Extracts obtained from *Hieracium pilosella* leaves have an antibacterial effect on grown cultures of veterinary pathogens: *Brucella abortis* and *Brucella melitensis*.³ The identification of flavonoids and phenolic acids in this plant species was mostly carried out on the material harvested in areas of New Zealand.⁴ The phenolic components most frequently represented in methanol extracts from all *Hieracium* species are: chlorogenic acid (3-{[3-(3,4-dihydroxyphenyl)-1-oxo-2-propenyl]oxy}-1,4,5-trihydroxycyclohexanecarboxylic acid), caffeic acid (3-(3,4-dihydroxyphenyl)-2-propenoic acid), and umbelliferone (7-hydroxy-2H-1-benzopyran-2-one), and of these, umbelliferone is the most active one.⁴⁻⁶ The phenolic acids and flavonoids present in the plants are natural antioxidants.^{7,8} They also have anti-mutagenic and anti-cancerogenic properties,⁹ cardio-protective¹⁰ and antimicrobial activity.¹¹ Chlorogenic, caffeic and dihydrocaffeic acid, which are present in many plant species, are cinnamic acid derivatives. These acids have anti-inflammatory, anti-mutagenic and anti-cancerogenic properties.¹² Antioxidants are important species which have the ability to protect the organism from the damage caused by a free radical-induced oxidative stress.¹³ Phenolic acids are mainly antioxidant active due to their redox properties, which allow them to act as reducing agents, hydrogen donors, singlet oxygen quenchers and metal chelators. Their antioxidant activity is generally based on the number and the location of hydroxyl groups present, as well as on the presence of a 2-3 double bond and 4-oxo function.^{14,15}

Free radicals contribute to more than one hundred disorders in humans, including atherosclerosis, arthritis, ischemia and reperfusion injuries of many tissues, central nervous system injury, gastritis and cancer.¹⁶⁻¹⁹ Due to environmental pollutants, radiation, chemicals, toxins, deep-fried and spicy foods, as well as physical stress, free radicals cause depletion of the antioxidants of the immune system, changes in gene expression and induce abnormal proteins. Oxidation processes are one of the most important routes for producing free radicals in food, drugs, and even in living systems.^{16,20,21}

Medicinal plants have been used for centuries as remedies for human diseases because they contain components of therapeutic value.^{22,23} Recently, the acceptance of traditional medicine as an alternative form of health care and the development of microbial resistance to the available antibiotics has led the authors to investigate the antimicrobial activity of medicinal plants.^{22,24,25} Moreover, the increasing use of plant extracts in the food, cosmetic and pharmaceutical industries suggests that, in order to determine the active compounds, a systematic study of medicinal plants is very important.^{13,22}

The anti-oxidative and antimicrobial activity of different extracts from dried and ground *Hieracium pilosella* L. (Asteraceae) whole plant material from south-east Serbia were studied. The qualitative and quantitative compositions of the extracts obtained were determined by HPLC analyses.

EXPERIMENTAL

Plant material

Hieracium pilosella L. whole plant was harvested in June 2005 in the area of southeast Serbia. The plant material was dried in the shade in an airy place and then stored in paperbags and kept at room temperature.

Standards

Chlorogenic acid was obtained from Sigma-Aldrich (Steinheim, Germany), and apigenin-7-*O*-glucoside and umbelliferone were purchased from Extrasynthese (Genay, France).

Solvents and reagents

Methanol and acetonitrile were of HPLC grade from Merck (Darmstadt, Germany). 1,1-Diphenyl-2-picrylhydrazyl (DPPH) was obtained from Sigma Chemicals Co., St. Louis, MO, USA. All other chemicals were of analytical-reagent grade (Sigma).

Extraction method

Dried, ground plant material (10 g) was extracted for 48 h at room temperature (plant material to solvent ratio: 1:20, m/v) employing the following solvents: methanol, dichloromethane:methanol (9:1), dichloromethane and ethyl acetate. All the extracts were filtered through No. 1 Whatman filter paper.

Determination of a total yield of extracted substance in Hieracium pilosella L. plant extracts

10 ml of extract was added into the vessel of a Scaltec SMO 1 apparatus (Scaltec Instruments, Germany). After drying at 105 °C, the contents of the dry residue mass were read on the apparatus display.

Free radical scavenger activity

The capacity of a compound to scavenge free 1,1-diphenyl-2-picrylhydrazyl (DPPH) radicals is determined by the use of the so-called DPPH test.²⁶⁻²⁹ The extracts obtained using the various solvents (10 ml) were evaporated on a rotary evaporator at 40 °C until dry, then dissolved in methanol and various concentrations of the methanolic extract solutions were prepared. A 1.0 ml of methanolic solution of DPPH radicals (3×10^{-4} mol dm⁻³) was added to 2.5 ml sample. The capacity of the scavenging free radicals was calculated using Eq. (1):

$$\text{DPPH radicals scavenging capacity} = 100 - \frac{100(A_S - A_B)}{A_C} \quad (1)$$

where A_S is the sample absorbance at 517 nm of the sample of a methanolic solution of the extract treated with the DPPH radical solution, A_B is the blank absorbance at 517 nm of the blank methanol solution of the extract not treated with the DPPH radical solution and A_C is the control absorbance at 517 nm of the control solution of a pure, non-irradiated methanolic solution of DPPH radical (1.0 ml of DPPH radical of 3×10^{-4} mol dm⁻³ concentration + 2.5 ml of methanol).

The absorbance of the samples was measured on a VARIAN UV-Vis Cary-100 Conc. spectrophotometer. The EC_{50} value (mg ml⁻¹) was determined for all the extracts. The antioxidant capacities of the samples were compared with those of butylated hydroxytoluene (BHT). A decrease by 50 % of the initial DPPH concentration was defined as the EC_{50} .

HPLC analysis

For the quantification of phenolic substances, the extracts of dry homogenized leaves and roots from individual plants were analyzed by HPLC under the following conditions. Appa-

ratus: Agilent 110 Series, Waldborn, Germany; column: Zorbax-Eclipse XDB-CN, 4.6×250 mm, 5 µm; eluent: acetonitrile:water = 30:70 v/v; flow rate: 1.0 ml min⁻¹; task volume: 20 µl; temperature: 25 °C; detection: UV detector at 205 nm.

The quantities of chlorogenic acid, apigenin-7-*O*-glucoside and umbelliferone were determined from calibration curves of the compounds, using external standards.

Microbiological tests

Microorganisms and substrates. The following microorganisms were used for the antimicrobial test. Bacteria: *Escherichia coli* (ATCC 25922), *Pseudomonas aeruginosa* (ATCC 9027), *Staphylococcus aureus* (ATCC 6538), *Bacillus subtilis* (ATCC 6633), *Salmonella enteritidis* (ATCC 13076) and *Klebsiella pneumoniae* (ATCC 13883); fungi: *Aspergillus niger* (ATCC 16404) and *Candida albicans* (ATCC 10231). Substrates used for microorganism growth: antibiotic agar no. 1 for microbiology for bacteria and tryptic soy agar for fungi (Merck, Darmstadt, Germany).

Disc diffusion test. The extracts evaporated on a rotary evaporator (40 °C) were dissolved in dimethyl sulfoxide (DMSO, BDH, Milan, Italy). The substrates were sterilized for 15 min in an autoclave at 121 °C. 0.50 ml of microorganism was added to 50 ml of agar and a 10 ml sample was poured into a petri dish. Filter paper discs (12.7 mm, Schleicher & Schuell) were placed on the inoculated substrate and impregnated with 70 µl of the sample. The plates are incubated for 18 h at 37 °C for the bacteria and 48 h at 25 °C for the fungi. All tests were performed in duplicate and the antibacterial activity is expressed as the average value of the inhibition zones (mm) realized by the plant extracts. The minimum inhibitory concentration (MIC) of the extracts is defined as the smallest extract concentration causing a visible inhibition of the microorganisms.

RESULTS AND DISCUSSION

The DPPH test is based on the exchange of hydrogen atoms between the antioxidant and the stable DPPH free radical. Practically, the reaction brings about the reduction of DPPH radicals to the corresponding hydrazine, which is manifested by a color change from violet to yellow, which is monitored spectrophotometrically. The results for methanol, dichloromethane:methanol, ethyl acetate and dichloromethane extracts, are shown in Fig. 1.

All the extracts show a higher DPPH radicals scavenging capacity after incubation (20 min) with a free radical solution.

The DPPH scavenging capacity of the studied extracts at a concentration of 0.18 mg ml⁻¹ decreased in the following sequence: MeOH > EtOAc > CH₂Cl₂:MeOH >> CH₂Cl₂, the values being 95.53, 94.54, 87.62, and 19.83 % (20 min incubation time) and 95.33, 67.7, 51.75, and 12.7 % (without incubation), respectively. The methanol extract showed the highest anti-oxidative activity. The EC₅₀ values for all extracts and BHT are given in Table I.

Unlike the examined extracts, the DPPH test performed without incubation showed that the standard BHT antioxidant did not attain the EC₅₀ value at a concentration of 0.18 mg ml⁻¹. In the case of DPPH test performed with a 20-min incubation, the BHT concentration necessary for reaching EC₅₀ was 0.021 mg ml⁻¹. The concentrations of the dichloromethane:methanol, ethyl acetate and dichloromethane extracts required to attain EC₅₀ were higher than that of BHT. In

producing this effect, the methanol extract concentration was lower than that of BHT. The obtained data show that the methanol extract was a better antioxidant than the BHT standard of the same concentration.

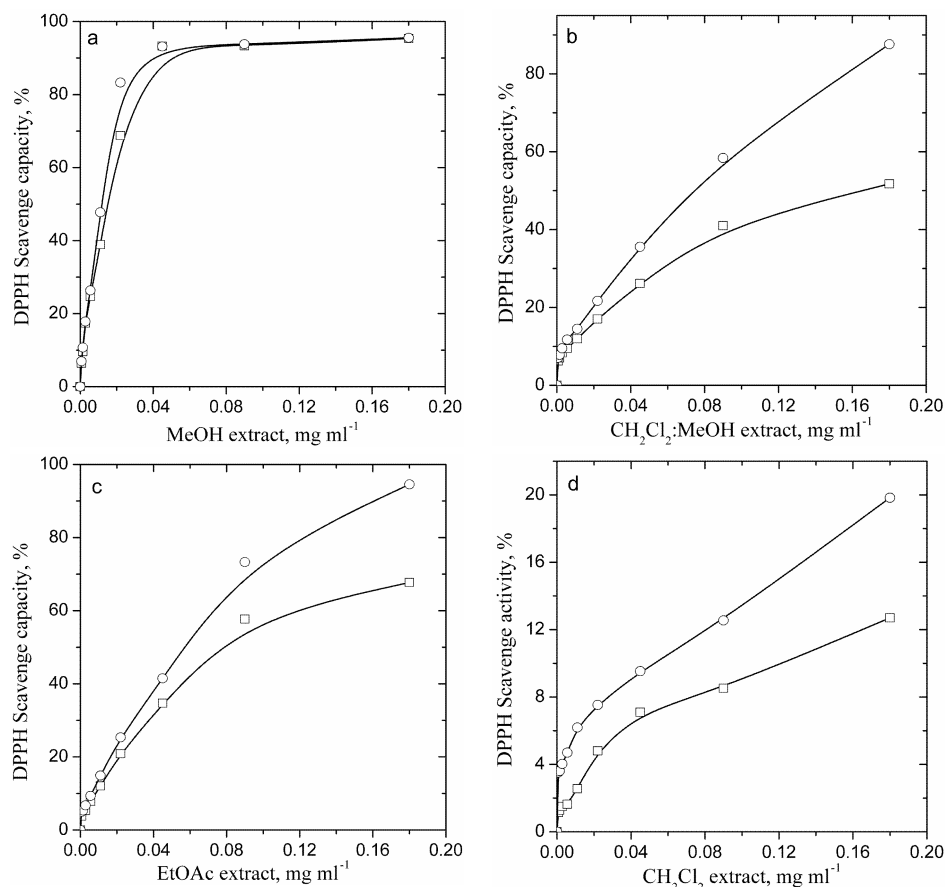


Fig. 1. DPPH scavenging capacity of the MeOH (a), CH₂Cl₂:MeOH (b), EtOAc (c) and CH₂Cl₂ (d) extracts of *Hieracium pilosella* L.; (□) without incubation; (○) 20 min of incubation.

The carriers of the anti-oxidative activity are phenolic acids and flavonoids extracted from the plant material.^{7,8} In the DPPH test, different extracts showed different anti-oxidative activities. This is the consequence of the different polarities of the employed solvents, which extract different components from the plant material and, therefore, the composition of the extracts differed.

Total quantities of substances extracted using the different solvents per 100 g of dry plant material are given in Table II, while the retention times and calibration curves of the estimated compounds in the *Hieracium pilosella* L. extracts are given in Table III.

TABLE I. EC_{50} values (mg ml^{-1}) of the different extracts

	Extract				
	MeOH	$\text{CH}_2\text{Cl}_2:\text{MeOH}$ (9:1)	EtOAc	CH_2Cl_2^a	BHT
Without incubation	0.015	0.167	0.079	> 0.18	EC_{50} not achieved
20 min incubation	0.012	0.075	0.058	> 0.18	0.021

TABLE II. Total quantity of dry substance extracted by the different solvents

Solvent	Total extract, g per 100 g of d.p.m. ^a
MeOH	12.9
$\text{CH}_2\text{Cl}_2:\text{MeOH}$ (9:1)	5.2
CH_2Cl_2	3.7
EtOAc	4.0

^aDry plant materialTABLE III. Calibration curves and retention times of the estimated compounds in the *Hieracium pilosella* L. extracts

Compound	Chlorogenic acid	Apigenin-7- <i>O</i> -glucoside	Umbelliferone
Retention time min	2.01	4.81	5.67
Concentration range $\mu\text{g ml}^{-1}$	1–500	0.15–15	4–670
Calibration curve ^a q	75.84	60.08	235.61
$P = q + rc$ r	30891.11	79938.97	153295.95
Correlation coefficient	0.9998	0.9997	0.9998

^a P , mAU: peak area; c , mg ml^{-1} : concentration of the standard sample; q and r : constants

Based on HPLC analysis and the calibration curves of the standard samples, the contents of the bioactive components were determined in all the extracts (Table IV).

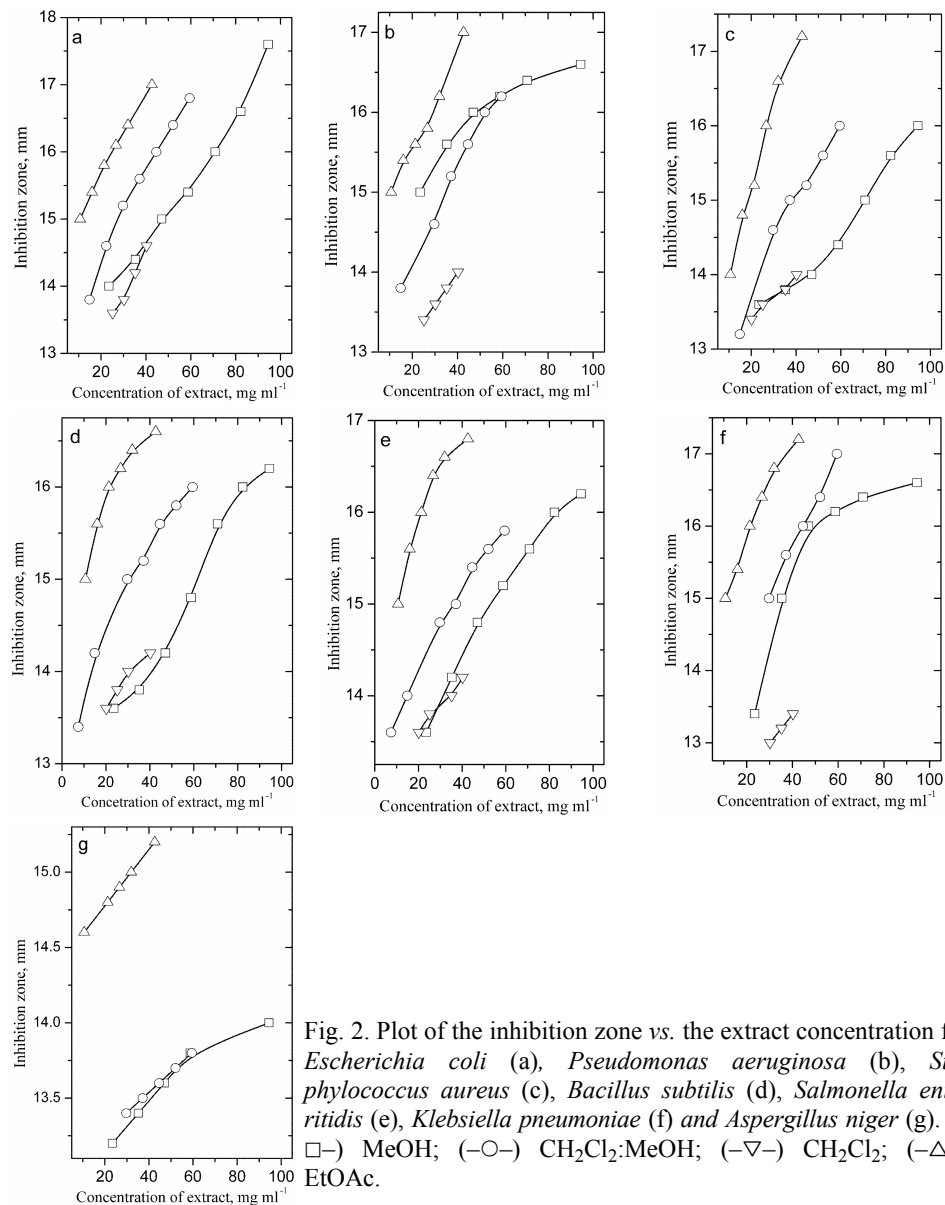
TABLE IV. The content of bioactive components in g per 100 g of the total dry extracts or the dry plant material

Extract	Chlorogenic acid		Umbelliferone		Apigenin-7- <i>O</i> -glucoside	
	Dry extract	Dry plant material	Dry extract	Dry plant material	Dry extract	Dry plant material
MeOH	35.45	4.58	2.54	0.32	1.20	0.150
$\text{CH}_2\text{Cl}_2:\text{MeOH}$ (9:1)	16.60	0.86	11.66	0.61	1.80	0.094
CH_2Cl_2	0.58	0.02	6.35	0.23	0.03	0.01
EtOAc	2.65	0.12	5.15	0.20	0.97	0.039

The highest quantities of chlorogenic acid and apigenin-7-*O*-glucoside were extracted using methanol: 4.58 and 0.15 g/100 g of d.p.m., respectively, and the highest yield of umbelliferone was obtained using dichloromethane:methanol, 0.61 g/100 g d.p.m. Chlorogenic acid is a natural antioxidant.^{7,8,23} The methanolic extract contained the highest quantity of chlorogenic acid and showed the highest antioxidant activity. Such a composition results in the extracts having dif-

ferent anti-oxidative and antimicrobial activities. Since phenolic acids are well-known natural antioxidants^{7,8} and have antimicrobial properties,¹¹ such an extract composition only confirms the good anti-oxidative properties, especially of the extracts obtained with methanol.

The results of the microbiological tests and MIC determinations are given in Fig. 2.



All the tested extracts (Fig. 2) demonstrated some antimicrobial activity. All the extracts concentrations less than 30 mg ml⁻¹ had an antimicrobial effect on the bacteria *Staphylococcus aureus* and *Bacillus subtilis*. All the extracts showed antimicrobial activity against *Escherichia coli*, whereby the ethyl acetate extract was active at the lowest concentration. In comparison to the other extracts, the ethyl acetate extract was active against the bacteria *Pseudomonas aeruginosa* and *Klebsiella pneumoniae* at the lowest concentration (Figs. 2b and 2f). The dichloromethane:methanol extract was active at the lowest concentration (7.44 mg ml⁻¹) against *Salmonella enteritidis* (Fig. 2e). The ethyl acetate extract had the best effect on the fungus *Aspergillus niger*, while dichloromethane extract had no effect at all (Fig. 2g). All the extracts studied were inactive against *Candida albicans*.

The MIC values of the different extracts are given in Table V.

TABLE V. MIC values (mg ml⁻¹) of the different extracts

Microorganism	Extract			
	MeOH	CH ₂ Cl ₂ :MeOH (9:1)	CH ₂ Cl ₂	EtOAc
<i>Escherichia coli</i>	11.75	14.87	25.16	10.66
<i>Pseudomonas aeruginosa</i>	23.5	14.87	25.16	10.66
<i>Staphylococcus aureus</i>	23.5	14.87	20.12	10.66
<i>Bacillus subtilis</i>	23.5	7.44	20.12	10.66
<i>Salmonella enteritidis</i>	23.5	7.44	20.12	10.66
<i>Klebsiella pneumoniae</i>	23.5	29.75	30.19	10.66
<i>Aspergillus niger</i>	23.5	29.75	No effect	10.66

The lowest MIC values for all microorganisms was shown by the ethyl acetate extract, while dichloromethane:methanol extract has a wide range of MIC values, the lowest MIC value (7.44 mg ml⁻¹) being for *B. subtilis* and *S. enteritidis*. The activity of the obtained extracts was more pronounced against bacterial than against fungal organisms. Some authors attribute the antimicrobial activity to the phenolic components.³⁰ Investigations have demonstrated the presence of flavonoids and triterpenes in the species of the genus *Hieracium*, which are carriers of antimicrobial activity.²² The antifungal compounds of the plants are not well known. However, the presence of flavonoids and terpenes and a certain degree of lipophilicity might determine the toxicity by interactions with the membrane constituents and their arrangement.²² However, it is difficult to compare the data with the literature because several variables influence the results, such as the environmental and climatic conditions of the plant, and the choice of the extraction method and the antimicrobial test. Moreover, standard criteria for the evaluation of the plant activity are lacking and therefore the results obtained by different authors differ widely.²²

CONCLUSIONS

The highest yield was obtained by extraction with methanol (12.9 g/100 g of dry plant material). Chlorogenic acid, apigenin-7-*O*-glucoside and umbelliferone

were detected in the highest quantities in the extracts. The qualitative and quantitative composition of the extracts depended on the solvent used. The highest radical scavenging effect was observed in a methanolic extract with and without incubation, $EC_{50} = 0.012$ and 0.015 mg ml^{-1} , respectively. The lowest *MIC* values for all microorganisms was shown by the ethyl acetate extract, while the dichloromethane:methanol extract had a wide range of *MIC* values, the lowest *MIC* value (7.44 mg ml^{-1}) being for *Bacillus subtilis* and *Salmonella enteritidis*.

Acknowledgements. This investigation was supported by the Ministry of Science of the Republic of Serbia under the project TR-6708 B. Ljiljana Stanojević is a recipient of a fellowship granted by the Ministry of Science of the Republic of Serbia.

ИЗВОД
АНТИОКСИДАТИВНА И АНТИМИКРОБНА АКТИВНОСТ
ЕКСТРАКТА *Hieracium pilosella* L.

ЉИЉАНА П. СТАНОЈЕВИЋ, МИХАЈЛО З. СТАНКОВИЋ, ВЕСНА Д. НИКОЛИЋ И ЉУБИША Б. НИКОЛИЋ

Технолошки факултет, Булевар ослобођења 124, 16000 Лесковац

Испитивана је антиоксидативна и антимикробна активност различитих екстраката добијених из целе биљке *Hieracium pilosella* L. (Asteraceae). Укупни суви екстракти одређени су за све екстракте, метанолни, дихлорметански, етилацетатни и дихлорметан:метанолни (9:1) и показано је да је највећи принос постигнут са метанолом ($12.9 \text{ g}/100 \text{ g}$ сувог биљног материјала). Квалитативни и квантитативни садржај је анализиран помоћу HPLC методе коришћењем екстерних стандарда. Идентификоване су три најзаступљеније компоненте у екстрактима: хлорогенска киселина, апигенин-7-О-глукозид и умбелиферон. Установљено је да квалитативни и квантитативни састав екстраката зависи од врсте растварача. Способност неутралисања 1,1-дифенил-2-пикрил-хидразил (DPPH) радикала екстрактима одређена је спектрофотометријски. Највећа способност неутралисања радикала остварује се метанолним екстрактом са инкубацијом и без ње ($EC_{50} = 0.012$, односно 0.015 mg ml^{-1}). Антимикробна активност на бактерије (*Escherichia coli*, *Pseudomonas aeruginosa*, *Staphylococcus aureus*, *Bacillus subtilis*, *Salmonella enteritidis* и *Klebsiella pneumoniae*) и гљиве (*Aspergillus niger* и *Candida albicans*) одређена је применом диск дифузионе методе. Одређене су минималне инхибиторне концентрације (*MIC*) за све испитиване екстракте за наведене микроорганизме.

(Примљено 28. јуна, ревидирано 22. октобра 2007)

REFERENCES

1. N. Randjelović, Z. Jeremić, V. Stamenković, *Healing Plants of Timok Region, Phytotherapy II*, Young Explorer Organization and Cultural and Educational Community of Zaječar, Zaječar, 1995, p. 72 (in Serbian)
2. S. D. Petrović, M. S. Gorunović, V. Wray, I. Merfort, *Phytochemistry* **50** (1999) 293
3. G. F. Bishop, A. J. Davy, *J. Ecol.* **82** (1994) 195
4. C. Zidorn, B. Schubert, H. Stuppner, *Biochem. Syst. Ecol.* **33** (2005) 855
5. S. D. Petrović, R. Löscher, M. S. Gorunović, I. Merfort, *Biochem. Syst. Ecol.* **27** (1999) 651
6. W. Makepeace, A. T. Dobson, D. Scott, *N. Z. J. Bot.* **23** (1985) 79
7. I. Konczak, S. Okuno, M. Yoshimoto, O. Yamakawa, *J. Biomed. Biotech.* **5** (2004) 287
8. M. Kosar, D. Dorman, K. Baser, R. Hiltunen, *Chromatographia* **60** (2004) 635

9. M. Kampa, V. I. Alexaki, G. Notas, A. P. Nifli, A. Nistikaki, A. Hatzoglou, *Breast Cancer Res.* **6** (2004) 63
10. R. A. A. Caccetta, K. D. Croft, L. J. Beilin, I. B. Puddey, *Am. J. Clin. Nutr.* **71** (2000) 67
11. A. M. Wen, P. Delaquis, K. Stanich, P. Toivonen, *Food Microbiol.* **20** (2003) 305
12. M. Y. Moridani, H. Scobie, A. Jamshidzadeh, P. Salehi, P. J. O'Brien, *Drug Metab. Dispos.* **29** (2001) 1432
13. J. M. Čanadanović-Brunet, S. M. Djilas, G. S. Cetković, V. T. Tumbas, *J. Sci. Food Agric.* **85** (2005) 265
14. F. Karadeniz, H. S. Burdurlu, N. Koca, Y. Soyer, *Turk. J. Agric. Forestry* **29** (2005) 297
15. P.-G. Pietta, *J. Nat. Prod.* **63** (2000) 1035
16. F. Pourmorad, S. J. Hosseinimehr, N. Shahabimajd, *Afr. J. Biotechnol.* **5** (2006) 1142
17. W. P. Shih, P. L. Lai, H. W. K. Jen, *Food Chem.* **99** (2006) 775
18. S. Lan, Y. Jun-Jie, C. Denys, Z. Kequan, M. Jeffrey, Y. Liangli (Lucy), *Food Chem.* **100** (2007) 990
19. T. Bektas, E. Ozgur, A. H. Askin, A. Enes, *Food Chem.* **100** (2007) 985
20. C. D. Dillard, J. B. German, *J. Sci. Food Agric.* **80** (2000) 1744
21. T. Aziz, E. D. Mehmet, M. Nazime, K. Ibrahim, G. Kudret, *Food Chem.* **101** (2007) 267
22. A. Nostro, M. P. Germanò, V. D'Angelo, A. Marino, M. A. Cannatelli, *Lett. Appl. Microbiol.* **30** (2000) 379
23. B. Lj. Milić, S. M. Djilas, J. M. Čanadanović-Brunet, M. B. Sakač, *Polyphenols in Plants*, Faculty of Technology, University of Novi Sad, Novi Sad, 2000, p.p. 277-309 (in Serbian)
24. C. Proestos, I. S. Boziaris, G.-J. E. Nychas, M. Komaitis, *Food Chem.* **95** (2006) 664
25. J.-P. Rauha, S. Remes, M. Heinonen, A. Hopia, M. Kahkonen, T. Kujala, *Int. J. Food Microbiol.* **56** (2000) 3
26. R. Aquino, S. Morelli, A. Tomaino, M. Pellegrino, A. Saija, L. Grumetto, C. Puglia, D. Ventura, F. Bonina, *J. Ethnopharmacol.* **79** (2002) 183
27. W. C. Choi, C. S. Kim, S. S. Hwang, K. B. Choi, J. H. Ahn, Y. M. Lee, H. S. Park, K. S. Kim, *Plant Sci.* **163** (2002) 1161
28. Li.-C. Lu, Y.-W. C. Chen, C.-C. Chou, *J. Food Drug Anal.* **11** (2003) 277
29. C. Sanchez-Moreno, *Food Sci. Techn. Int.* **8** (2002) 121
30. B. Mezzeti, G. Orzalesi, C. Rossi, V. Bellavita, *Planta Med.* **18** (1970) 326.



www.shd.org.yu

J. Serb. Chem. Soc. 73 (5) 541–545 (2008)
JSCS–3735

JSCS@tmf.bg.ac.yu • www.shd.org.yu/JSCS

Short communication

SHORT COMMUNICATION

Stereospecific ligands and their complexes. Synthesis and characterization of the *s-cis*-K[Ru(*S,S*-eddp)Cl₂] \cdot 3H₂O

VERICA V. GLODJOVIĆ and SREĆKO R. TRIFUNOVIĆ*

Department of Chemistry, Faculty of Science, University of Kragujevac,
Radoja Domanovića 12, P. O. Box 60, 34000 Kragujevac, Serbia

(Received 2 August, revised 10 December 2007)

Abstract: In the reaction of ruthenium(III) chloride and an edda-like ligand ethylenediamine-*N,N'*-di-*S,S*-2-propionic acid (*S,S*-eddp) in aqueous solution led to the formation of only one of the three possible geometrical isomers potassium-*s-cis*-dichlorido-(ethylenediamine-*N,N'*-di-*S,S*-2-propionato)-ruthenate(III)-trihydrate, *s-cis*-K[Ru(*S,S*-eddp)Cl₂] \cdot 3H₂O. The assumed geometry of the complex was based on its electronic absorption and infrared spectra.

Keywords: ruthenium(III) complex; *S,S*-ethylenediamine-*N,N'*-di-*S,S*-propionate ligand; electronic absorption and infrared spectra.

INTRODUCTION

The synthesis and pharmacological evaluation of new compounds bearing metal ions other than platinum is a field of growing interest.^{1,2} Complexes based on ruthenium, one of the platinum group metals, have been proposed as potential antitumour substances,^{3–8} demonstrating remarkable antitumour activity and anti-metastatic behaviour, as well as lower systematic toxicity than platinum compounds.^{9–12} Recent biochemical studies demonstrated that the new ruthenium compounds bind proteins in a tight covalent manner.⁹

Today, ruthenium complexes with polyaminopolycarboxylic chelating agents constitute a new group of potential anticancer compounds.^{2,3,13} The most representative example, *cis*-H[Ru(H₂-pdta)Cl₂], (H₄-pdta = 1,3-propanediamine-tetraacetic acid), binds rapidly to serum proteins through surface histidines, damages nuclear DNA, inhibits DNA recognition and DNA lysis by restriction enzymes, alters the conformation of pHV14 DNA, stimulates NADPH oxidase and a respiratory burst in phagocytic neutrophils and elicits phosphorylation of tyrosine residues.^{2,9,14,15}

In an effort to improve the antitumour properties of ruthenium compounds, a series of new Ru(III) complexes was prepared with stereospecific ligands similar

* Corresponding author. E-mail: srecko@kg.ac.yu
doi: 10.2298/JSC0805541G

to the linear quadridentate edda ligand (edda = ethylenediamine-*N,N'*-acetic acid ion), such as the *S,S*-eddp ligand (*S,S*-eddp = ethylenediamine-*N,N'*-di-*S,S*-2-propionic acid ion), by changing the substituent on the chiral carbon atom.

The *S,S*-eddp (*S,S*-eddp = *S,S*-ethylenediamine-*N,N'*-di-2-propionate ion) is similar to the edda ligand and it can form three possible geometrical isomers, *s-cis*, *uns-cis* and *trans* (Fig. 1), when it is coordinated as a tetradentate agent together with two additional monodentate ligands in octahedral Ru(III) complexes. With a known absolute configuration, on coordination to a Ru(III) ion, the *S,S*-eddp ligand forms complexes maintaining the *S* configuration of both carbon atoms, yielding complexes with a $\Delta\Delta\Delta$ (net Δ) absolute configuration.^{16,17} However, the orientation of the methyl groups of the *S,S*-eddp ligand, in complexes can be different after coordination to a metal ion and two diastereoisomers can theoretically be formed for every geometric isomer.

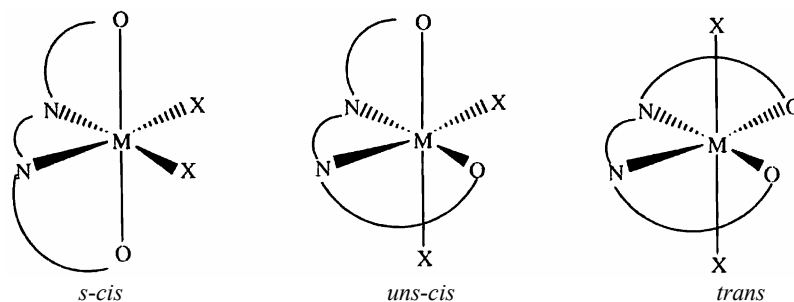


Fig. 1. Possible geometric isomers of the $[\text{Ru}(\text{S,S-eddp})\text{Cl}_2]^-$ complex.

As part of continuing studies on this important class of complexes, the synthesis and characterization of the new Ru(III) complex, *s-cis*- $\text{K}[\text{Ru}(\text{S,S-eddp})\text{Cl}_2] \cdot 3\text{H}_2\text{O}$, in which the chelating agent ethylenediamine-*N,N'*-di-*S,S*-2-propionic acid acts as tetradentate ligand is presented here.

EXPERIMENTAL

Materials

Ethylenediamine-*N,N'*-di-*S,S*-2-propionic acid (*S,S*-eddp) was prepared using a previously described procedure.¹⁸ Commercial hydrated ruthenium(III) chloride was dissolved in concentrated HCl and refluxed for 30 min. After concentration to dryness, the compound was stored under CaCl_2 .

Synthesis of the complex *s-cis*- $\text{K}[\text{Ru}(\text{S,S-eddp})\text{Cl}_2] \cdot 3\text{H}_2\text{O}$

The new ruthenium(III) complex, *s-cis*- $\text{K}[\text{Ru}(\text{S,S-eddp})\text{Cl}_2] \cdot 3\text{H}_2\text{O}$, was synthesized by heating, on a steam bath (2 h), an aqueous solution of *S,S*-eddp with RuCl_3 obtained as described above (molar ratio = 1:1). After this process, the pH of the system was adjusted to 3.0 and the mixture refluxed for 3 h, evaporated to a small volume and left overnight. After adding acetone, a black powder of the complex formed. The complex is stable on air and soluble in water. An aqueous solution (0.10 %) gave $[\alpha]_{\text{D}} = -142^\circ$ ($[M]_{\text{D}} = -663$). Anal. Calcd. (%) for *s-cis*- $\text{K}[\text{Ru}(\text{S,S-eddp})\text{Cl}_2] \cdot 3\text{H}_2\text{O} \equiv \text{KRuC}_8\text{H}_{20}\text{N}_2\text{O}_7\text{Cl}_2$ ($M_r = 467.33 \text{ g mol}^{-1}$): C, 20.56; H, 4.31; N, 6.00. Found: C, 20.69; H, 4.65; N, 6.16.

Physical measurements

Electronic absorption spectra were recorded on a Perkin–Elmer Lambda 35 double-beam UV-Vis spectrophotometer. An aqueous 1×10^{-3} mol dm⁻³ solution of the complex was used for this measurement. The infrared spectra were recorded on a Perkin–Elmer FTIR 31725-X spectrophotometer using the KBr pellet technique. The $[\alpha]_D^{20}$ value was measured in a 1.0 dm tube at 20 °C using a Perkin–Elmer SP polarimeter. Elemental microanalyses for C, H, and N were performed by standard methods.

RESULTS AND DISCUSSION

Electronic absorption spectrum

The absorption maxima in the corresponding electronic absorption spectrum of the isolated *s-cis*-[Ru(*S,S*-eddp)Cl₂]⁻ complex are summarized in Table I. The corresponding data for the similar [Ru(edda-type)L]⁻ complexes are given for comparison.

TABLE I. Electronic absorption spectra of Ru(III) complexes with some tetradentate ligands

Complex	λ_{\max} / nm	ϵ_{\max} / m ² mol ⁻¹	Ref.
[Ru(edta)H ₂ O] ⁻	350	68.0	19
	280	280.0	
<i>s-cis</i> -[Ru(eddp)Cl ₂] ⁻	470	60.0	8
	300	214.0	
<i>s-cis</i> -[Ru(H ₂ edta)Cl ₂] ⁻	470	70.0	20
	300	190.0	
[Ru(<i>S,S</i> -eddp)Cl ₂] ⁻	464	69.4	This work
	307	232.4	

The electronic absorption spectra of the ruthenium(III) complexes polyaminopolycarboxylic chelating agents contain bands that in most cases can be interpreted as arising from one or more of the following types of transitions: d–d, interligand, metal to ligand charge transfer, ligand to metal charge transfer and ligand field. The electronic spectrum of an aqueous solution of the prepared *s-cis*-K[Ru(*S,S*-eddp)Cl₂] \cdot 3H₂O complex shows bands at 307 nm ($\epsilon = 69.4$ m² mol⁻¹) and 464 nm ($\epsilon = 232.4$ m² mol⁻¹). The registered absorptions may be attributed to the ligand to metal charge transfer band ($\pi_{\text{Cl}} \rightarrow \pi_{\text{Ru}}^*$) and the d–d transition, respectively.

The two symmetrical absorption bands suggest that the isolated [Ru(*S,S*-eddp)Cl₂]⁻ complex has pseudo-octahedral symmetry (Table I). Based on a comparison of the positions of its absorption band maxima and the molar absorbances, it can be concluded that the isolated K[Ru(*S,S*-eddp)Cl₂] \cdot 3H₂O complex has *s-cis* geometry (Fig. 1).

Infrared spectrum

The isolated complex shows a rather broad absorption band near 1600 cm⁻¹ (a strong band at 1580 cm⁻¹ and a shoulder at about 1630 cm⁻¹) of the asymmetric stretching frequencies of the coordinated carboxylate groups of the *S,S*-

-eddp ligand. The lack of absorption between 1700–1750 cm^{-1} indicates that the carboxyl groups of *S,S*-eddp are coordinated to the central Ru(III) ion and are not present as free acid groups. The strong asymmetric stretching band of the coordinated carboxylate groups, which is less influenced by the coordination effects, lies in the expected region at 1399 cm^{-1} . The N–H stretching band of the *s-cis*- $\text{K}[\text{Ru}(\text{S,S-eddp})\text{Cl}_2]\cdot 3\text{H}_2\text{O}$ complex appears at 3434 cm^{-1} .

CONCLUSIONS

Based on the electronic absorption and infrared spectra of potassium-dichlorido-(ethylenediamine-*N,N'*-di-*S,S*-2-propionato) ruthenate(III) trihydrate, $\text{K}[\text{Ru}(\text{S,S-eddp})\text{Cl}_2]\cdot 3\text{H}_2\text{O}$, prepared by the direct synthesis from RuCl_3 and *S,S*-eddp in aqueous solution, the *s-cis* geometrical configuration is proposed.

Acknowledgment. This work was supported by Ministry of Science of the Republic Serbia, Project No 142008B. The authors are grateful to Ms. Snežana Trifunović for the elemental analyses.

ИЗВОД

СТЕРЕОСПЕЦИФИЧНИ ЛИГАНДИ И ЊИХОВИ КОМПЛЕКСИ. II. СИНТЕЗА И КАРАКТЕРИЗАЦИЈА *s-cis*- $\text{K}[\text{Ru}(\text{S,S-eddp})\text{Cl}_2]\cdot 3\text{H}_2\text{O}$

ВЕРИЦА В. ГЛОЂОВИЋ И СРЕЂКО Р. ТРИФУНОВИЋ

*Институт за хемију, Природно–математички факултет у Краљевуцу,
Радоја Домановића 12, б. бр. 60, 34000 Краљевац*

У реакцији између рутенијум(III)-хлорида и едда-типа лиганда, етилендиамин-*N,N'*-ди-*S,S*-2-пропионска киселина (*S,S*-еддп) у воденом раствору настао је само један од могућа три геометријска изомера калијум-*s-cis*-дихлорида-(етилендиамин-*N,N'*-ди-*S,S*-2-пропионато) рутенат(III)-трихидрат, *s-cis*- $\text{K}[\text{Ru}(\text{S,S-eddp})\text{Cl}_2]\cdot 3\text{H}_2\text{O}$. Геометрија насталог комплекса је претпостављена на основу електронских апсорпционих и инфрацрвених спектра.

(Примљено 2. августа, ревидирано 10. децембра 2007)

REFERENCES

1. M. J. Clarke, *Coord. Chem. Rev.* **236** (2003) 209
2. K. Akdi, R. A. Vilaplana, S. Kamah, J. A. R. Navaro, J. M. Salas, F. González-Vílchez, *J. Inorg. Biochem.* **90** (2002) 51
3. M. J. Clarke, F. Zhu, D. R. Frasca, *Chem. Rev.* **99** (1999) 2511
4. J. Reedijk, *Proc. Natl. Acad. Sci. USA* **100** (2003) 3611
5. G. Mestroni, E. Alessio, G. Sava, S. Pacor, M. Coluccia, A. Boccarelli, *Metal-Based Drugs* **1** (1994) 41
6. M. Coluccia, G. Sava, F. Loseto, A. Nassi, A. Boccarelli, D. Giordano, E. Alessio G. Mestroni, *Eur. J. Cancer* **29A** (1993) 1873
7. A. Anagnostopoulou, E. Moldreheim, N. Katsaros, E. Sletten, *J. Biol. Inorg. Chem.* **4** (1999) 199
8. S. R. Grgurić-Šipka, R. A. Vilaplana, J. M. Pérez, M. A. Fuertes, C. Alonso, Y. Alvarez, T. J. Sabo, F. González-Vílchez, *J. Inorg. Biochem.* **97** (2003) 215

9. L. Messori, F. González-Vilchez, R. A. Vilaplana, E. Piccioli, E. Alessio, B. K. Keppler, *Metal-Based Drugs* **7** (2000) 335
10. E. Gallori, C. Vettori, E. Alessio, F. González-Vilchez, R. A. Vilaplana, P. Orioli, A. Casini, L. Messori, *Arch. Biochem. Biophys.* **376** (2000) 156
11. *Metal Complexes in Cancer Chemotherapy*, B. K. Keppler, Ed., VCH, Weinheim, 1993
12. S. R. Grgurić-Šipka, R. A. Vilaplana, J. M. Perez, M. A. Fuertes, C. Alonso, Y. Alvarez, T. J. Sabo, F. Gonzales-Vilchez, *J. Inorg. Biochem.* **97** (2003) 215
13. R. A. Vilaplana, M. G. Basallote, C. Ruiz, E. Gutierrez-Puebla, F. González-Vilchez, *J. Chem. Soc. Chem. Commun.* (1991) 100
14. F. González-Vilchez, R. A. Vilaplana, G. Blasco, L. Messori, *J. Inorg. Biochem.* **71** (1998) 45
15. M. Carballo, R. A. Vilaplana, G. Márquez, M. Conde, F. J. Bedoya, F. González-Vilchez, F. Sobrino, *Biochem. J.* **328** (1997) 559
16. P. F. Coleman, J. I. Legg, J. Steele, *Inorg. Chem.* **13** (1974) 2193
17. M. J. Jun, Y. B. Park, S. R. Choi, *Polyhedron* **8** (1989) 1205
18. L. N. Schoenberg, D. W. Cooke, C. F. Liu, *Inorg. Chem.* **7** (1968) 2386
19. T. Matsubara, C. Creutz, *Inorg. Chem.* **18** (1979) 1956
20. N. A. Ezerskaya, T. P. Solovih, O. N. Evstafjeva, L. K. Shubockin, N. K. Belskij, *Zh. Neorg. Khim.* **20** (1975) 1036 (in Russian).



www.shd.org.yu

J. Serb. Chem. Soc. 73 (5) 547–554 (2008)

JSCS–3736

JSCS@tmf.bg.ac.yu • www.shd.org.yu/JSCS

UDC 539.124:534.24:547.235

Original scientific paper

Partitioning of π -electrons in rings of diaza-derivatives of acenes

SONJA STANKOVIĆ[#], JELENA ĐURĐEVIĆ, IVAN GUTMAN^{#*} and
RADMILA MILENTIJEVIĆ

Faculty of Science, University of Kragujevac, P. O. Box 60, 34000 Kragujevac, Serbia

(Received 17 December 2007)

Abstract: A few years ago, a method was proposed for assessing the π -electron content (EC) of rings in heteroatom-containing benzenoid molecules. In this work, the effect of two nitrogen atoms at the opposite sides of a linear benzenoid molecule on the partitioning of its π -electrons was investigated. The results obtained can be explained by means of resonance-theoretical arguments.

Keywords: partitioning of π -electrons in rings; π -electron content of ring; aza-derivatives of acenes; resonance theory.

INTRODUCTION

Recent studies¹ have shown that acenes and their various derivatives can be used as organic semiconductors and are thus of great practical importance for electronics.² This, in particular, was found³ to be the case with aza-derivatives of acenes. In a previous work,⁴ the π -electron properties of monoaza acenes was considered. Here, the studies are extended to diaza species.

In 2004, Randić and Balaban^{5,6} developed a method that makes it enabled the π -electron content of rings of polycyclic conjugated molecules to be assessed. This method was mainly applied to benzenoid and coronoid hydrocarbons.^{5–23} Eventually, the method was extend to heteroatom-containing molecules.^{24–26} The respective expression for the π -electron content of a ring R reads:²⁴

$$EC(R) = 2 \sum_{*} \tilde{P}_{rs}^{HR} + \sum_{**} \tilde{P}_{rs}^{HR} \quad (1)$$

where \tilde{P}_{rs}^{HR} is the modified Ham–Ruedenberg bond order and where \sum_{*} and \sum_{**} indicate, respectively, summation over those bonds rs belonging solely to the ring R , and summation over the bonds rs that are shared by the ring R and another ring. The modified Ham–Ruedenberg bond order is given by:²⁴

$$\tilde{P}_{rs}^{HR} = P_{rs}^{HR} + \frac{A_{rr}}{\delta_r} P_{rr}^{HR} + \frac{A_{ss}}{\delta_s} P_{ss}^{HR} \quad (2)$$

* Corresponding author. E-mail: gutman@kg.ac.yu

Serbian Chemical Society member.

doi: 10.2298/JSC0805547S

where P_{rs}^{HR} is the ordinary Ham–Ruedenberg bond order,²⁷ δ_r and δ_s are, respectively, the degrees²⁸ of the vertices r and s , whereas A_{rr} and A_{ss} are the corresponding diagonal elements of the adjacency matrix.²⁸ In the case of nitrogen-containing conjugated molecules, the following standard HMO parameterization is employed:²⁹

$$A_{rr} = \begin{cases} 0.5 & \text{if the atom in position } r \text{ is nitrogen} \\ 0.0 & \text{if the atom in position } r \text{ is carbon} \end{cases}$$

Recently, rules for the effect of a nitrogen atom on the partitioning of π -electrons in rings of monoaza acenes were established.⁴ The most important of these are the following:

When the nitrogen atom is in position α (see Fig. 1), then the minimal value of the π -electron content is in the ring R_1 to which the nitrogen atom belongs. The π -electron contents of the other rings monotonically increase as their distance from R_1 increases. Therefore, the terminal ring R_h has the maximal EC value.

If the nitrogen atom is in position β (see Fig. 1), then the π -electron content of the ring R_1 is maximal and of its first neighbor minimal. The π -electron contents of the rings R_3, R_4, \dots monotonically increase with the distance from R_1 , becoming maximal at the terminal ring R_h .

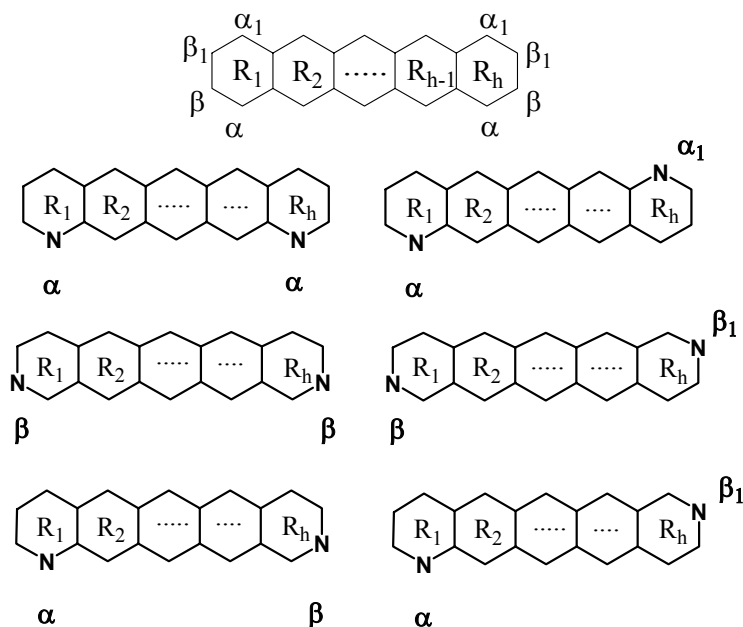


Fig. 1. The diaza-derivatives of acenes and the labeling of the positions of the nitrogen atoms. There are two different positions of the nitrogen atoms (α or α_1 and β or β_1), but there are six diaza-derivatives ($\alpha\alpha$, $\alpha\alpha_1$, $\beta\beta$, $\beta\beta_1$, $\alpha\beta$ and $\alpha\beta_1$).

As seen from the above rules, the effect of a heteroatom located in a terminal ring of an acene extends to the other terminal ring. Bearing this in mind, it seems to be purposeful to investigate the effect of two nitrogen atoms, located at the opposite sides of the acene molecule.

π -ELECTRON CONTENT OF RINGS OF DIAZA-ACENES

In order to best express the effects of heteroatoms on the partitioning of π -electrons in polycyclic aromatic compounds, the difference between the EC value of the heteroatom-containing molecule (h.c.m.) and the EC value of the parent hydrocarbon (p.h.) is used:⁴

$$\Delta EC(R) = EC(R)_{\text{h.c.m.}} - EC(R)_{\text{p.h.}} \quad (3)$$

The general forms of diaza-acenes with nitrogen atoms in the terminal rings, as well as the labeling of their hexagons are shown in Fig. 1. As can be seen, the nitrogen atoms can be in two different positions (α or α_1 and β or β_1). Consequently, there are six different arrangements of two nitrogen atoms ($\alpha\alpha$, $\alpha\alpha_1$, $\beta\beta$, $\beta\beta_1$, $\alpha\beta$ and $\alpha\beta_1$).

The ΔEC values of all rings of the six possible diaza-acenes with h hexagons, $2 \leq h \leq 10$, were calculated. Some of these results (for $h \leq 6$) are collected in Tables I, II, and III.

TABLE I. The ΔEC values of the rings of $\alpha\alpha$ and $\alpha\alpha_1$ diaza-acenes with h hexagons; notation the same as in Fig. 1. Positive (resp. negative) $\Delta EC(R)$ means that the π -electron content of the ring R has increased (resp. decreased) relative to the π -electron content of the same ring in the parent hydrocarbon

h	Position	$\Delta EC(R_1)$	$\Delta EC(R_2)$	$\Delta EC(R_3)$	$\Delta EC(R_4)$	$\Delta EC(R_5)$	$\Delta EC(R_6)$
2	$\alpha\alpha$	0.0	0.0	–	–	–	–
	$\alpha\alpha_1$	0.0	0.0	–	–	–	–
3	$\alpha\alpha$	–0.0146	0.0293	–0.0146	–	–	–
	$\alpha\alpha_1$	–0.0182	0.0363	–0.0182	–	–	–
4	$\alpha\alpha$	–0.0181	0.0181	0.0181	–0.0181	–	–
	$\alpha\alpha_1$	–0.0216	0.0216	0.0216	–0.0216	–	–
5	$\alpha\alpha$	–0.0181	0.0105	0.0152	0.0105	–0.0181	–
	$\alpha\alpha_1$	–0.0211	0.0124	0.0174	0.0124	–0.0211	–
6	$\alpha\alpha$	–0.0166	0.0047	0.0119	0.0119	0.0047	–0.0166
	$\alpha\alpha_1$	–0.0191	0.0059	0.0133	0.0133	0.0059	–0.0191

The results show similar displacements of the π -electrons in the cases $\alpha\alpha$, $\alpha\alpha_1$, as well as in the cases $\beta\beta$, $\beta\beta_1$, and $\alpha\beta$, $\alpha\beta_1$. Therefore, attention was focused on the cases $\alpha\alpha$, $\beta\beta$ and $\alpha\beta$. From the ΔEC values given in Tables I, II, and III, the following conclusions can be reached:

If the nitrogen atoms are in positions α (or α_1), then they cause a decrease of the π -electron content of the rings R_1 and R_h (see Table I).

TABLE II. Same data as in Table I but for $\beta\beta$ and $\beta\beta_1$ diaza-acenes

h	Position	$\Delta EC(R_1)$	$\Delta EC(R_2)$	$\Delta EC(R_3)$	$\Delta EC(R_4)$	$\Delta EC(R_5)$	$\Delta EC(R_6)$
2	$\beta\beta$	0.0	0.0	–	–	–	–
	$\beta\beta_1$	0.0	0.0	–	–	–	–
3	$\beta\beta$	0.0546	–0.1093	0.0546	–	–	–
	$\beta\beta_1$	0.0515	–0.1029	0.0515	–	–	–
4	$\beta\beta$	0.0707	–0.0707	–0.0707	0.0707	–	–
	$\beta\beta_1$	0.0673	–0.0673	–0.0673	0.0673	–	–
5	$\beta\beta$	0.0770	–0.0652	–0.0234	–0.0652	0.0770	–
	$\beta\beta_1$	0.0740	–0.0633	–0.0214	–0.0633	0.0740	–
6	$\beta\beta$	0.0805	–0.0670	–0.0135	–0.0135	–0.0670	0.0805
	$\beta\beta_1$	0.0780	–0.0658	–0.0122	–0.0122	–0.0658	0.0780

TABLE III. Same data as in Table I but for $\alpha\beta$ and $\alpha\beta_1$ diaza-acenes

h	Position	$\Delta EC(R_1)$	$\Delta EC(R_2)$	$\Delta EC(R_3)$	$\Delta EC(R_4)$	$\Delta EC(R_5)$	$\Delta EC(R_6)$
2	$\alpha\beta$	–0.0873	0.0873	–	–	–	–
	$\alpha\beta_1$	–0.0851	0.0851	–	–	–	–
3	$\alpha\beta$	–0.0431	–0.0332	0.0763	–	–	–
	$\alpha\beta_1$	–0.0390	–0.0398	0.0789	–	–	–
4	$\alpha\beta$	–0.0296	0.0024	–0.0480	0.0753	–	–
	$\alpha\beta_1$	–0.0258	–0.0011	–0.0514	0.0783	–	–
5	$\alpha\beta$	–0.0237	0.0064	–0.0020	–0.0573	0.0767	–
	$\alpha\beta_1$	–0.0206	0.0045	–0.0041	–0.0592	0.0795	–
6	$\alpha\beta$	–0.0200	0.0039	0.0072	–0.0062	–0.0639	0.0790
	$\alpha\beta_1$	–0.0174	0.0027	0.0059	–0.0075	–0.0650	0.0814

If the nitrogen atoms are in position α (or α_1), the π -electron content of the other rings monotonically increase towards the center of the molecule. In particular, if h is odd, then the maximal EC value is at the ring $R_{(h+1)/2}$; if h is even, then the two rings $R_{h/2}$ and $R_{h/2+1}$ have greatest π -electron content.

If the nitrogen atoms are in position β (or β_1), then (contrary to the case of α -substitution) the greatest value of the π -electron content is in rings R_1 and R_h .

If the nitrogen atoms are in position β (or β_1), then the minimal ΔEC values are in the neighboring rings (R_2 and R_{h-1}). The π -electron contents of the other rings monotonically increase with distance from the terminal rings (see Table II).

If one nitrogen atom is in position α , and the other in position β (or β_1), then the π -electron contents of all rings are the result of two simultaneously, but in opposite sense acting, effects. Thus, the ring R_1 , containing nitrogen in position α , has the minimal ΔEC value, whereas the ring R_h , containing nitrogen in position β (or β_1), shows the maximal ΔEC value (see Table III).

These regularities are in agreement with the displacements of π -electrons caused by a single heteroatom (nitrogen).^{4,25,26} The main differences are the con-

sequence of the simultaneous effect of two nitrogen atoms. In the subsequent section, it will be shown that these results are in agreement with the (qualitative) predictions of the resonance theory.

RESONANCE-THEORETICAL ANALYSIS

In this section, a resonance-theoretical analysis of the partitioning of π -electrons in the rings of acenes is described. Without loss of generality, only the case $h = 5$ (pentacene) will be considered. We first outline First, the resonance-theoretical approach to the $\beta\beta$ -forms is outlined.

It was shown elsewhere⁴ that only ionic resonance structures need to be taken into account. The most important of these are the ionic structures with minimal charge separation. However, these structures result in the same distribution of π -electrons as in Kekulé structures, *i.e.*, as in the parent hydrocarbon.⁴ Therefore, only the ionic structures with greater charge separation are considered. The relevant ionic structures of $\beta\beta$ diaza-pentacene are depicted in Fig. 2.

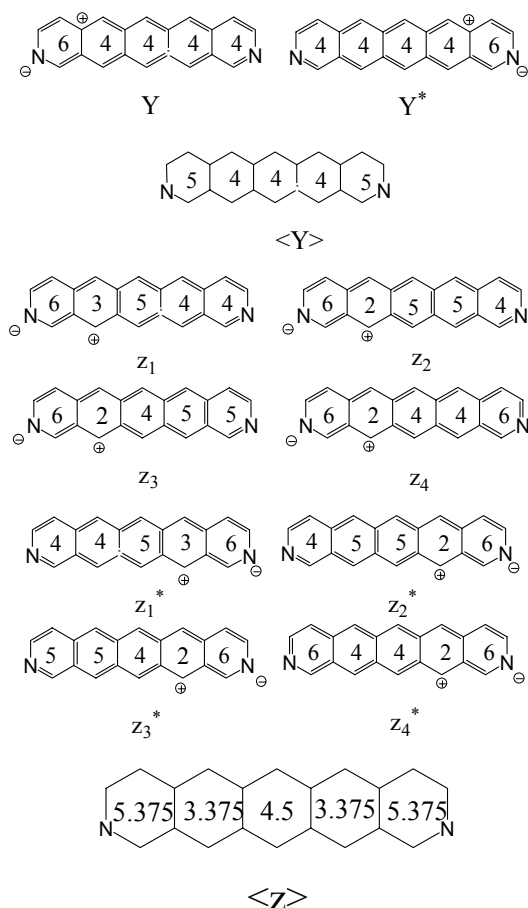


Fig. 2. The considered ionic resonance forms of $\beta\beta$ diaza-pentacene. The numerals inscribed in the rings indicate the number of π -electrons belonging to that ring; for details see text.

The structures Y , Y^* have positive charges in the *para* position to the negatively charged nitrogen atom. The next-significant structures are those with a positive charge at the neighboring ring ($z_1, \dots, z_4, z_1^*, \dots, z_4^*$). These forms are responsible for the differences between the EC values. Thus, by averaging the π -electron contents of rings Y and Y^* (denoted by $\langle Y \rangle$), it can be seen that the terminal rings have the greatest π -electron contents. For the displacement of π -electrons among the internal rings, one has to use resonance forms with still greater charge separation ($z_1, \dots, z_4, z_1^*, \dots, z_4^*$) have to be employed. The average of the π -electron contents of these species (denoted by $\langle Z \rangle$) yields: $EC(R_3) > EC(R_2)$, $EC(R_3) > EC(R_4)$, *i.e.*, $EC(R_2) < EC(R_3) < EC(R_4)$.

As can be seen, the diagrams depicted in Fig. 2 explain in a qualitative manner the results given in Table II.

The analogous resonance forms of $\alpha\alpha$ diaza-pentacene are depicted in Figs. 3 and 4. Their resonance-theoretical analysis proceeds in a similar manner.

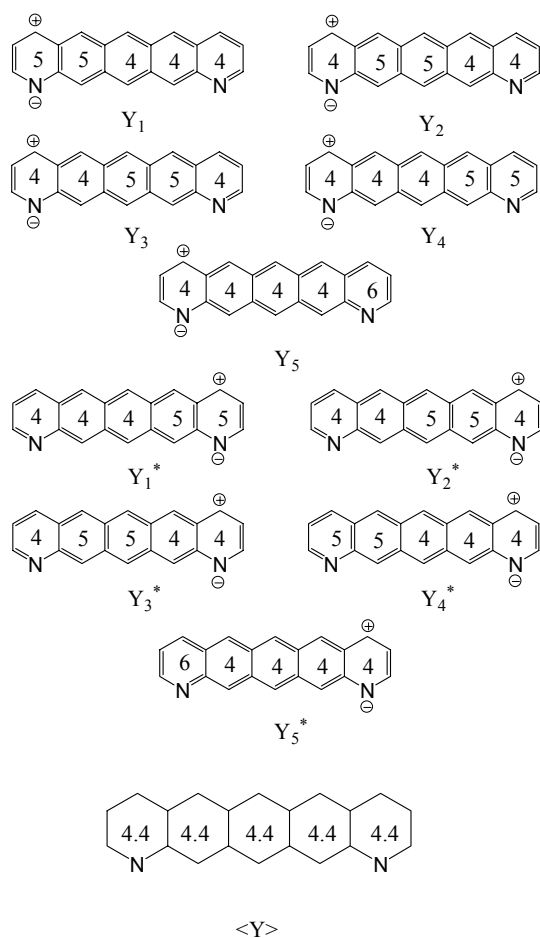


Fig. 3. The Y -type ionic structures of $\alpha\alpha$ diaza-pentacene, analogous to those depicted in Fig. 2.

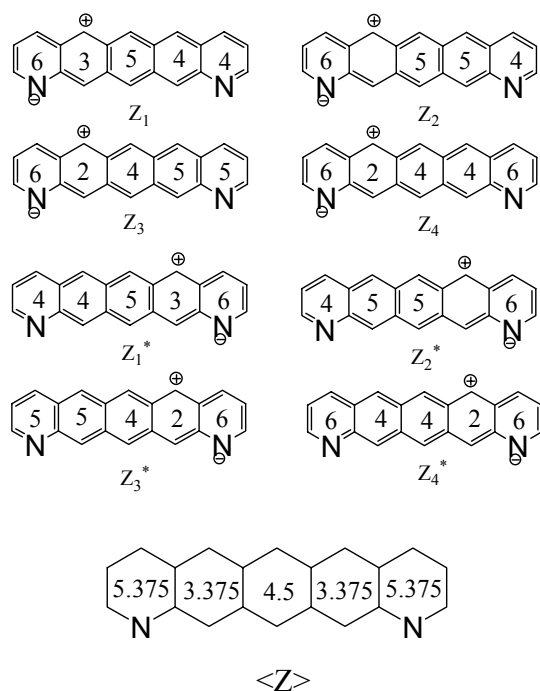


Fig. 4. The Z-type ionic structures of $\alpha\alpha$ diaza-pentacene, analogous to those depicted in Fig. 2.

Equal EC values are arrived at from Y_1, \dots, Y_5^* . However, this implies that the EC values increase relative to the parent hydrocarbon in rings R_1 and R_5 , whereas they decrease in rings R_2 , R_3 and R_4 . By taking into account the Z-type structures, one obtains $EC(R_3) > EC(R_2)$, i.e., $EC(R_3) > EC(R_4)$. In summary, one obtains: $EC(R_1) < EC(R_2) < EC(R_3)$, which is in agreement with the calculated results (cf. Table I).

The same reasoning can be applied also to $\alpha\beta$ -type diaza-acenes, the details of which are omitted.

ИЗВОД

РАСПОДЕЛА π -ЕЛЕКТРОНА ПО ПРСТЕНОВИМА У ДИАЗА-ДЕРИВАТИМА АЦЕНА

СОЊА СТАНКОВИЋ, ЈЕЛЕНА ЂУРЂЕВИЋ, ИВАН ГУТМАН и РАДМИЛА МИЛЕНТИЈЕВИЋ

Природно-математички факултет у Крагујевцу

Недавно је предложена метода за рачунање π -електронског садржаја прстенова бензеноидних молекула који садрже хетероатом. У овом раду проучавана је расподела π -електрона у аценима који садрже два атома азота на супротним крајевима линеарног ланца. Добијени резултати објашњени су помоћу резонанционе теорије.

(Примљено 17. децембра 2007)

REFERENCES

1. J. E. Anthony, *Angew. Chem. Int. Ed.* **46** (2007) 2

2. J. Wu, W. Pisula, K. Müllen, *Chem. Rev.* **102** (2007) 718
3. M. Winkler, K. N. Houk, *J. Am. Chem. Soc.* **129** (2007) 1805
4. A. T. Balaban, B. Furtula, I. Gutman, R. Kovačević, *Polyc. Arom. Comp.* **27** (2007) 51
5. M. Randić, A. T. Balaban, *Polyc. Arom. Comp.* **24** (2004) 173
6. A. T. Balaban, M. Randić, *J. Chem. Inf. Comput. Sci.* **44** (2004) 50
7. I. Gutman, T. Morikawa, S. Narita, *Z. Naturforsch.* **59a** (2004) 295
8. A. T. Balaban, M. Randić, *New J. Chem.* **28** (2004) 800
9. D. Vukičević, M. Randić, A. T. Balaban, *J. Math. Chem.* **36** (2004) 271
10. I. Gutman, *Indian J. Chem.* **43A** (2004) 1615
11. I. Gutman, Ž. Tomović, K. Müllen, J. P. Rabe, *Chem. Phys. Lett.* **397** (2004) 412
12. A. T. Balaban, M. Randić, *J. Math. Chem.* **37** (2005) 443
13. I. Gutman, S. Gojak, N. Turković, B. Furtula, *MATCH Commun. Math. Comput. Chem.* **53** (2005) 139
14. I. Gutman, B. Furtula, N. Turković, *Polyc. Arom. Comp.* **25** (2005) 87
15. I. Gutman, M. Randić, A. T. Balaban, B. Furtula, V. Vučković, *Polyc. Arom. Comp.* **25** (2005) 211
16. I. Gutman, G. Stojanović, Z. Bošković, N. Radulović, P. Rašić, *Polyc. Arom. Comp.* **25** (2005) 345
17. I. Gutman, B. Furtula, S. Jeremić, N. Turković, *J. Serb. Chem. Soc.* **70** (2005) 1199
18. I. Gutman, A. T. Balaban, M. Randić, C. Kiss-Toth, *Z. Naturforsch.* **60a** (2005) 171
19. I. Gutman, N. Turković, *Monatsh. Chem.* **136** (2005) 713
20. B. Furtula, I. Gutman, N. Turković, *Indian. J. Chem.* **44A** (2005) 13
21. I. Gutman, S. Milosavljević, B. Furtula, N. Cmiljanović, *Indian. J. Chem.* **44a** (2005) 13
22. I. Gutman, N. Turković, B. Furtula, *Indian. J. Chem* **45** (2006) 1601
23. I. Gutman, S. Gojak, N. Radulović, B. Furtula, *Monatsh. Chem.* **137** (2006) 277
24. I. Gutman, *MATCH Commun. Math. Comput. Chem.* **56** (2006) 345
25. I. Gutman, B. Furtula, R. Kovačević, *J. Serb. Chem. Soc.* **72** (2007) 655
26. A. T. Balaban, I. Gutman, S. Stanković, *Polycyclic Aromat. Compd.* **28** (2008) 85
27. N. S. Ham, K. Ruedenberg, *J. Chem. Phys.* **29** (1958) 1215
28. I. Gutman, O. E. Polansky, *Mathematical Concepts in Organic Chemistry*, Springer-Verlag, Berlin, 1986
29. A. Streitwieser, *Molecular Orbital Theory for Organic Chemists*, Wiley, New York, 1961.



www.shd.org.yu

J. Serb. Chem. Soc. 73 (5) 555–560 (2008)
JSCS–3737

Journal of
the Serbian
Chemical Society



JSCS@tmf.bg.ac.yu • www.shd.org.yu/JSCS

UDC 546.289'161+546.28'161:531.64:517.956.2

Original scientific paper

Franck–Condon factors and r-centroids for the diatomic fluorides of germanium and silicon

S. KANAGAPRABHA, R. RAJESWARA PALANICHAMY* and V. SATHIYABAMA

Department of Physics, N. M. S. S. V. N College, Madurai – 625 019, Tamilnadu, India

(Received 7 November 2006, revised 9 February 2007)

Abstract: A suitable potential energy function was found by analysing the potential functions proposed by Morse, Mohammad and Rafi *et al.* for the $A^2\Sigma^+ - X^2\Pi_{3/2}$ and $B^2\Sigma^+ - X^2\Pi_{3/2}$ band systems of GeF and the $^1\Sigma - ^1\Pi$ band system of SiF. It was found that the potential proposed by Rafi *et al.* is in close agreement with the Rydberg–Klein–Rees (R–K–R) potential. Using this potential, the wave functions were evaluated by the Wentzel–Kramer–Brillouin (W–K–B) method. The Franck–Condon factors and r-centroids were computed by a numerical integration technique. The results are compared with available theoretical values. The intensities of the various bands were investigated.

Keywords: Franck–Condon factor; r-centroid; potential function; GeF and SiF.

INTRODUCTION

Spectroscopic research on the intensities in molecular spectra has two main components: (a) experimental intensity measurements in emission or absorption and (b) theoretical studies (including *ab initio* quantum mechanical calculation) of molecular potentials, eigenfunctions and the quantities derived there from, such as Franck–Condon (F–C) factors and r-centroids.¹ Detailed knowledge of F–C factors and r-centroids is essential for the calculation of many important data, such as radiative life times, vibrational temperatures of the sources and relative band strengths. The intensity distribution of various bands in any band system is mainly governed by the F–C factors. Singh² analysed the vibrational translation probabilities and r-centroids for diatomic fluorides of Si and Ge. Previously, the F–C factors and r-centroids were evaluated with the wave function computed using the Wentzel–Kramer–Brillouin (W–K–B) method for the SiH molecule.³ Nagarajan *et al.*⁴ computed the F–C factors and r-centroids for the SiF molecule. In the previous works,^{2,4} the Morse potential⁵ was used to find the wave function but not all of them obey the Morse potential.⁵ In this work, a suitable potential energy function was found by analysing the potential functions proposed by

* Corresponding author. E-mail: rrpcaspd2003@yahoo.com

doi: 10.2298/JSC0805555K

Morse,⁵ Mohammad⁶ and Rafi *et al.*⁷ for the $A^2\Sigma^+-X^2\Pi_{3/2}$ and $B^2\Sigma^+-X^2\Pi_{3/2}$ band systems of GeF and the $^1\Sigma-^1\Pi$ band system of SiF. It was found that the potential proposed by Rafi *et al.*⁷ is in close agreement with the Rydberg–Klein–Rees potential.^{8–10} Hence, this problem was revisited with the Rafi *et al.*⁷ potential and the wave functions were evaluated using the W–K–B method. The F–C factors and r-centroids were computed by numerical integration techniques.

F–C factors and r-centroids

The intensity of each individual transition between vibrational levels for an allowed electronic transition is governed by F–C factors. The intensity of a v', v'' transition in emission is given by:

$$I_{v',v''} = (164/3h^4c^3)E_{v',v''}^4 \left[\int_0^\infty \Psi_1(v') R_e(r) \Psi_2(v'') dr \right]^2 \quad (1)$$

where c is the velocity of light, $E_{v',v''}$ is the energy difference and R_e is the electronic transition moment. When R_e varies only slowly with r , R_e may be replaced by an average value, $R_{e,av}$. The quantity in the square brackets of Eq. (1) can then be written as:

$$R_{v',v''} = R_e \int_0^\infty \Psi_1(v') \Psi_2(v'') dr \quad (2)$$

Equation (2) defines the so-called vibrational transition moment. The integral in the bracket in Eq. (2) is called the overlap integral and its square is known as the F–C factor. Thus, the F–C factor can be written as:

$$q_{v',v''} = \left[\int_0^\infty \Psi_1(v') \Psi_2(v'') dr \right]^2 \quad (3)$$

where $\Psi_1(v')$ and $\Psi_2(v'')$ are the wave functions corresponding to the vibrational states v' and v'' , respectively.

The r-centroid is a unique value of internuclear separation, which may be associated with a $v \rightarrow v''$ band and is defined as:

$$r_{v',v''} = \frac{\int r \Psi(v') \Psi(v'') dr}{\int \Psi(v') \Psi(v'') dr} \quad (4)$$

RESULTS AND DISCUSSION

The molecular constants for the $A^2\Sigma^+-X^2\Pi_{3/2}$ and $B^2\Sigma^+-X^2\Pi_{3/2}$ band systems of GeF and the $^1\Sigma-^1\Pi$ band system of SiF are given in Table I. The wave functions were obtained by the W–K–B method following the procedure of Wu.¹¹ Then, the F–C factors for the $A^2\Sigma^+-X^2\Pi_{3/2}$ and $B^2\Sigma^+-X^2\Pi_{3/2}$ band systems of GeF were determined by the numerical integration technique and the

values are given in Table II and Table III. For comparison, the F-C factors calculated by Singh² are also given in parentheses. From Table II, it can be seen that the (0-2) band is the most intense one of the $A^2\Sigma^+-X^2\Pi_{3/2}$ band system, although the intensities of the other bands (2-2), (1-0) and (0-1) are also comparable with that of the (0-2) band. The results are in close agreement with the values computed by Singh² for the (0,1) and (0,3) bands. For all the other bands, there is a small deviation. This is because in this work the Rafi *et al.*⁷ potential function was employed, whereas Singh² used the Morse potential function for computation of the wave function. From Table III, it can be seen that the (0-0) band is the most intense of the $A^2\Sigma^+-X^2\Pi_{3/2}$ band system. The intensities of the other bands (3-2), (1-0), (1-3) and (4-2) are comparatively intense. The F-C factors computed for $^1\Sigma-^1\Pi$ band system of SiF molecule are given in Table IV, together with the values calculated by Nagarajan *et al.*⁴ It can be seen from Table IV that the (0-0) band is the most intense one, followed by the bands (1-0), (1-1), (2-1) and (3-2) bands, which are also intense.

TABLE I. Molecular constants of GeF and SiF molecules

Molecules	States	Molecular constants						
		$\omega_e / \text{cm}^{-1}$	D_e / cm^{-1}	$R_e / \text{\AA}$	B_e / cm^{-1}	$\alpha_e / \text{cm}^{-1}$	$\mu / 10^{-23} \text{ g}$	$\omega_e x_e / \text{cm}^{-1}$
GeF	$X^2\Pi_{3/2}$	667.33	35343.6	1.7443	0.36659	0.00266	2.519938	3.15
	$A^2\Sigma^+$	413.03	37943.46	1.8659	0.32035	0.00299	2.519938	1.124
	$B^2\Sigma^+$	796.99	43951.91	1.6817	0.39440	0.00255	2.519938	3.613
SiF	$^1\Sigma$	1011.20	53256.53	1.5500	0.62200	0.00041	1.837054	4.8
	$^1\Pi$	856.70	39039.09	1.6030	0.57950	0.00043	1.837054	4.7

TABLE II. Franck-Condon factors for the $A^2\Sigma^+-X^2\Pi_{3/2}$ band system of GeF

v'/v''	0	1	2	3	4	5
0	0.1214 (0.182)	0.2407 (0.258)	0.2978 (0.2275)	0.1413 (0.1444)	0.0394	0.0052
1	0.2643 (0.334)	0.0484 (0.108)	0.0049 (0.0155)	0.0566 (0.069)	0.1120	0.1606
2	0.1804 (0.252)	0.0839 (0.0175)	0.2681 (0.162)	0.0458 (0.098)	0.0002	0.0449
3	0.0153 (0.180)	0.1579 (0.128)	0.0660 (0.0385)	0.0349 (0.034)	0.0736	0.1960
4	0.0504	0.0970	0.0142	0.0375	0.0156	0.0089
5	0.0729	0.0434	0.3411	0.0001	0.0242	0.0307

For $A^2\Sigma^+-X^2\Pi_{3/2}$ and $B^2\Sigma^+-X^2\Pi_{3/2}$ band systems of GeF, the r-centroids were computed using the wave function computed by the W-K-B method. The evaluated values of the r-centroids are given in Tables V and VI. The r-centroid values calculated by Singh² are also given in parentheses for comparison. From Table V, it can be seen that the r-centroid value is high for the (4-4) band. The values for the other bands (0-4), (0-5), (1-4) and (1-5) are comparable with that

of the (4–4) band. From Table VI, it can be seen that the r-centroid value is high for the (3–1) and (5–3) bands. For the ${}^1\Sigma-{}^1\Pi$ band system of SiF, the computed r-centroid values are given in Table VII. For comparison, the r-centroids calculated by Nagarajan *et al.*⁴ are also given in parentheses. From Table VII, it can be seen that the r-centroid value for the (4–0) band has a higher value compared to the other bands. It is found that the values calculated in this study are in close agreement with those computed by Singh² and Nagarajan *et al.*,⁴ for some bands, while there are small deviations for some other bands.

TABLE III. Franck–Condon factors for the $B^2\Sigma^+-X^2\Pi_{3/2}$ band system of the GeF molecule

v'/v''	0	1	2	3	4	5
0	0.4872 (0.512)	0.0493 (0.333)	0.1915 (0.1175)	0.0468 (0.030)	0.0141 (0.005)	0.0046 (0.020)
1	0.3639 (0.3485)	0.0041 (0.0535)	0.2523 (0.2805)	0.2245 (0.2065)	0.01378 (0.0168)	0.0551 (0.002)
2	0.0955 (0.1135)	0.0498 (0.3142)	0.0035 (0.0095)	0.0793 (0.1375)	0.1768 (0.1605)	0.1560 (0.4495)
3	0.0206 (0.0235)	0.1112 (0.215)	0.0432 (0.1735)	0.0015 (0.0858)	0.1095 (0.046)	0.1118 (0.0355)
4	0.0085 (0.0017)	0.1416 (0.1155)	0.2162 (0.211)	0.0396 (0.0675)	0.0819 (0.523)	0.0004 (0.0015)
5	0.0002 (0.0024)	0.0725 (0.0015)	0.1562 (0.1365)	0.1805 (0.105)	0.0063 (0.002)	0.0102

TABLE IV. Franck–Condon factors for the ${}^1\Sigma-{}^1\Pi$ band system of SiF molecule

v'/v''	0	1	2	3	4	5
0	0.6625 (0.602)	0.1619 (0.297)	0.0809 (0.082)	0.0265 (0.017)	0.0030	0.6625 (0.602)
1	0.3211 (0.314)	0.3084 (0.145)	0.2002 (0.316)	0.1663 (0.163)	0.0932	0.3211 (0.314)
2	0.1005 (0.074)	0.3659 (0.363)	0.0676 (0.007)	0.1435 (0.228)	0.1776	0.1005 (0.074)
3	0.0185 (0.010)	0.1351 (0.160)	0.3228 (0.293)	0.0027 (0.016)	0.0912	0.0185 (0.010)
4	0.0006 (0.000)	0.0780 (0.032)	0.2077 (0.228)	0.1806 (0.188)	0.0038	0.0006 (0.000)
5	0.6625 (0.602)	0.1619 (0.297)	0.0809 (0.082)	0.0265 (0.017)	0.0030	0.6625 (0.602)

TABLE V. r-Centroids for the $A^2\Sigma^+-X^2\Pi_{3/2}$ band system of the GeF molecule

v'/v''	0	1	2	3	4	5
0	1.8130 (1.802)	1.8460 (1.8415)	1.8710 (1.877)	1.9173 (1.910)	1.9733	1.9914
1	1.7808 (1.7745)	1.8347 (1.8175)	1.7660 (1.855)	1.9031 (1.890)	1.9503	1.9591
2	1.7401 (1.743)	1.8341 (1.793)	1.8299 (1.833)	1.9396 (1.869)	1.6953	1.9227

TABLE V. Continued

v'/v''	0	1	2	3	4	5
3	1.5826 (1.702)	1.8153 (1.764)	1.8500 (1.8085)	1.7977 (1.847)	1.9844	1.9393
4	1.8512	1.8086	1.6501	1.8889	2.0015	1.6268
5	1.7561	1.8705	1.7822	0.9156	1.9008	2.0520

TABLE VI. r-Centroids for $B^2\Sigma^+-X^2\Pi_{3/2}$ band system of the GeF molecule

v'/v''	0	1	2	3	4	5
0	1.718 (1.716)	1.680 (1.672)	1.645 (1.627)	1.593 (1.5795)	1.541 (1.5265)	1.537 (1.4585)
1	1.767 (1.7675)	1.747 (1.7245)	1.681 (1.681)	1.655 (1.637)	1.621 (1.591)	1.590 (1.5405)
2	1.832 (1.8185)	1.8011 (1.7755)	1.769 (1.733)	1.676 (1.690)	1.637 (1.647)	1.614 (1.602)
3	1.787 (1.870)	1.872 (1.826)	1.791 (1.7835)	1.459 (1.7415)	1.697 (1.6995)	1.612 (1.657)
4	1.832 (1.922)	1.845 (1.8775)	1.853 (1.834)	1.811 (1.792)	1.766 (1.750)	1.641 (1.7085)
5	1.455 (1.9755)	1.865 (1.929)	1.856 (1.8845)	1.873 (1.8415)	1.802 (1.7995)	1.773 (1.7585)

TABLE VII. r-Centroids for the $^1\Sigma-^1\Pi$ band system of the SiF molecule

v'/v''	0	1	2	3	4
0	1.57812 (1.576)	1.66833 (1.523)	1.68932 (1.472)	1.70321 (1.420)	1.77614
1	1.52432 (1.637)	1.57137 (1.585)	1.68216 (1.532)	1.69184 (1.481)	1.68393
2	1.47979 (1.679)	1.51988 (1.646)	1.54269 (1.597)	1.70369 (1.541)	1.71522
3	1.42256 (1.762)	1.45379 (1.706)	1.52266 (1.650)	1.27250 (1.599)	1.71479
4	2.06379 (1.833)	1.45631 (1.771)	1.46030 (1.715)	1.51068 (1.665)	1.92671

CONCLUSIONS

A suitable potential energy function was fitted for the $A^2\Sigma^+-X^2\Pi_{3/2}$ and $B^2\Sigma^+-X^2\Pi_{3/2}$ band systems of GeF and the $^1\Sigma-^1\Pi$ band system of SiF and the Franck–Condon factors and r-centroids values were evaluated. It was found that, for the $^1\Sigma-^1\Pi$ band system of GeF and for the $^1\Sigma-^1\Pi$ band system of SiF, the (0,0) band is the most intense. However, for the $A^2\Sigma^+-X^2\Pi_{3/2}$ band system of GeF, the (0,2) band is the most intensive. The obtained results are compared with the values computed by Singh² and Nagarajan *et al.*⁴ It is found that the calculated values are in close agreement with them only for a few bands. For all the other bands, there is a deviation. This may be because different potential functions were employed for the computation and to the different methods adopted for the computation.

Acknowledgement. The authors are indebted to the college management for their constant encouragement.

ИЗВОД

ФРАНК–КОНДОНОВИ ФАКТОРИ И Γ -ЦЕНТРОИДИ ЗА ДВОАТОМСКЕ
ФЛУОРИДЕ ГЕРМАНИЈУМА И СИЛИЦИЈУМА

S. KANAGAPRABHA, R. RAJESWARA PALANICHAMY и V. SATHIYABAMA

Department of Physics, N. M. S. S. V. N College, Madurai – 625 019, Tamilnadu, India

Анализом функција потенцијалне енергије које су предложили Morse, Mohammad и Rafi са сарадницима, нађене су погодне функције за $A^2\Sigma^+-X^2\Pi_{3/2}$ и $B^2\Sigma^+-X^2\Pi_{3/2}$ системе трака GeF и $^1\Sigma^-1\Pi$ систем SiF. Установљено је да је потенцијал који је предложио Rafi са сарадницима у доброј сагласности са Rydberg–Klein–Rees потенцијалом. Користећи овај потенцијал израчунате су таласне функције помоћу Wentzel–Kramer–Brillouin методе. Франк–Кондонови фактори и Γ -центриди су израчунати нумеричком интеграцијом. Резултати су упоређени са доступним теоријским вредностима. Испитивани су интензитети различитих трака.

(Примљено 7. новембра 2006, ревидирано 9. фебруара 2007)

REFERENCES

1. M. Singh, J. Chaturvedi, *Astrophys. Space Sci.* **1** (1987) 135
2. J. Singh, *Ind. J. Pure App. Phys.* **13** (1974) 204
3. R. Rajeswarapalanichamy, R. Veluchamy, *Ind. J. Pure App. Phys.* **29** (1991) 274
4. K. Nagarajan, M. Fernandez Gomez, J. J. Lopez Gonzalez, N. Rajamanickam, *J. Astron Astrophys. Suppl. Sep.* **129** (1998) 157
5. P. M. Morse, *Phys. Rev.* **34** (1929) 57
6. S. N. Mohammad, *Ind. J. Pure Appl. Phys.* **23** (1985) 188
7. M. Rafi, A. Bakry, N. Al-Senanj, Fayyazuddin, *Ind. J. Phys.* **74B** (2000) 485
8. R. Rydberg, *Z. Phys.* **73** (1931) 376
9. O. Klein, *Z. Phys.* **76** (1932) 221
10. A. L. G. Rees, *Proc. Roy. Soc. London* **59** (1947) 998
11. W. T. You, *Proc. Phys. Soc.* **65A** (1952) 63.



www.shd.org.yu

J. Serb. Chem. Soc. 73 (5) 561–568 (2008)

JSCS–3738

Journal of
the Serbian
Chemical Society



JSCS@tmf.bg.ac.yu • www.shd.org.yu/JSCS

UDC 778.38+77.035:546.62+546.131–71

Original scientific paper

Investigation of the pitting of aluminum induced by chloride ions by holographic microphotography

LIANG LI¹, CHAO WANG^{1,3*}, SHENHAO CHEN^{2,3},
XIANMIN HOU² and XUEGENG YANG²

¹Department of Chemistry, Xuzhou Normal University, Xuzhou 221009, ²Department of Chemistry, Shandong University, Jinan 250100 and ³State Key Laboratory for Corrosion and Protection, Shenyang 110016, P. R. China

(Received 29 October 2007, revised 7 January 2008)

Abstract: Holographic microphotography was used to investigate the dynamic processes of pitting during anodic dissolution of aluminum in a solution containing chloride ions. The induction and the follow-up propagation processes of the pitting were observed in real-time. A simple model of the propagating process of the pitting was deduced from the result of the holograms of the Al/electrolyte interface. The results prove that holographic microphotography is a useful tool to study the dynamic processes of pitting.

Keywords: holography; pitting; aluminum; chloride ions.

INTRODUCTION

Passive films are easily formed on the surfaces of Al and its alloys in open air and solutions without aggressive ions. However, aluminum and its alloys are much more susceptible to pitting than other metals and a great variety of anions can bring about pitting, such as Cl^- , Br^- , *etc.*¹ The study of pitting corrosion is of particular interest and importance in many scientific and technological applications. Many techniques, such as radiotracer techniques,^{2,3} adsorption from solution onto powders,⁴ X-ray photoelectron spectroscopy (XPS),^{5–8} X-ray absorption spectroscopy (XAS),^{6,7} and Auger spectroscopy⁵ are used to investigate the pitting of Al and Al-alloys caused by chloride ions. Various theories on pitting corrosion have been formulated. It was proposed that the first step in the pitting process is the adsorption of chloride onto the oxide-covered surface due to attractive forces, mainly coulombic ones, and the induction of the adsorbent by the approaching ion.⁹ In neutral solutions, the oxide film on aluminum has a positive surface charge,¹⁰ and the adsorption of chloride ions is most likely favored on a positively charged oxide surface, as ion–ion forces are attractive in nature. This

* Corresponding author. E-mail: wangc@xznu.edu.cn

doi: 10.2298/JSC0805561L

adsorption process is further enhanced under an anodic potential. According to the point defect model (PDM) proposed by Macdonald *et al.*,¹¹ defects exist in the oxide film. The breakdown of the passivity of the Al electrode is caused by the adsorption of the chloride ions into the surface oxygen vacancies. There are still many problems concerning the pitting of Al and Al-alloys (such as deterministic factors in pit initiation), which need to be studied further.¹² Opinions differ on how the pitting is initially induced with the presence of aggressive ions and how the pits propagate. Answers to the above unsettled questions can cast light on the mechanism of the pitting. To observe *in-situ* the initiation and the propagation processes of pitting, new experimental methods are required.

Based on the principles of holographic interferometry techniques for measuring microsurface dissolution, Habib *et al.*¹³ developed a mathematical model and an optical corrosion-meter¹⁴ to characterize the electrochemical and mechanochemical properties of metallic materials, such as localized corrosion of stainless steel,¹⁵ and the anodic dissolution behavior of carbon steel in seawater, with and without inhibitor.¹⁶ It was proposed that holographs have many potential applications in the field of electrochemistry, which are yet to be explored.

Holographic microphotography was employed to study the dynamic processes during the electrodisolution of iron in sulfuric acid solutions.¹⁷⁻¹⁹ Recently, digital holography was used to study the anodic dissolution processes of an iron electrode.^{20,21}

In this study, holography was employed to observe *in situ* how the pitting is initially induced by chloride ions and how the pits propagate on the surface of an aluminum electrode.

EXPERIMENTAL

A three-electrode system was used. The working electrode, 1.8 mm×1.0 mm, prepared from aluminum of industrial purity (0.031 % Mn, 0.17 % Si, 0.01 % Cu, 0.29 % Fe, 0.05 % Zn) was carefully embedded in resin, and only the end of the Al specimen was exposed to solution. The specimen was polished with # 600 and # 1200 emery papers to a mirror-like surface and then washed with alcohol and double distilled water in an ultrasonic bath before each experiment. The counter electrode was a large platinum sheet. A saturated calomel electrode (SCE) with Luggin capillary tip set at 2 mm from the working electrode surface served as a reference electrode. All potentials reported here are referred to SCE. All electrolytes were prepared from analytical grade reagents and double distilled water. In each run, 50 ml of the tested solution was used. The electrochemical experiments were performed at room temperature with a CHI602A electrochemical station.

The dynamic processes of the electrode/electrolyte interface during the anodic dissolution of the electrode were videotaped synchronically by a Sony digital recorder. The holograms presented here were transferred from the digital videotape with the aid of a computer. The electrochemical cell and the light path are shown in Fig. 1. The working and the counter electrodes were placed horizontally, facing each other. For details of the procedures of holographic microphotography, previous publications can be referred to.¹⁷⁻¹⁹

Before the experiments in which the morphology of Al electrode was observed using a scanning electron microscope (FEI QUANT200-ESEM), the sample was first rinsed with anhydrous ethanol and then with double distilled water.

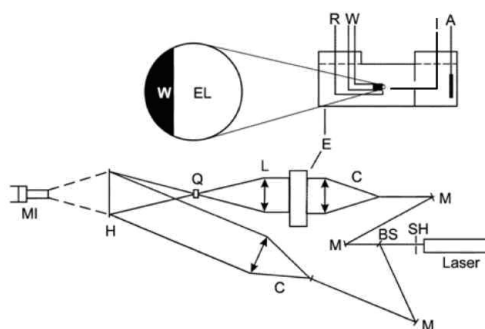


Fig. 1. Schematic diagram of the arrangement for holographic microphotography and the configuration of the electrochemical cell. SH – shutter; BS – beam splitter; M – mirror; C – collimator; L – imaging lens; Q – phase filter; H – holographic plate; MI – microscope; E – electrochemical cell; W – working electrode; R – reference electrode; A – counter electrode; I – chloride ion injection tube.

RESULTS

The $j-t$ curve of the Al electrode in 3.5 % NaCl solution at $-0.55 V_{SCE}$ is shown in Fig 2. The holograms of the electrode/electrolyte interface taken at different points illustrated in Fig. 2 during the initiation and the propagation of pits on the surface of the electrode in 3.5 % NaCl solution are displayed in Fig. 3.

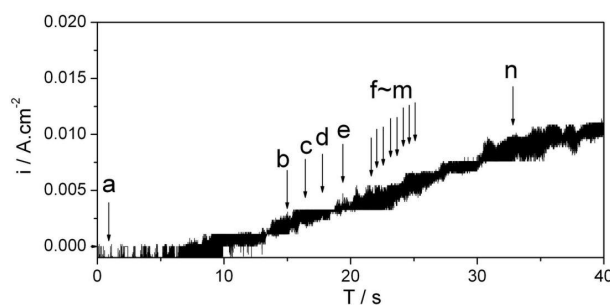


Fig. 2. The $i-t$ curve of the Al electrode in 3.5 % NaCl solution at $-0.55 V_{SCE}$.

Initiation of pitting

Figures 3a–3f correspond to points a to f in Fig. 2. Figure 3a exhibits the interface at the start of the electrodisolution of the Al electrode. The dark and bright fringes are straight and parallel to each other, indicating that there are concentration gradients at the electrode/electrolyte interface. However, after about 15 s of anodic dissolution of the Al electrode, as shown in Fig. 3b, the fringes bend at one point towards the electrode surface and then small trumpet-like fringes appear at other points (Figs. 3c–3e). The appearance of the fringe bend and trumpet-like fringes indicates that the concentration gradient at the electrode/electrolyte interface is no longer uniform. In other word, the concentrations are higher in the areas with trumpet-like fringes than elsewhere, which was caused by the initiation of pitting. About 4 s later than the hologram shown in Fig. 3e, one of the trumpet-like fringes had expanded (Fig. 3f). This indicates that the

pitting had entered the propagating process. These trumpet-like fringes appeared in many areas near the surface of the electrode, indicating that many pits were initiated. However, only some of the pits propagate (Figs. 3b–3e) while the others were repassivated.

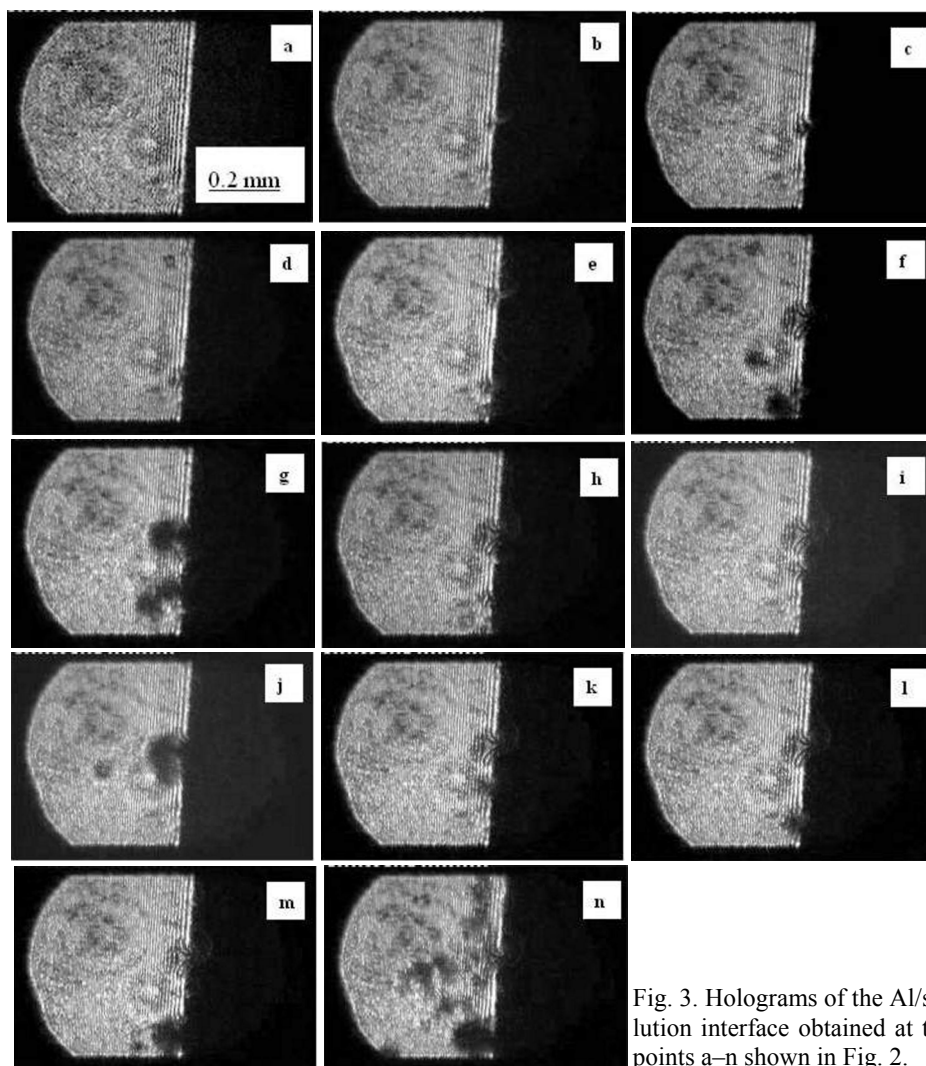


Fig. 3. Holograms of the Al/solution interface obtained at the points a–n shown in Fig. 2.

Propagation of pitting

After the trumpet-like fringes had expanded (Fig 3f), corrosion products emerged in the local area (Fig. 3g). As these products diffused away from the surface of the Al electrode, more trumpet-like fringes appeared, indicating more pits were propagating, as shown in Figs. 3h and 3i. As the products re-emerge

(Fig. 3j), more and more pits propagate (Figs. 3k–3m), until the entire electrode is activated (Fig. 3n). Then the object wave was blocked by the quickly accumulated products, so the fringes could no longer be observed afterwards.

Surface morphology

After the electrochemical experiment (Fig. 2), an ESEM micrograph of the electrode was taken. Figure 4 shows pits with different diameters and depths, indicating that these pits were at different stages of the propagation processes.

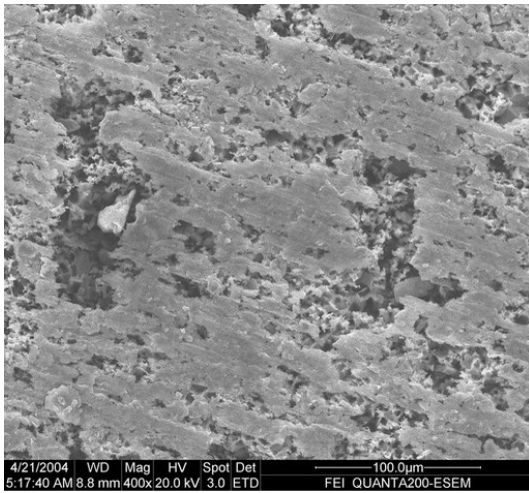


Fig. 4. An ESEM micrograph of the electrode after the experiment shown in Fig. 2.

DISCUSSION

If the dark and bright fringes are straight and parallel to the surface of the electrode, there may be iso-concentration planes parallel to the electrode surface. C1, C2 and C3 in Fig. 5 show that there is a concentration boundary layer near the electrode surface. This concentration boundary layer caused a gradient of the refraction index. The actual imaging interferes with the reconstructed one on the holographic plate and fringes appeared whenever the following condition was satisfied:¹⁷

$$\Delta n = \frac{(2k+1)\lambda}{2d}$$

where Δn is the difference in the refractive index, d is the optical length over which the refractive index was different, λ is wavelength of the light and k is an integer representing the order of the fringe.

When light passes through different concentration planes, different Δn values will be produced. The dark or bright fringe is caused by different values of Δn .

However, if the dark and bright fringes are neither straight nor parallel to the surface of the electrode, there was no iso-concentration planes parallel to the electrode surface. Trumpet-like pits gradually emerged and expanded (from Fig. 3b

to Fig. 3n) along the fringes towards the electrode surface, indicating different periods of pitting. This can be explained as follows: the fringes bend because the concentration in the area is higher than that in other areas at the electrode/electrolyte interface. As the trumpet-like fringes appear (Fig. 3b), pits start to form on the surface of the electrode. The trumpet-like fringes expand with the increase of the concentrations in the local area, indicating that the pits propagate. As more and more pits propagate, the Al electrode is finally activated.

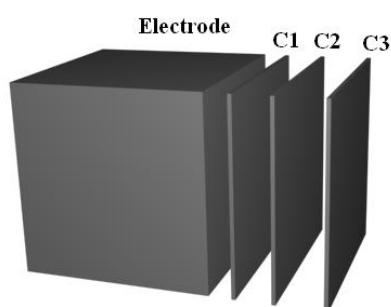


Fig. 5. Illustration of the iso-concentration plane during the general dissolution of the Al electrode.

In order to visualize better how the chloride ions attack the oxide film, a small amount of chloride ions was injected into the vicinity of the electrode surface during the anodic polarization of Al in neutral Na_2SO_4 solution, in which medium an oxide film is readily formed on the electrode surface. The $j-t$ curve of aluminum electrodes in 0.50 M Na_2SO_4 at $-0.50 \text{ V}_{\text{SCE}}$ is shown in Fig. 6. After 0.50 ml 3.5 % NaCl solution had been injected towards the surface of the electrode, the current increased rapidly.

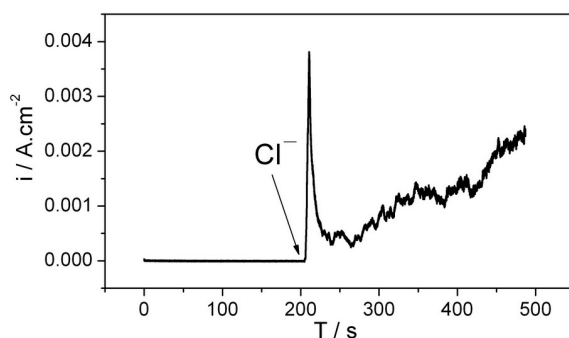


Fig. 6. The $i-t$ curve of the electrode in 0.50 M Na_2SO_4 at $-0.50 \text{ V}_{\text{SCE}}$ after injection of 0.50 ml 3.5 % NaCl solution near the surface of the electrode.

The anodic oxidation of aluminum in near-neutral solutions, *e.g.*, Na_2SO_4 , leads to the growth of thin barrier-type oxide films, normally less than 50 nm thick.²² The first step in the pitting process is the adsorption of chloride on the positively charged surface.^{9,10} The adsorption of the anions leads to the generation of cation vacancies at the film/solution interface.¹¹ The oxide film with defects caused by chloride ions becomes mechanically stressed and damaged by

the pores and flaws, and finally, the passive film on the surface of the electrode is broken. As the pits on the surface of the Al electrode propagate, the current increases (Fig. 6).

According to the obtained results, a simple model of the propagating process of a pit was developed, as shown in Fig. 7. During the propagating process of a pit, both its diameter and depth develop synchronously, which is verified by the fact that there are pits with different diameters and depths shown in Fig. 4, and the trumpet-like fringes (Fig. 3) emerge and expand during different periods of the anodic dissolution of the electrode.



Fig. 7. Schematic diagram of the propagation process of a pit.

CONCLUSIONS

The bending of the fringes and the appearance of trumpet-like ones at the electrode/electrolyte interface indicate the initiation of the pitting, because the concentrations are higher in the pitting areas than elsewhere. The expansion of these trumpet-like fringes indicates propagation of the pitting.

A simple model of the propagation process of a pit has been deduced from the experiment results, and it was found that both the diameter and the depth of a pit develop synchronously.

Acknowledgement. This work was supported by the Natural Science Foundation (No. 05KJB150130 and 06KJB150108) of the Jiangsu Education Committee of China, the Jiangsu Qing-Lan Project of China (QL200616), the Chinese National Science Fund (No.20573069) and Special Funds for the Major State Basic Research Projects (No.2006CB605004). The Project was also sponsored by SRF for ROCS, SEM of the P. R. China.

ИЗВОД

ИСПИТИВАЊЕ ПИТИНГ КОРОЗИЈЕ АЛУМИНИЈУМА ИЗАЗВАНЕ ХЛОРИДНИМ ЈОНИМА КОРИШЋЕЊЕМ ХОЛОГРАФСКЕ МИКРОФОТОГРАФИЈЕ

LIANG LI¹, CHAO WANG^{1,3}, SHENHAO CHEN^{2,3}, XIANMIN HOU² и XUEGENG YANG²

¹Department of Chemistry, Xuzhou Normal University, Xuzhou 221009, ²Department of Chemistry, Shandong University, Jinan 250100 и ³State Key Laboratory for Corrosion and Protection, Shenyang 110016, P. R.China

Холографска микрофотографија је коришћена за испитивање динамичких процеса питинг корозије током анодног растварања алуминијума у раствору хлоридних јона. Почетак и развој питинга праћени су у реалном времену. На основу холограма границе фаза алуминијум/електролит изведен је једноставан модел развоја питинга. Резултати потврђују да се холографска микрофотографија може успешно користити за испитивање динамичких процеса питинга.

(Примљено 29. октобра 2007, ревидирано 7. јануара 2008)

REFERENCES

1. Z. Szklarska-Smialowska, *Pitting Corrosion of Metals*, NACE Press, Houston, TX, 1986, pp. 7, 201
2. J. O. 'M. Bockris, Y. Kang, *J. Solid State Electrochem.* **1** (1997) 17
3. A. Kolics, J. C. Polkinghorne, A. E. Thomas, A. Wieckowski, *Chem. Mater.* **10** (1998) 812
4. D. M. Dražić, S. K. Zečević, R. M. Atanasoski, A. R. Despić, *Electrochim. Acta* **28** (1983) 751
5. L. D. Atanasoska, D. M. Dražić, A. R. Despić, A. Zalar, *J. Electroanal. Chem.* **182** (1985) 179
6. P. M. Natishan, W. E. O'Grady, E. McCafferty, D. E. Ramaker, K. Pandya, A. Russell, *J. Electrochem. Soc.* **146** (1999) 1737
7. S. Yu, W. E. O'Grady, D. E. Ramaker, P. M. Natishan, *J. Electrochem. Soc.* **147** (2000) 2952
8. A. Kolics, A. S. Besing, P. Baradlai, R. Haasch, A. Weickowski, *J. Electrochem. Soc.* **148** (2001) B251
9. J. H. de Boer, in *Advances in Colloid Science*, H. Mark, Vol. III, E. J. W. Verwey, Eds., Interscience Publishers, New York, 1950, p. 1
10. E. McCafferty, *Corros. Sci.* **45** (2003) 1421
11. D. D MacDonal, *Pure Appl. Chem.* **71** (1999) 951
12. Z. Szklarska-Smialowska, *Corros. Sci.* **41** (1999) 1743
13. K. Habib, *Optics and Lasers in Engineering* **18** (1993) 115
14. K. Habib, F. Al-Sabti, H. Al-Mazedi, *Optics and Lasers in Engineering* **27** (1997) 227
15. K. Habib, K. Bouresli, *Electrochim. Acta* **44** (1999) 4635
16. K. Habib, K. Muhana, *Electrochem. Commun.* **4** (2002) 54
17. C. Wang, S. Chen, X. Yu, *Electrochim. Acta* **39** (1994) 577
18. C. Wang, S. Chen, H. Ma, *J. Electrochem. Soc.* **145** (1998) 2214
19. C. Wang, S. Chen, X. Yu, *Electrochim. Acta* **43** (1998) 2225
20. X. Yang, S. Chen, C. Wang, L. Li, *J. Serb. Chem. Soc.* **71** (2006) 67
21. S. Chen, *J. Serb. Chem. Soc.* **71** (2006) 1091
22. K. Shimizu, H. Habazaki, P. Skeldon, G. E. Thompson, G. C. Wood, *Electrochim. Acta* **45** (2000) 1805.



www.shd.org.yu

J. Serb. Chem. Soc. 73 (5) 569–576 (2008)
JSCS–3739

JSCS@tmf.bg.ac.yu • www.shd.org.yu/JSCS

UDC 615.33+615.276+546.723:66.094.3:543.4/.5

Original scientific paper

An indirect atomic absorption spectrometric determination of ciprofloxacin, amoxicillin and diclofenac sodium in pharmaceutical formulations

MAHMOUD MOHAMED ISSA¹, R'AFAT MAHMOUD NEJEM^{1*},
MONZER AL-KHOLY¹, NASER SAID EL-ABADLA²,
RAFIK SOBHI HELLES¹ and AKILA AMIN SALEH³

¹Analytical Chemistry, Department of Chemistry, Alqaqa University, P. O. Box 4051, Gaza,

²Organic Chemistry, Department of Chemistry, Alqaqa University, Gaza, Palestine and

³Analytical Chemistry, Ain Shams University, Cairo, Egypt

(Received 23 May, revised 7 December 2007)

Abstract: A highly sensitive indirect atomic absorption spectrophotometric (AAS) method has been developed for the determination of very low concentrations of ciprofloxacin, amoxicillin and diclofenac sodium. The method is based on the oxidation of these drugs with iron(III). The excess of iron(III) was extracted into diethyl ether and then the iron(II) in the aqueous layer was aspirated into an air–acetylene flame and determined by AAS. The linear concentration ranges were 25–400, 50–500 and 60–600 ng ml⁻¹ for ciprofloxacin, amoxicillin and diclofenac sodium, respectively. The results were statistically compared with the official method using *t*- and *f*-test at *p* < 0.05. There were insignificant interferences from most of the excipients present. The intra- and inter-day assay coefficients of variation were less than 6.1 % and the recoveries ranged from 95 to 103 %. The method was applied for the analysis of these drug substances in their commercial pharmaceutical formulations.

Keywords: ciprofloxacin; amoxicillin; diclofenac sodium; indirect atomic absorption spectrometry.

INTRODUCTION

Ciprofloxacin, chemically 1,4-dihydro-1-cyclopropyl-6-fluoro-4-oxo-7-(1-piperazinyl)-3-quinolinecarboxylic acid (Fig. 1a), is a quinolone antibiotic drug with a broad spectrum of activity against a variety of gram positive and gram-negative bacteria. It is mainly used to treat respiratory infections (*Klebsiella pneumoniae*, *Pseudomonas aeruginosa*, *Haemophilus influenzae*), urinary tract infections, for gastrointestinal surgery, typhoid fever, gonorrhoea b (enterotoxigenic strains of *Escherichia coli*), and septicaemia. Ciprofloxacin acts by inhibiting the

* Corresponding author. E-mail: rafatnejem@alqaqa.edu.ps

doi: 10.2298/JSC0805569I

bacterial enzymes DNA gyrase. Amoxicillin (Fig. 1b) is the only phenolic penicillin used as an antibacterial drug. It is a moderate-spectrum β -lactam antibiotic used to treat bacterial infections caused by susceptible microorganisms. Amoxicillin is susceptible to degradation by β -lactamase-producing bacteria and so may be administered together with clavulanic acid to decrease its susceptibility. Diclofenac sodium is described as the salt of 2-[(2,6-dichlorophenyl)amino]benzene acetic acid (Fig. 1c). It is a non-steroidal anti-inflammatory drug of the cyclo-oxygenase (COX) inhibitor type. It is used for the treatment of rheumatoid arthritis, osteoarthritis, and ankylosing spondylitis, and for a variety of non-rheumatic inflammatory conditions.

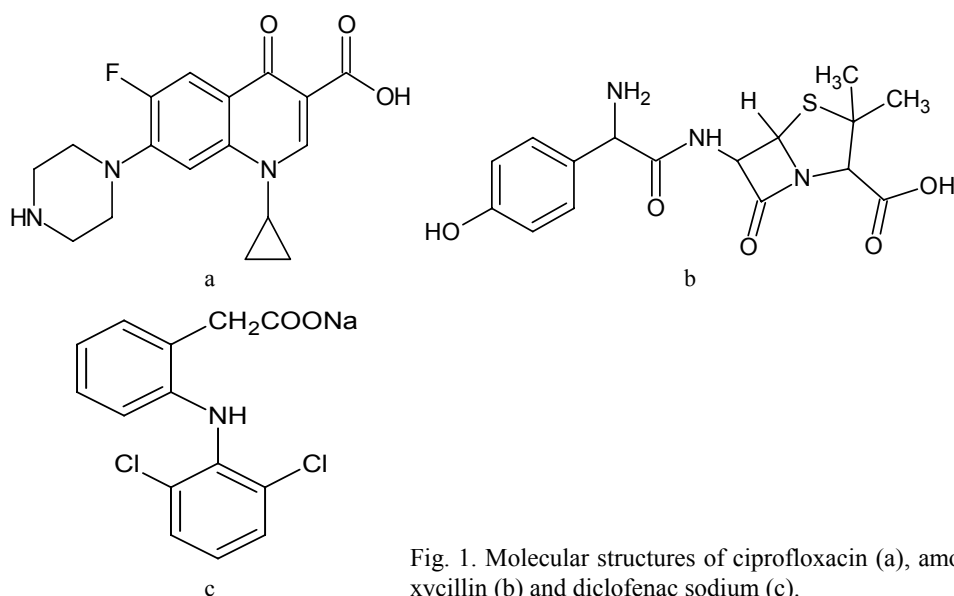


Fig. 1. Molecular structures of ciprofloxacin (a), amoxicillin (b) and diclofenac sodium (c).

Several methods have been reported for the quantitative analysis of the cited drugs, such as spectrophotometry,¹⁻⁴ flow injection,⁵ fluorimetry,⁶ titrimetry,^{7,8} electrophoresis,⁹ microbiology,^{10,11} HPLC^{12,13} and AAS¹⁴⁻¹⁶ methods.

The reduction process of iron(III) to iron(II) by certain drugs, such as paracetamol,¹⁷ diclofenac,¹⁸ salbutamol sulphate,¹⁹ captopril,²⁰ amoxicillin²¹ and ciprofloxacin,²¹ was used as the basis for their quantification based on a colorimetric method.

The present work aims to develop a highly sensitive, simple and rapid atomic absorption spectrometric method for application in quality control analysis. The proposed method is based on the reduction of iron(III) by the investigated drugs (ciprofloxacin, amoxicillin and diclofenac sodium). The excess of iron(III) was extracted into diethyl ether²² and then iron(II) in aqueous layer was determined by AAS. The reaction method is simple since it is a single step process.

EXPERIMENTAL

Apparatus

The atomic absorption measurements were performed using a Perkin-Elmer AAS, Model A Analyst 100 spectrophotometer equipped with an iron hollow-cathode lamp under the following conditions: wavelength, 302.1 nm; lamp current, 30 mA; slit width, 0.2 nm; air/acetylene ratio, 3.5/1.5. A UV/Vis spectrophotometer (Spectro 23 Labomed Inc. USA) with quartz cells was used for all spectrophotometric measurements.

Chemicals and solutions

Analytical grade ciprofloxacin, amoxicillin and diclofenac sodium standards were obtained from the Middle East Pharmaceutical and Cosmetics Laboratories, Palestine. Various pharmaceutical formulations of ciprofloxacin, amoxicillin and diclofenac sodium were obtained commercially. These formulations contained only the investigated drug and were not in combination with other drugs.

Ferric sulphate was purchased from Sigma. Hydrochloric acid (32 %) was supplied by BDH and diethyl ether by Carlo Erba. Solutions of 2.60×10^{-5} M ciprofloxacin ($10 \mu\text{g ml}^{-1}$), 2.38×10^{-5} M amoxicillin ($10 \mu\text{g ml}^{-1}$) and 3.14×10^{-5} M diclofenac sodium ($10 \mu\text{g ml}^{-1}$) were prepared in 0.10 M HCl. A 1.00×10^{-4} M ferric sulphate solution ($40 \mu\text{g ml}^{-1}$) was also prepared in 0.10 M HCl. Standard solutions were prepared by serial dilution. All the employed chemicals were of analytical grade. Deionised water was used for the preparation of all solutions.

Procedure

Six 2.5 ml standard solutions of ciprofloxacin (25–400 ng ml^{-1}), amoxicillin (50–500 ng ml^{-1}) or diclofenac sodium (60–600 ng ml^{-1}) were pipetted into a series of 10 ml volumetric flasks. To each flask, 1.5 ml of 1.0×10^{-5} M ferric sulphate was added. The mixtures were heated using a boiling water bath for 10 min (100 °C). After cooling, 4.0 ml of 12 M HCl was added and the excess iron(III) was extracted with three portions of 10 ml of diethyl ether using a separatory funnel. Then the aqueous layer containing iron(II) was aspirated into an air-acetylene flame. The absorbance of iron(II) was measured at 302.1 nm, and the iron concentration was determined from a previously constructed calibration curve.

RESULTS AND DISCUSSION

It was found that ciprofloxacin, amoxicillin and diclofenac sodium were very weak reducing agents at room temperature. The oxidation of these compounds was non-quantitative, slow and time-consuming. However, on heating at 100 °C using a boiling water bath, the given drugs immediately reduced iron(III) to iron(II) in amounts which corresponded to the concentration of the drugs. The amount of iron(II) was determined by AAS.

Response characteristics

The equations of the calibrations describing the relation between drug concentration and atomic absorbance measurements obtained for ciprofloxacin, amoxicillin and diclofenac sodium are summarized as:

Ciprofloxacin:	$A = 1.510c - 0.007$	($R = 0.9991$)
Amoxicillin:	$A = 1.021c - 0.005$	($R = 0.9986$)
Diclofenac sodium:	$A = 0.9832c - 0.0003$	($R = 0.9998$)

where A and c are the absorbance and concentration (in $\mu\text{g ml}^{-1}$) of the drug, respectively. R is the correlation coefficient. The linear concentration ranges were 25–400 ng ml^{-1} for ciprofloxacin, 50–500 ng ml^{-1} for amoxicillin and 60–600 ng ml^{-1} for diclofenac sodium, based on AAS measurements. The proposed method exhibited a high sensitivity for the three drugs, which are 3.1, 4.4 and 4.5 ng ml^{-1} for ciprofloxacin, amoxicillin and diclofenac sodium, respectively.

Comparison of the proposed and official method using the t -test and f -test ($p < 0.05$) showed the high accuracy and precision of the AAS method. The results obtained by the proposed and official method²³ are summarized in Table I.

TABLE I. Assay of commercial tablet formulations by the AAS method and the official method²³

Drug	Official method ²³			Proposed AAS method		
	Found	t -Test ^a	f -Test ^b	Found	t -Test ^a	f -Test ^b
Ciprofloxacin, 500 mg/tablet	498.3±2.8	1.66	2.6	496.7±3.7	1.32	2.2
Amoxicillin, 500 mg/capsule	499.6±4.2	0.64	2.9	502.4±4.4	1.78	3.1
Diclofenac, 100 mg/tablet	100.2±2.9	1.05	2.3	101.5±3.1	0.78	1.7

^a $t_{\text{tab}}(n=5) = 2.776$; ^b $f_{\text{tab}}(5,5) = 6.390$

The intraday, interday precisions and recoveries were tested (Table II). These data indicate that the method was reproducible within and between days. The mean percentage recovery ranged from 95 to 103 % ($RSD < 6.1$ %).

TABLE II. Intraday and interday assay of ciprofloxacin, amoxicillin and diclofenac sodium

Drug	$c / \mu\text{g ml}^{-1}$	Intraday assay			Interday assay		
		Found $\mu\text{g ml}^{-1}$	Recovery %	RSD %	Found $\mu\text{g ml}^{-1}$	Recovery %	RSD %
Ciprofloxacin	0.10	0.103±0.006	103.0	5.8	0.098±0.005	98.0	5.1
	0.40	0.39±0.01	97.5	2.6	0.406±0.01	101.5	2.2
Amoxicillin	0.20	0.19±0.01	95.0	4.7	0.196±0.01	98.0	5.1
	0.50	0.48±0.02	96.0	4.2	0.490±0.03	98.0	6.1
Diclofenac sodium	0.24	0.235±0.01	97.9	4.7	0.238±0.01	99.2	5.5
	0.60	0.61±0.03	101.7	5.2	0.590±0.03	98.3	5.8

The effects of the presence of common excipients (dextrose, glucose, saccharine sodium, starch, talc and magnesium stearate) were tested (Table III). There were no significant interferences due to the presence of any of these excipients.

Selecting the optimum solvent for an efficient extraction

Several organic solvents were tested to extract Fe(III) in the presence of Fe(II), *i.e.*, 1,2-dichloroethane, chloroform and diethyl ether. To select the suitable solvent, atomic absorbance values caused by the presence of Fe(II) and Fe(III) were measured after extraction with each of the three different organic solvents. The most suitable solvent for the extraction of only Fe(III) in the presence of Fe(II) was diethyl ether. The amount of extracted Fe(III) metal depen-

ded on the concentration of the acid. The maximum extraction value was attained with ≈ 6 M HCl, where approximately 99.99 % of the iron(III) was extracted.

TABLE III. Recovery of ciprofloxacin, amoxycillin and diclofenac sodium in the presence of common excipients ($10 \mu\text{g ml}^{-1}$) using the proposed method

Interfering material	Drug recovery, %		
	Ciprofloxacin	Amoxycillin	Diclofenac sodium
Sucrose	99.9 \pm 1.7	103.0 \pm 1.1	100.4 \pm 2.2
Glucose	101.0 \pm 2.2	101.0 \pm 1.8	101.0 \pm 1.4
Saccharin sodium	98.5 \pm 1.2	99.6 \pm 2.1	102.0 \pm 1.7
Starch	102.0 \pm 1.6	100.2 \pm 1.3	99.20 \pm 2.1
Talc	99.8 \pm 2.0	99.6 \pm 2.1	100.1 \pm 1.7
Magnesium stearate	97.2 \pm 2.8	100.5 \pm 1.7	100.8 \pm 2.2

Effect of temperature

The effect of the temperature was investigated by heating the reaction mixtures of these drugs in a water bath at different temperatures for 10 min. The absorbance was found to increase with increasing reaction temperature. The maximum absorbance was observed at 100 °C, as shown in Fig. 2. The time of heating is important to ensure complete reaction. Different heating time intervals were investigated at a constant temperature (100 °C); 10 min was found to be the optimal interval time to achieve complete reaction, as is shown in Fig. 3.

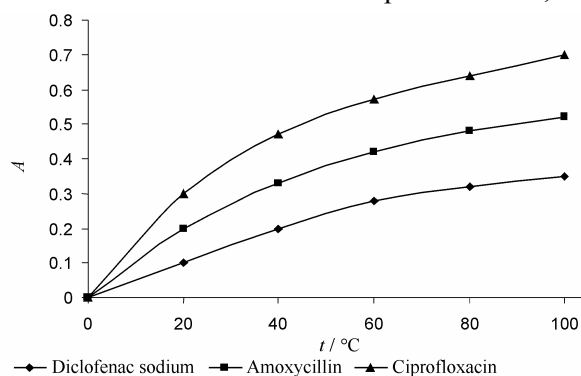


Fig. 2. Effect of temperature on the oxidation reactions of the drugs, ciprofloxacin $0.4 \mu\text{g ml}^{-1}$, amoxycillin $0.5 \mu\text{g ml}^{-1}$, and diclofenac sodium $0.3 \mu\text{g ml}^{-1}$.

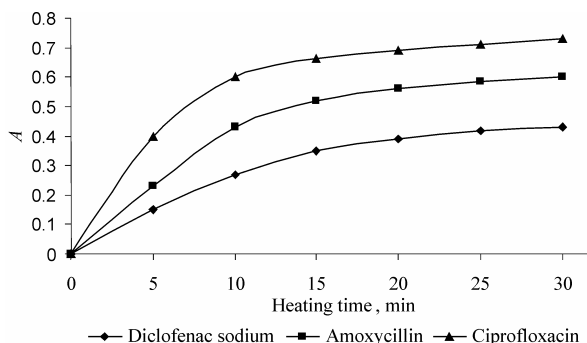


Fig. 3. Effect of heating time on the oxidation reactions of the drugs, ciprofloxacin $0.4 \mu\text{g ml}^{-1}$, amoxycillin $0.5 \mu\text{g ml}^{-1}$, and diclofenac sodium $0.3 \mu\text{g ml}^{-1}$.

Effect of pH

The effect of pH on the response of the oxidation reactions was determined by recording the absorption of ciprofloxacin (400 ng ml^{-1}), amoxicillin (500 ng ml^{-1}) and diclofenac sodium (300 ng ml^{-1}) at different pH values. The absorption vs. pH graph, Fig. 4, showed the absorbance was almost independent of pH in the range 1.0–2.5 for ciprofloxacin, amoxicillin and diclofenac sodium.

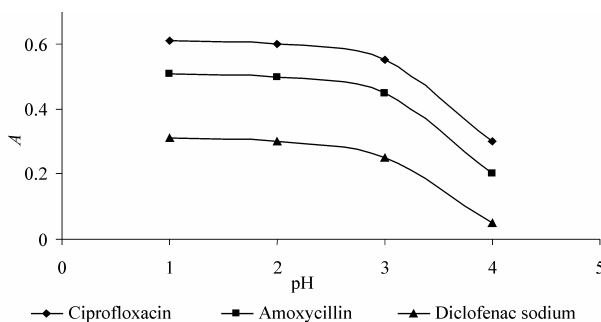


Fig. 4. Effect of pH on the oxidation reactions of the drugs, ciprofloxacin $0.4 \text{ } \mu\text{g ml}^{-1}$, amoxicillin $0.5 \text{ } \mu\text{g ml}^{-1}$, and diclofenac sodium $0.3 \text{ } \mu\text{g ml}^{-1}$.

Iron(III)/Drug mole ratio

For the stoichiometric relation of the oxidation reaction of the drugs, different amounts of iron(III), 0.2–2.5 ml aliquots ($1.0 \times 10^{-5} \text{ M}$ ferric sulphate) were added to 2.5 ml aliquots of solutions of the drugs, $1.19 \times 10^{-6} \text{ M}$ ciprofloxacin, $1.04 \times 10^{-6} \text{ M}$ amoxicillin and $1.88 \times 10^{-6} \text{ M}$ diclofenac sodium. The maximum absorbance was attained with a five-fold, ten-fold and two-fold amount of iron(III) for ciprofloxacin, amoxicillin and diclofenac sodium, respectively (Fig. 5). Thus, 1.5 ml of a $1 \times 10^{-6} \text{ M}$ ferric sulphate solution was employed to achieve a constant and maximum absorbance for the three drugs.

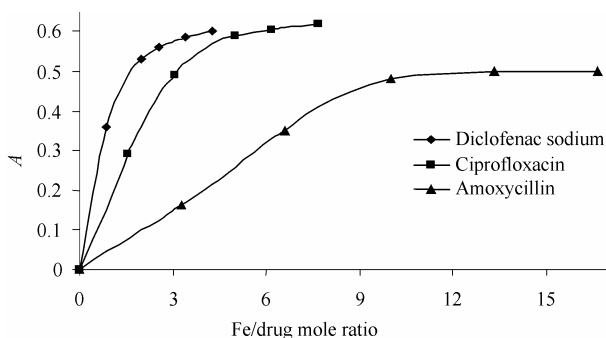


Fig. 5. Effect of iron(III) concentration on the drugs, ciprofloxacin $0.4 \text{ } \mu\text{g ml}^{-1}$, amoxicillin $0.5 \text{ } \mu\text{g ml}^{-1}$, and diclofenac sodium $0.3 \text{ } \mu\text{g ml}^{-1}$.

CONCLUSIONS

The AAS method is highly sensitive and, moreover, it can be used for routine analysis of the investigated drugs in raw materials and pharmaceutical formulations. The method is simple and rapid since it is a single step process. The

statistical parameters and the recovery tests data clearly indicate the reproducibility and accuracy of the method. The results demonstrate that the method has an equivalent accuracy and precision as the official methods, as found from the *t*- and *f*-tests.

ИЗВОД

ИНДИРЕКТНО ОДРЕЂИВАЊЕ ЦИПРОФЛОКСАЦИНА, АМОКСИЦИЛИНА И НАТРИЈУМ-ДИКЛОФЕНАКА У ФАРМАЦЕУТСКИМ ФОРМУЛАЦИЈАМА АТОМСКОМ АПСОРПЦИОНОМ СПЕКТРОМЕТРИЈОМ

MAHMOUD MOHAMED ISSA¹, R'AFAT MAHMOUD NEJEM¹, MONZER AL-KHOLY¹, NASER SAID EL-ABADLA², RAFIK SOBHI HELLES¹ и AKILA AMIN SALEH³

¹Analytical Chemistry, ²Organic Chemistry, Department of Chemistry, Alaqsa University, Gaza, Palestine и

³Analytical Chemistry, Ain Shams University, Cairo, Egypt

Развијена је високоосетљива индиректна атомска апсорпциона спектрометријска метода (AAS) за одређивање веома ниских концентрација ципрофлоксацина, амоксицилина и натријум-диклофенака. Метода се заснива на оксидацији лекова помоћу Fe(III). После уклањања вишка Fe(III) диетил-етром, Fe(II) се по аспирирању водене фазе у пламену ваздух–ацетилен одређује помоћу AAS. Линеарност је потврђена у опсегу концентрација 25–400 ng·ml⁻¹ за ципрофлоксацин, 50–500 ng·ml⁻¹ за амоксицилин и 60–600 ng·ml⁻¹ за натријум-диклофенак. Резултати су упоређени са официналном методом применом *t*- и *f*-теста за *p* < 0.05. Нису утврђене значајне интерференције са најчешће коришћеним ексципијенсима. Коефицијент варијације је у свим случајевима мањи од 6,1 %, а проценат приноса у опсегу од 95 до 103 %. Метода је примењена у анализи поменутих лековитих супстанци у комерцијалним фармацеутским препаратима.

(Примљено 23. маја, ревидирано 7. децембра 2007)

REFERENCES

1. M. A. El-Dilamony, S. A. Amin, *Anal. Lett.* **37** (2004) 1151
2. A. S. Amin, A. L. El-Ansary, Y. M. Issa, *Talanta* **41** (1994) 691
3. Q. Li, Z. Yang, *Anal. Lett.* **39** (2006) 763
4. Q. M. Al-Abachi, H. Haddi, M. A. Al-Abachi, *Anal. Chim. Acta* **554** (2005) 184
5. W. Cao, J. Yang, C. Sun, Y. Chem, Q. Gao, *Luminescence* **20** (2005) 20
6. D. L. Ming, Y. H. Yan, F. Mi, *Spectrochim. Acta* **61** (2005) 281
7. M. A. Abulkibash, M. S. Sultan, M. A. Al-Olyan, M. S. Al-Ghannam, *Talanta* **61** (2003) 239
8. Z. S. Qureshi, T. Qayoom, H. I. Mraud, *J. Pharm. Biomed Anal.* **23** (2000) 773
9. A. Macia, F. Borrull, C. Aguilar, M. Calull, *Electrophoresis* **25** (2004) 428
10. M. A. Gonzalez, F. Uribe, S. D. Moisen, A. P. Fuster, A. Selen, P. G. Welling, B. Painter, *Antimicrob. Agents Chemother.* **26** (1984) 741
11. L. K. Anderson, L. R., Luman, A. W. Moats, P. A. Hansen, E. J. Rushing, *J. AOAC Int.* **85** (2002) 546
12. X. Du, C. Li, K. H. Sun, H. C. Nightingale, H. Charles, P. D. Nicolau, *J. Pharm. Biomed Anal.* **39** (2005) 648
13. K. M. Sowinski, M. B. Kays, *J. Clin. Pharm Therap.* **29** (2004) 381
14. G. H. Ragab, A. S. Amin, *Spectrochim. Acta* **60** (2004) 973
15. Y. Li, H. Lang, H. Li, Z. Xie, *Fenxi Huaxue* **28** (2000) 1252 (in Chinese)

16. H. Salem, K. Kelani, A. Shalaby, *Scient. Pharm.* **69** (2001) 189
17. T. Z. Liu, K. H. Oka, *Clin. Chem.* **26** (1980) 69
18. K. El-Sousi, M. A. Ahmed, M. M. Issa, *Bull Fac. Pharm.* **40** (2002) 201
19. B. Kanakapura, P. H. Chandrashekar, *Ind. Sci. Asia* **29** (2003) 141
20. N. Rahman, N. Anwar, M. Kashif, N. Hoda, *Acta Pharm.* **56** (2006) 347
21. B. S. Nagaralli, J. Seetharamappa, M. B. Melwanki, *J. Pharm. Biomed. Anal.* **29** (2002) 859
22. A. I. Vogel, *Vogel's Textbook of Quantitative Inorganic Analysis*, 4th Ed., Longman Press, New York, 1978, p.157
23. E. G. C. Clarke, *Clarke's Analysis of Drugs and Poisons*, Pharmaceutical Press, London, 2006 (<http://www.medicinescomplete.com/mc/clarke/current/whatsnew.htm>).



www.shd.org.yu

J. Serb. Chem. Soc. 73 (5) 577–583 (2008)

JSCS–3740

Transformation of a petroleum pollutant during soil bioremediation experiments

B. JOVANČIĆEVIĆ^{1,2*#}, M. ANTIĆ^{3#}, M. VRVIĆ^{1,2#}, M. ILIĆ^{2#}, M. NOVAKOVIĆ^{1#},
R. M. SAHEED¹ and J. SCHWARZBAUER⁴

¹Department of Chemistry, University of Belgrade, Studentski trg 12–16, 11001 Belgrade,

²Centre of Chemistry, ICTM, Belgrade, ³Department of Agriculture, University of Belgrade, Belgrade, Serbia and ⁴Institute of Geology and Geochemistry of Petroleum and Coal, Aachen University, Aachen, Germany

(Received 24 October 2007)

Abstract: The experiment of *ex situ* soil bioremediation was performed at the locality of the Oil Refinery in Pančevo (alluvial formation of the Danube River, Serbia) polluted with an oil type pollutant. The experiments of biostimulation, bioventilation and reinoculation of an autochthonous microbial consortium were performed during the six-month period (May–November 2006). The changes in the quantity and composition of the pollutant, or the bioremediation effect, were monitored by analysis of the samples of the polluted soil taken in time spans of two weeks. In this way, from the beginning until the end of the experiment, 12 samples were collected and marked as P₁–P₁₂ (Pančevo 1–Pančevo 12). The results obtained showed that more significant changes in the composition of the oil pollutant occurred only during the last phases of the experiment (P₈–P₁₂). The activity of microorganisms was reflected in the increase of the quantity of polar oil fractions, mainly fatty acid fractions. In this way, the quantity of total eluate increased, and the quantity of the insoluble residue was reduced to a minimum, whereby the oil pollutant was transformed to a form that could be removed more efficiently and more completely from the soil, as a segment of the environment.

Keywords: bioremediation; oil type pollutant; soil; Pančevo Oil Refinery; alkanes; fatty acids.

INTRODUCTION

The fate of an oil type pollutant in the environment can be monitored most accurately by determining its quantity and studying its composition in polluted samples from the same or a neighbouring locality during different time periods. For example, in this way, oil microbiological transformations were monitored in

* Corresponding author. E-mail: bjovanci@chem.bg.ac.yu

Serbian Chemical Society member.

doi: 10.2298/JSC0805577J

samples of ground waters during a period of almost three years in the locality of the Oil Refinery in Pančevo (Serbia), which belongs to an alluvial formation of the Danube River.¹⁻⁴ The samples of ground waters were taken from the same piezometer. An identical method was applied for determining the quantity of hydrocarbons and the composition at the molecular level was defined using the instrumental techniques, gas chromatography (GC) and gas chromatography combined with mass spectrometry (GC-MS). However, these studies obviously lasted too long.

Simulation of natural conditions in the laboratory with the simultaneous intensification of only specified factors affecting the intensity and rate of transformation enabled time saving and relevant conclusions to be reached. Thus, the course of the biodegradation of an oil pollutant in a sample of surface water (alluvial formation of the Danube River, Serbia) was accelerated under the laboratory conditions during ninety days by exposing the pollutant to the influence of those microorganisms identified in the natural environment but at a much higher concentration.⁵ There are also numerous other examples. Rosa and Trigüis⁶ assessed the behaviour of oil pollutants during a laboratory investigation of bioremediation (using nutrients) in tropical coast sediments. Bioremediation experiments on oil polluted soils were also performed using white rot fungus, *Pleurotus tuberregium* (Fr.) Sing.⁷ A similar method was used to monitor the fate of other non-oil organic pollutants, *e.g.*, polycyclic aromatic hydrocarbons (PAHs),^{8,9} polychlorinated biphenyls (PCBs) and polychlorinated dibenzo-*para*-dioxins (PCDD/Fs).^{10,11}

The mentioned experiments of bioremediation offered the opportunity to not only gain fundamental knowledge of the fate of pollutants in the environment, but also to assess to what extent bioremediation as a technique may be applied to refine polluted water, soil or sediments.

In this paper, the results of a study of the decomposition of an oil-type pollutant during *ex situ* bioremediation of soil from the pilot heap (halde) of approximately 150 m³ at the Petroleum Refinery Pančevo (Serbia) are presented. Experiments of biostimulation, bioventilation and re-inoculation of autochthonous microbial consortium were performed during a period of six months.

EXPERIMENTAL

The experiment of soil bioremediation was performed at the locality of the Oil Refinery in Pančevo (alluvial formation of the Danube River, Serbia) polluted with an oil type pollutant. It lasted for 6 months (May–November 2006). The changes in the quantity and composition of the pollutant, *i.e.*, the bioremediation effect, were monitored by analysis of the polluted soil samples taken in time spans of two weeks. In this way, from the beginning until the end of the experiment, 12 samples were collected and denoted as P₁–P₁₂ (Pančevo 1–Pančevo 12).

Approximately, a quantity of 150 m³ of polluted soil was collected from five locations from the refinery's property. The samples were mechanically homogenized. Poplar cutting was added to the soil (10 % of total volume) in order to increase its aeration. Esters of long

chain alcohols and fatty acids were added as biodegradable substrates active at the surface (0.20 kg m^{-3}), and manure from poultry farms as a source of nitrogen and phosphorus for biostimulation (approx. 5 %). Thereafter, the soil was formed into a halde shape and aeration pipes and a gutter system for collecting seepage water were installed. Manual stirring of the soil material every two weeks ensured homogenization and additional aeration of the halde content. The halde was protected from direct external influences by a green house.

The titre of microorganisms was determined by serial dilution on agar plates incubated at 26°C . Nutrient agar was used for bacteria, Sabouraud glucose agar with chloramphenicol for yeasts and moulds and a mineral base medium with 2000 ppm diesel fuel was used for hydrocarbon-degrading microorganisms.

The population growth of the microorganisms and intensification of the biodegradation process in addition to biostimulation was achieved by re-inoculation of zymogenous microorganisms. Bacteria strains which are able to decompose hydrocarbons were spawned in the laboratory bioreactor. 10 dm^3 of biomass of high density (up to 10^9 CFU cm^{-3}) of activated microorganisms were deposited on the experimental halde once a week during the monitoring of the bioremediation.

The organic substance from samples P_1 – P_{12} was Soxhlet extracted with chloroform for 36 h and quantified. The group composition in the extracts was determined and fractions of saturated hydrocarbons, aromatic hydrocarbons, alcohols and fatty acids were isolated by column chromatography. GC–MS was applied for analysis of some of the compounds in fractions. Fatty acids were detected as methyl esters formed during the elution step. Detailed descriptions of the analytical procedure and applied analytical techniques were discussed in previous papers.^{3,12}

RESULTS AND DISCUSSION

The contents of the organic substance in the samples P_1 – P_{12} , as well as the results obtained by chromatographic separation of the isolated extracts are given in Table I.

TABLE I. Extracted content of organic matter in samples P_1 – P_{12} and the results obtained by column chromatography of the isolated extracts

Sample	Date of sampling	Organic substance from soil, %	Saturated HC in eluate, %	Aromatics in eluate, %	Alcohols in eluate, %	Fatty acids in eluate, %
P_1	10/05/2006	5.9	46.4	9.5	27.4	16.7
P_2	24/05/2006	4.8	53.3	13.0	26.0	7.8
P_3	12/06/2006	5.9	45.9	10.8	32.4	10.8
P_4	28/06/2006	5.7	54.4	14.4	21.1	10.0
P_5	12/07/2006	5.5	51.2	12.8	24.4	11.6
P_6	26/07/2006	4.6	45.5	17.0	26.1	11.4
P_7	14/08/2006	4.2	53.2	13.9	21.5	11.4
P_8	30/08/2006	6.6	58.1	6.5	25.8	9.7
P_9	13/09/2006	4.5	53.6	10.1	21.7	14.5
P_{10}	04/10/2006	6.1	49.4	19.5	23.4	7.8
P_{11}	19/10/2006	5.3	39.2	19.6	26.8	14.4
P_{12}	10/11/2006	4.1	33.3	17.1	32.4	17.1

The extractable contents of organic substance ranged from 4.1 to 6.6 %. However, although the last analyzed sample contained the least amount in the

extract, a regular decreasing trend in the total extract amount with the increasing time of bioremediation was not observed.

Changes in the contents of the four isolated fractions of P₁ to P₁₂ also showed no significant regularity. Only for the content of saturated hydrocarbons was perhaps an evenly decreasing trend from 58.1 → 33.3 % for P₈ (sample taken on 30/08/2006) to P₁₂ (10/11/2006) observed (Table I). Based on this observation, it may be concluded that the microbiological decomposition of the alkane fraction occurred in the second part of the bioremediation experiment. It is very well known that saturated hydrocarbons, compared to other fractions in oil, are the least resistant to biodegradation.¹³ Therefore this reduction in the contents of the alkane fraction may be considered as an expected and logical result.

The results of the group composition of the extracts given in Table I represent the quantities of some fractions recalculated to the total eluate. However, a much more realistic picture on the changes in composition of the oil pollutant during the performed bioremediation experiment (especially for samples P₈ to P₁₂) can be obtained if the calculation includes also the residue remaining on the column during the chromatographic separation. Then the results of the contents of the four isolated fractions in the 12 examined samples become obviously different (Table II).

TABLE II. Results obtained by column chromatography of the isolated extracts (including the column residue)

Sample	Saturated HC in extract, %	Aromatics in extract, %	Alcohols in extract, %	Fatty acids in extract, %	Column residue, %
P ₁	37.1	7.6	21.9	13.3	20.0
P ₂	38.7	9.4	18.9	5.7	27.4
P ₃	32.7	7.7	23.1	7.7	28.8
P ₄	47.6	12.6	18.4	8.7	12.6
P ₅	41.5	10.4	19.8	9.4	18.9
P ₆	38.8	14.6	22.3	9.7	14.6
P ₇	40.8	10.6	16.5	8.7	23.4
P ₈	35.3	3.9	15.7	5.9	39.2
P ₉	33.3	6.3	13.5	9.0	37.8
P ₁₀	34.9	13.8	16.5	5.5	29.4
P ₁₁	35.0	17.5	23.9	12.9	10.7
P ₁₂	32.4	16.7	31.5	16.7	2.8

This calculation avoids the detected reduction of the alkane fraction from P₈ to P₁₂. In this phase of the bioremediation process, an obvious increase in the content of the fatty acid fraction (5.9 → 16.7 %, Table II) occurred. GC-MS analysis confirmed that these fractions were dominated by *n*-fatty acids (Fig. 1).

The quantities of the aromatic and alcohol fractions increased, with certain deviations, from sample P₈ to sample P₁₂. If, however, the values for these two fractions are summed, the increasing trend was even more obvious. The detected regularities are very clear if the values are presented as a histogram (Fig. 2).

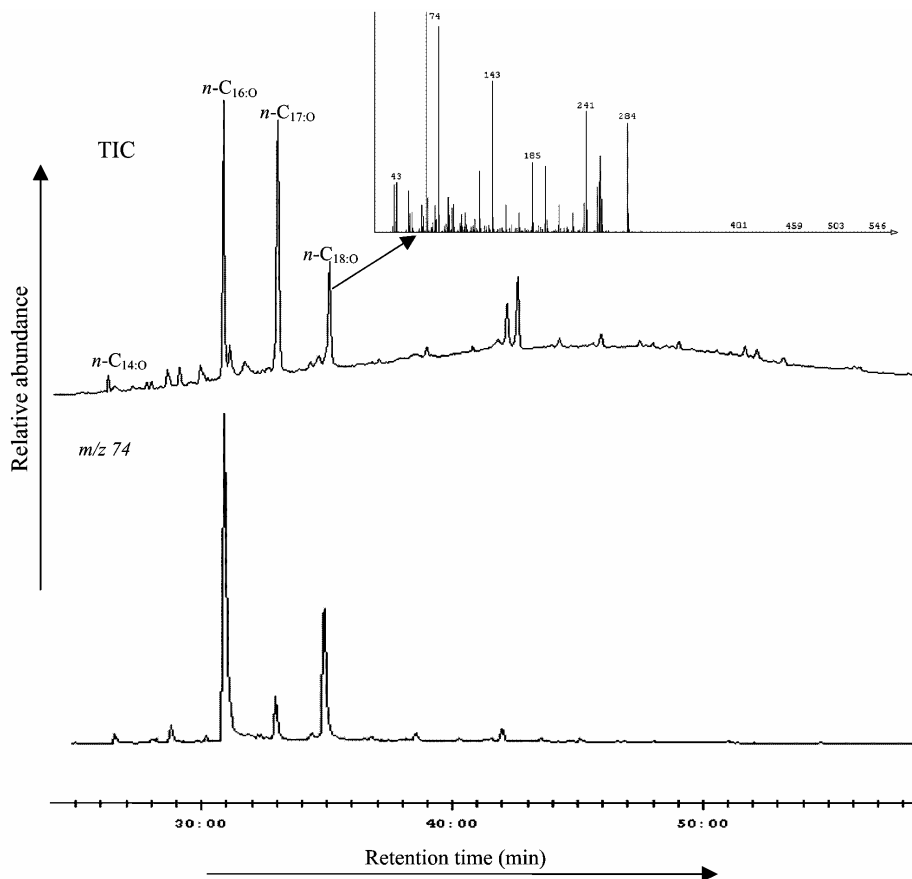


Fig. 1. Total ion chromatogram (TIC) of the fatty acid fraction and related chromatogram of mass m/z 74 (typical for fatty acid esters) of the P_{10} extract, characteristic for all the investigated samples. As additional proof of the presence of fatty acids (or their esters), the entire mass spectrum which matches the peak of $n\text{-C}_{18}$ fatty acid esters is also given.

For the part of the bioremediation experiment covered by samples P_8 to P_{12} , the most obvious results are the reduction of the amount of residue remaining on the column (39.2 \rightarrow 2.8 %) and the increase in the total amount of eluate (60.8 \rightarrow 97.2 %, Table II; Fig. 2). Based on this observation, it may be concluded that the activity of the microorganisms contributed to the minimization of the insoluble part in the oil pollutant. The results of the group composition of the extracts showed that this activity also resulted in an increase of all polar fractions (aromatics, alcohols and fatty acids) and that the quantity of the saturated hydrocarbon fraction remained approximately constant. The detected reduction in the quantity of this fraction for samples P_8 – P_{12} based on the results presented in Table I (calculated only for the eluate mass) is only apparent and is the consequence of the increased quantities of the other fractions.

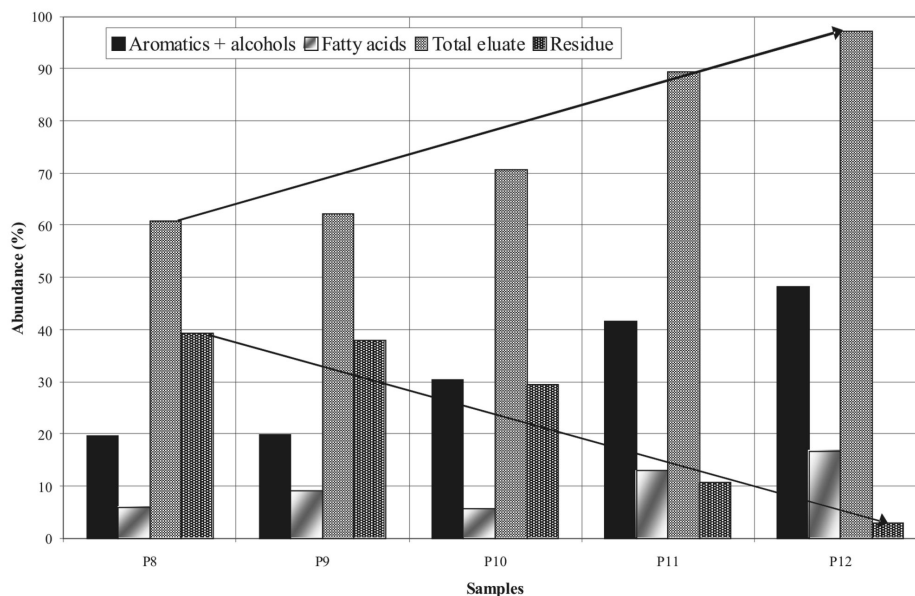


Fig. 2. Contents of total aromatics and alcohols, fatty acids, total eluate and the column residue for samples P₈ – P₁₂.

CONCLUSIONS

An *ex situ* experiment of the bioremediation of oil polluted soil from the locality of the Oil Refinery in Pančevo (alluvial formation of the Danube River, Serbia) was performed during a period of 6 months (May–November 2006). The effect of the bioremediation was monitored by analysis of samples of the polluted soil taken in time intervals of two weeks (12 samples in total; samples P₁–P₁₂). The obtained results showed that significant changes in the composition of the oil pollutant occurred only during the last phases of the experiment (samples P₈–P₁₂). The activity of the microorganisms was reflected in an increase in the quantity of the polar oil fractions, most obvious for the fatty acid fractions. In this way, the quantity of the total eluate increased (60.8 → 97.2 %) and the quantity of the insoluble residue diminished (39.2 → 2.8 %). Thus, the oil pollutant was transformed into a form which could be removed more efficiently and more completely from the soil, as a segment of the environment.

Acknowledgements. The Alexander von Humboldt Foundation and the Ministry of Science of the Republic of Serbia are thanked for supporting this research.

ИЗВОД
ТРАНСФОРМАЦИЈЕ ЗАГАЂИВАЧА НАФТНОГ ТИПА ЗА ВРЕМЕ
ЕКСПЕРИМЕНТА БИОРЕМЕДИЈАЦИЈЕ

Б. ЈОВАНЧИЋЕВИЋ^{1,2}, М. АНТИЋ³, М. ВРВИЋ^{1,2}, М. ИЛИЋ², М. НОВАКОВИЋ¹,
R. M. SAHEED¹ и J. SCHWARZBAUER⁴

¹Хемијски факултет, Универзитет у Београду, Студентски брз 12–16, 11001 Београд, ²ИХТМ – Центар за хемију, Вежошева 12, 11000 Београд, ³Пољопривредни факултет, Универзитет у Београду и ⁴Institute of Geology and Geochemistry of Petroleum and Coal, Aachen University, Aachen, Germany

Извођени су експерименти *ex situ* биоремедијације земљишта на локалитету Рафинерије нафте Панчево (алувијална формација реке Дунав). Експерименти су извођени у току периода од шест месеци (мај–новембар 2006. године). Промене у количини и саставу нафтног загађивача (биоремедиациони ефекат), праћене су анализом узорака који су узимани у временским размацима од две недеље. На тај начин, у току шест месеци сакупљено је 12 узорака означених са P₁–P₁₂ (Pančevo 1–Pančevo 12). Добијени резултати показали су значајне промене у саставу нафтног загађивача само у последњој фази експеримента (P₈–P₁₂). Активност микроорганизама огледала се у повећању количине поларних нафтних компонената, на првом месту фракције масних киселина. На тај начин, у овој фази експеримента, повећана је количина укупног елуата, а количина нерастворног остатка сведена је на минималну вредност, чиме је нафтни загађивач доведен у облик који се ефикасније може уклонити из земљишта, као сегмента животне средине.

(Примљено 24. октобра 2007)

REFERENCES

1. B. Jovančičević, P. Polić, *Fresenius Environ. Bull.* **9** (2000) 232
2. B. Jovančičević, P. Polić, D. Vitorović, G. Scheeder, M. Teschner, H. Wehner, *Fresenius Environ. Bull.* **10** (2001) 178
3. B. Jovančičević, P. Polić, M. Vrvic, G. Scheeder, M. Teschner, H. Wehner, *Environ. Chem. Lett.* **1** (2003) 73
4. B. Jovančičević, M. Vrvic, J. Schwarzbauer, H. Wehner, G. Scheeder, D. Vitorović, *Water Air Soil Pollut.* **183** (2007) 225
5. M. Antić, B. Jovančičević, M. Ilić, M. Vrvic, J. Schwarzbauer, *Environ. Sci. Pollut. Res.* **13** (2006) 320
6. A. P. Rosa, J. A. Trigüis, *Environ. Sci. Pollut. Res.* **14** (2007) 470
7. O. Isikhuemhen, G. Anoliefo, O. Oghale, *Environ. Sci. Pollut. Res.* **10** (2003) 108
8. T. F. Guerin, *Environ. Sci. Pollut. Res.* **7** (2000) 19
9. D. Haddox, T. Cutright, *J. Soils Sediments* **3** (2003) 41
10. B. Campanella, C. Bock, P. Schröder, *Environ. Sci. Pollut. Res.* **9** (2002) 73
11. S. Saponaro, L. Bonomo, *J. Soils Sediments* **3** (2003) 165
12. B. Jovančičević, M. Antić, T. Šolević, M. Vrvic, A. Kronimus, J. Schwarzbauer, *Environ. Sci. Pollut. Res.* **12** (2005) 205
13. J. K. Volkman, R. Alexander, R. I. Kagi, G. W. Woodhouse, *Geochim. Cosmochim. Acta* **47** (1983) 785.



www.shd.org.yu

J. Serb. Chem. Soc. 73 (5) 585–593 (2008)

JSCS–3741

JSCS@tmf.bg.ac.yu • www.shd.org.yu/JSCS

UDC 669.22+669.4:622.234.4+669.53

Original scientific paper

Lead and silver extraction from waste cake from hydrometallurgical zinc production

DUŠAN D. STANOJEVIĆ^{1*}, MILOŠ B. RAJKOVIĆ²,
DRAGAN V. TOŠKOVIĆ¹ and MILANA A. TOMIĆ³

¹Faculty of Technology, University of East Sarajevo, Karakaj b.b., 76000 Zvornik, Republic of Srpska, Bosnia and Herzegovina, ²Institute of Food Technology and Biochemistry, Faculty of Agriculture, University of Belgrade, Nemanjina 6, 11080 Zemun and ³Higher Technological School of Professional Studies in Šabac, H. Veljkova 10, 15000 Šabac, Serbia

(Received 30 October, revised 7 December 2007)

Abstract: This paper presents the experimental results of the extraction of lead and silver from a lead–silver waste cake obtained in the process of hydrometallurgical zinc production. While controlling the pH value, the lead–silver cake was leached at a temperature close to boiling point in different concentrations of aqueous calcium chloride solutions. The experiments were performed applying different ratios between the mass of cake and the volume of the leaching agent under different durations of the process. It was concluded that at the optimal process parameters (pH 2.0–2.5; CaCl₂ concentration, 3.6 mol dm⁻³; temperature, 95 °C; solid/liquid ratio, 1:5), the leaching efficiency of lead and silver could reach the approximate value of 94 %. Applying the same optimal process parameters, the method was applied to the leaching of a lead–silver cake in a magnesium chloride solution, but with significantly lower efficiencies. The results show that leaching of lead and silver in a calcium chloride solution could be a prospective method for increasing the recovery of lead and silver during hydrometallurgical zinc production.

Keywords: lead–silver cake; chloride solutions; leaching; metal recovery.

INTRODUCTION

All over the world, more than 85 % of super high grade quality zinc (min. content, 99.995 %) is produced by the hydrometallurgical process.^{1,2}

In contemporary hydrometallurgical zinc production, greatest importance is given to the maximum possible extraction of present other metals present in the raw materials, especially, zinc, cadmium, copper, lead and silver. This has been confirmed through the number of procedures (jarosite, hematite, goetite, *etc.*) applied in the production practice for the last several decades.^{3–7} The aim of the

* Corresponding author. E-mail: ducca@sbb.co.yu

doi: 10.2298/JSC0805585S

previously mentioned procedures is to obtain a more economic process by increasing the efficiency of leaching, as a major production phase of metal extraction. An increased leaching efficiency is obtained by prolonged leaching time in a solution with higher sulfuric acid concentrations and at higher temperature. Simultaneously, however, in addition to zinc and other useful metals, useless iron is also extracted. The dissolved iron must be eliminated from the process, which is realized by transferring it into some poorly soluble iron compounds (jarosite, hematite, goetite, *etc.*).⁶ The leached residue in the jarosite technology of iron elimination is called lead–silver cake (Pb–Ag cake), containing lead, zinc, copper, cadmium, silver and other metals.⁸ A lead–silver cake can sometimes contain up to 25 % lead and more than 500 g t⁻¹ of silver, representing an important economic by-product of the jarosite technology which can be valorized by conventional pyrometallurgical methods in lead smelters, while the jarosite precipitate has never had commercial importance.^{9–13}

Under real industrial conditions and for different technological reasons, a Pb–Ag cake can contain higher quantities of iron, and less lead and silver. Such a Pb–Ag cake is not appropriate for pyrometallurgical treatment as the process is difficult. Due to the possible appearance of low metal content Pb–Ag cakes, as well as other similar wastes in hydrometallurgical zinc production, it is very important to define an appropriate procedure which will enable, as much as possible, the lead and silver present to be valorized from these wastes.^{14–16}

The process of leaching in aqueous calcium and magnesium chloride solutions was selected and examined by choosing possible procedures in order to attain effective valorization of the metals present in Pb–Ag cakes.^{9–11,14,17,18} A leaching medium convenient for such a purpose should effectively dissolve lead and silver compounds but not iron(III) compounds.¹⁰ Bearing in mind the chemical composition of Pb–Ag cakes, as well as the properties of the metal compounds present, it can be assumed that lead is present predominantly in the form of PbSO₄ and silver in the form of AgCl. Complex soluble chlorides, such as of [PbCl₃]⁻ and [PbCl₄]²⁻, *i.e.*, [AgCl₂]⁻, [AgCl₃]²⁻ and [AgCl₄]³⁻ types, are obtained from these compounds by leaching in concentrated solutions of alkaline and earth-alkaline chlorides.^{11,12} Thermodynamic analysis of the formation of lead and silver complex chlorides shows that CaCl₂ and MgCl₂ solutions could possibly be used as effective leaching agents for lead and silver from their compounds in Pb–Ag cakes.^{14,15,17,18}

EXPERIMENTAL

Regarding the influence of temperature on transfer of silver and lead from their sparingly soluble compounds into readily soluble complex chlorides, it was experimentally shown that the efficiency of this process increases with increasing temperature.^{14,15} Due to significant water evaporation from the reaction pulp at temperatures close to the boiling point, the working temperature in the conducted experiments was limited at 95 °C. The leaching experiments

were conducted in a tightly closed apparatus consisting of a five-necked one-liter glass flask. A stirrer with a water-valve, thermometer, condenser, dropping funnel for introduction of the $\text{Ca}(\text{OH})_2$ suspension and a pH electrode were introduced through the upper necks. Such an equipped vessel was placed into a heating mantle with an automatic regulator, providing the required temperature in the vessel.

Figure 1 illustrates a schematic drawing of the reaction vessel employed in the leaching experiments with chloride solution.

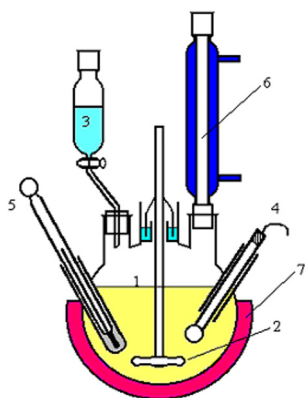


Fig. 1. Schematic presentation of the reaction flask employed for the leaching experiments. 1 – Flask filled with reaction mixture; 2 – propeller stirrer with a water-seal; 3 – dropping funnel for $\text{Ca}(\text{OH})_2$; 4 – electrode for measurement of the pH; 5 – thermometer; 6 – condenser; 7 – heating mantle.

A CaCl_2 solution was initially used as the leaching agent whereas later an MgCl_2 was used. Both solutions were prepared from analytical grade reagents.¹⁹

The chemical composition of the Pb–Ag cake was as follows: Pb, 6.1 %; Cu, 0.32 %; Cd, 0.15 %; Ag, 0.016 %; Zn, 6.0 % and Fe, 23.6 %. It was obtained from an industrial hydrometallurgical production of zinc.^{1,2,20,21}

These experiments were performed in a number of series. The concentrations of lead, silver and iron in the liquid phase formed by leaching and in the solid residue from which the leaching was performed were determined in all cases. Based on these data and according to mass balance in solid and liquid phase, extraction of these metals in relation to their content in Pb–Ag cake was calculated.

Leaching into a CaCl_2 solution

The process of leaching of the Pb–Ag cake into calcium chloride solution was examined in order to check the efficiency of the leaching of lead and silver in the form of complex chlorides, as well as to determine the effects of the following parameters on the leaching process: pH value; solid–liquid ratio in reaction pulp (ratio between the mass of the Pb–Ag cake and the volume of leaching agent); concentration of the leaching agent and the duration of the leaching.

Before the start of a leaching experiment, the appropriate quantity of CaCl_2 solution was added to measured amount of dry Pb–Ag cake in the reaction flask. Water vapor was condensed in the reflux condenser in order to prevent a change in the composition of the reaction mixture during heating. A water seal was used to prevent the evaporation of water vapor near the spindle of the stirrer. A decrease of the pH of the reaction mixture during the leaching process was prevented by the addition of $\text{Ca}(\text{OH})_2$. Under these conditions, Fe(III) remained as sparingly soluble hydroxide.

Leaching into $MgCl_2$ solution

The series of experiments on leaching into $MgCl_2$ solution were performed under the optimized operation procedures determined during leaching into $CaCl_2$ solution, using the same Pb–Ag cake and apparatus.

Two series of experiments were performed in order to determine the influence of temperature and time on the leaching process. In both series, the other relevant process parameters remained constant with values previously defined as optimal in the process of leaching into $CaCl_2$ solution, *i.e.*, pH of the reaction pulp 2.0–2.5, ratio between the mass of the cake and the volume of the leaching agent, S:L = 1:5, concentration of the leaching agent 400 g dm^{-3} and stirring rate of the reaction pulp 400 rpm.

After each experiment, the solid phase was separated by filtration, and then the cake was rinsed with hot water in order to extract the maximum amount of leached metals.

RESULTS AND DISCUSSION

Leaching into $CaCl_2$ solution

In the first series of experiments, the influence of the pH value on leaching efficiency of lead and silver was examined. The obtained results are shown in Fig. 2, which shows that the efficiency of lead and silver extraction decreased with increasing pH value.

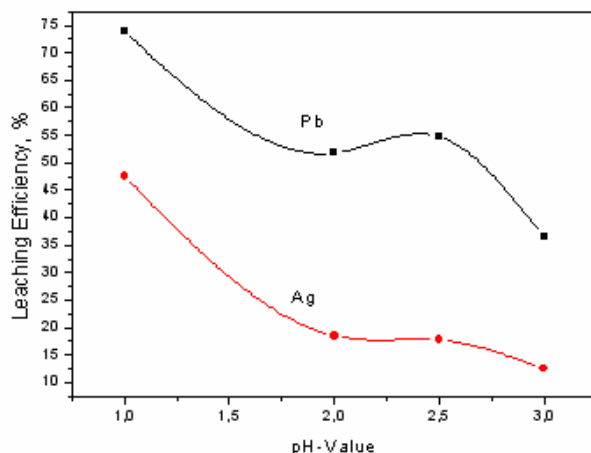


Fig. 2. Influence of pH on the efficiency of Pb and Ag leaching from the Pb–Ag cake. Leaching conditions: $t = 95 \text{ }^\circ\text{C}$; solid:liquid ratio, 1:2; duration of leaching, 12 h; $c(\text{CaCl}_2) = 3.0 \text{ mol dm}^{-3}$. The solid residue after leaching was not rinsed with water.

However, since conditions of low pH values enabled the undesirable transfer of iron into the solution, the optimal pH value for leaching was determined to be between 2.0 and 2.5. Under such conditions, iron was not extracted while the efficiency of lead and silver extraction was approximately 51–55 % for lead and 17–18 % for silver.

In the second series of experiments, the ratio of S:L in the reaction pulp was examined (the ratio of the mass of dry Pb–Ag cake to the volume of leaching solution, kg dm^{-3}). The solid:liquid ratio was changed from $1.0 \text{ kg:}2.0 \text{ dm}^{-3}$ to $1.0 \text{ kg:}7.0 \text{ dm}^{-3}$. The same leaching process parameters as in the first series of experiments were employed. The results of the second series of experiments are

presented in Fig. 3, which shows that the efficiency of lead and silver extraction first increased and then decreased with decreasing S:L ratio. At an S:L ratio 1.0 kg:5.0 dm⁻³, the highest efficiency of extraction detected for lead was 75.9 and for silver 67.2 %.

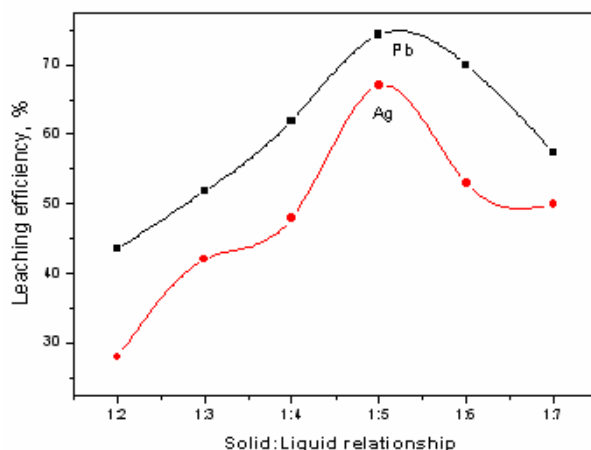


Fig. 3. Influence of the S:L ratio in the leaching pulp on the efficiency of Pb and Ag leaching from the Pb–Ag cake. Leaching conditions: $t = 95\text{ }^{\circ}\text{C}$; duration of leaching, 12 h; $c(\text{CaCl}_2) = 3.0\text{ mol dm}^{-3}$. The solid residue after leaching was not rinsed with water.

In the third series of experiments, the influence of the CaCl₂ concentration on the efficiency of lead and silver extraction from the Pb–Ag cake was examined. The results of the third series of experiments are shown in Fig 4, which shows that the efficiency of lead and silver extraction increased with increasing concentration of CaCl₂. The best results were obtained when a CaCl₂ concentration of 3.6 mol dm⁻³ was employed. Under these conditions, the extraction of lead was approximately 75 % and that of silver 78 %.

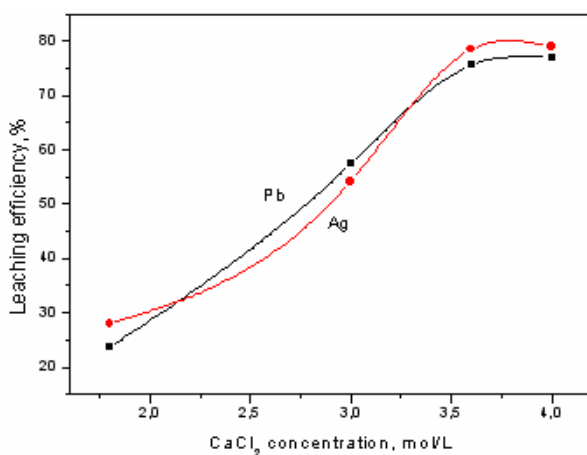


Fig. 4. Influence of the CaCl₂ concentration on the efficiency of Pb and Ag leaching from the Pb–Ag cake. Leaching conditions: $t = 95\text{ }^{\circ}\text{C}$; solid:liquid ratio, 1:5; duration of leaching, 12 h. The solid residue after leaching was not rinsed with water.

In the fourth series of experiments, the influence of the duration of leaching on the efficiency of lead and silver extraction was determined. Since the results

of the previous series of experiments indicate that the duration of leaching should not be shorter than 8 h, duration times of 8, 12 and 14 h were chosen. The results of the fourth series of experiments are shown in Fig. 5, from which it can be seen that the optimal duration of leaching was 12 h since prolonging the time to 14 h led to no further improvement in the extraction efficiency. The extraction efficiency after 14 h for both lead and silver was 94 %.

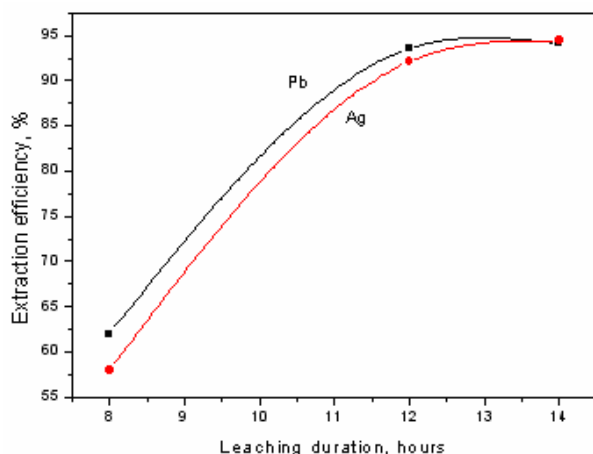


Fig. 5. Influence of the leaching duration on the efficiency of Pb and Ag leaching from the Pb–Ag cake. Leaching conditions: $t = 95\text{ }^{\circ}\text{C}$; solid:liquid ratio, 1:5; $c(\text{CaCl}_2) = 3.6\text{ mol dm}^{-3}$. The solid residue after leaching was not rinsed with water.

Leaching into MgCl_2 solution

In the first series of experiments of leaching into MgCl_2 solution, the influence of the leaching temperature on the efficiency of lead and silver extraction was investigated. The results of the first series of experiments on leaching into MgCl_2 solution are shown in Fig. 6, from which it can be seen that increasing the temperature did not result in an essentially higher leaching efficiency, *i.e.*, the maximum leaching efficiency did not exceed 45 % and 22 % for lead and silver, respectively.

In the second series of experiments, the influence of the duration of the leaching on the efficiency of the extraction of lead and silver was examined. These results are shown in Fig. 7, from which it can be seen that prolonging the time of leaching did not significantly improve the leaching efficiency. The maximal obtained values were 40–45 % and 20–25 % for lead and silver, respectively.

In order to compare the efficiency of CaCl_2 and MgCl_2 solutions for leaching lead and silver from Pb–Ag cake of the same chemical composition, a CaCl_2 solution and a MgCl_2 solution with the same mass concentrations of 400 g dm^{-3} (3.6 mol dm^{-3} CaCl_2 and 4.2 mol dm^{-3} MgCl_2) were used as the leaching agents with the leaching parameters: temperature, $95\text{ }^{\circ}\text{C}$; duration of leaching, 7 h, pH value from 2.0 to 2.5; ratio S:L, 1:5. The residue after leaching was not rinsed with hot water. A diagram comparing the efficiency of leaching of Pb–Ag cake

by CaCl_2 and MgCl_2 solution is shown in Fig. 8, from which it can be seen that the efficiencies of leaching lead and silver with the CaCl_2 solution were 80.5 and 72.0 %, respectively, while those of the same metals with the MgCl_2 solution were 39.0 and 24.6 %, respectively.

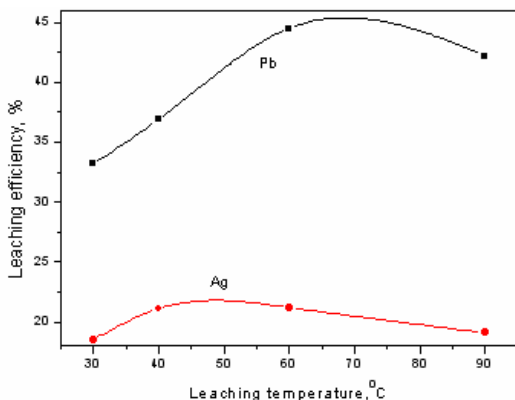


Fig. 6. Dependence of leaching efficiency of Pb and Ag from Pb–Ag cake by MgCl_2 solution, on the temperature of leaching. Leaching conditions: leaching duration, 3 h; pH of the reaction pulp, 2.0–2.5; S:L ratio, 1:5; $c(\text{MgCl}_2) = 400 \text{ g dm}^{-3}$; stirring speed, 400 rpm.

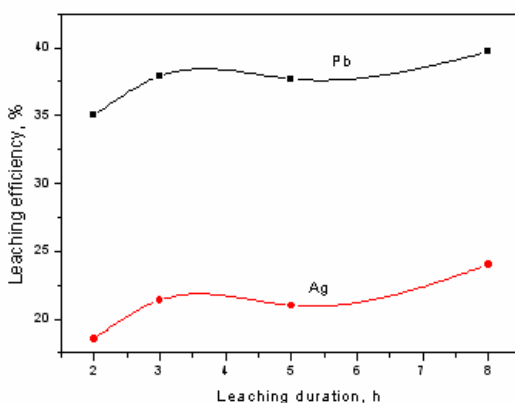


Fig. 7. Dependence of the efficiency of Pb and Ag leaching from the Pb–Ag cake by MgCl_2 solution on the duration of leaching. Leaching conditions: $t = 60 \text{ °C}$; pH value of the reaction pulp, 2.0–2.5; S:L ratio, 1:5; $c(\text{MgCl}_2) = 400 \text{ g dm}^{-3}$; stirring speed, 400 rpm.

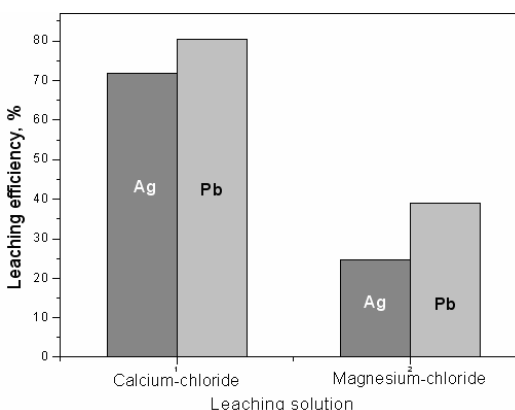


Fig. 8. Comparison of the efficiency of Pb and Ag leaching in CaCl_2 and MgCl_2 solutions under identical conditions. Leaching conditions: $t = 95 \text{ °C}$; leaching duration, 7 h; pH value of the reaction pulp, 2.0–2.5; S:L ratio, 1:5; $c(\text{MgCl}_2) = c(\text{CaCl}_2) = 400 \text{ g dm}^{-3}$; Stirring speed, 400 rpm. The solid residue after leaching was not rinsed with hot water.

CONCLUSIONS

The experimental results of leaching Pb–Ag cake in CaCl₂ and MgCl₂ solutions show that the CaCl₂ solution enabled a significantly better leaching efficiency of lead and silver than the MgCl₂ solution.

Optimal conditions for lead and silver leaching in CaCl₂ solution are: a 3.6 mol dm⁻³ (400 g dm⁻³) solution of leaching agent; pH value of leaching 2.0–2.5; temperature of leaching 95 °C; S:L ratio, 1:5 in the reaction mixture and rinsing the solid residue after leaching with hot water.

Under these conditions, the efficiency of lead and silver extraction from Pb–Ag cake was approximately 94 %, whereby iron was not extracted but remained in the solid residue.

Acknowledgements. The authors are grateful to Ministry of Technology of the Republic of Srpska and “Zorka – Non-Ferrous Metallurgy” from Šabac, for giving support and financial participation in the completion of the research which resulted in this scientific paper.

ИЗВОД

ЕКСТРАКЦИЈА СРЕБРА И ОЛОВА ИЗ ОТПАДНОГ ТАЛОГА ПРИ ХИДРОМЕТАЛУРШКОЈ ПРОИЗВОДЊИ ЦИНКА

ДУШАН Д. СТАНОЈЕВИЋ¹, МИЛОШ Б. РАЈКОВИЋ², ДРАГАН В. ТОШКОВИЋ¹ И МИЛАНА А. ТОМИЋ³

¹Технолошки факултет Универзитета у Источно Сарајеву, Каракај б.б., 56000 Зворник, Република Српска, Босна и Херцеговина, ²Институт за прехрамбену технологију и биохемију, Пољопривредни факултет Универзитета у Београду, Немањина б, 11080 Земун и ³Висока технолошка струковна школа Шабац, Хајдук Вељкова 10, 15000 Шабац

У раду су приказани резултати испитивања извлачења олова и сребра из оловно–сребрног отпадног талоба при хидрометалуршком процесу производње цинка. При контролисаној рН вредности, оловно–сребрни талоб је лужен на температури блиској температури кључања у воденом раствору калцијум-хлорида различитих концентрација, при различитом односу масе талоба и запремине средства за лужење, уз различито трајање процеса. Доказано је да при оптималним изабраним вредностима параметара процеса (рН 2,0–2,5; концентрација CaCl₂: 3,6 mol dm⁻³; температура: 95 °C; однос чврсто:течно, 1:5), може бити излужено око 94 % сребра и олова. При истим параметрима метод је примењен за лужење оловно–сребрног талоба у раствору магнезијум-хлорида, али су ефекти лужења били значајно слабији. Добијени резултати показују да лужење олова и сребра у раствору калцијум-хлорида може бити перспективан метод повећања искоришћења олова и сребра у процесу хидрометалуршке производње цинка.

(Примљено 30. октобра, ревидирано 7. децембра 2007)

REFERENCES

1. R. Vračar, *Extractive Metallurgy of Zinc*, Scientific Book, Belgrade, 1997, p. 53 (in Serbian)
2. B. Nikolić, *Metallurgy of Zinc*, Institute for Chemistry, Technology and Metallurgy, Belgrade, 1996, p. 7
3. D. Stanojević, M. B. Rajković, M. Jakšić, in *Proceedings of the II Yugoslav Symposium on Chemical and Process Engineering*, Book of papers, Dubrovnik, (1987), 10-III-5

4. D. J. MacKinnon, J. M. Brannen, *Zinc Electrowinning from Chloride Electrolyte*, Mining Engineering, Society for Mining, Metallurgy and Exploration, Inc., Littleton, 1982, p. 409
5. D. J. De Biasio, C. J. Krauss, CA 978137, 1971
6. S. M. Rothman, in *Proceedings of International Symposia on Industrial Electrochemistry*, Madras, India, (1976), p. 55
7. M. L. Connolly, R. N. Honey, C. J. Krauss, in *Proceedings of the 6th Annual Hydrometallurgical Meeting, Cominco Metallurgy Bulletin*, Trail, Canada, (1977), p. 151
8. R. H. Farmer, in *Proceedings of Extractive Metallurgy Division Symposium on Electrometallurgy*, Cleveland, OH, USA, (1968), p. 242
9. Norwegian Patent No. 142406, (1980)
10. Yu. V. Baiamakov, A. I. Zhurin, *Electrolysis in hydrometallurgy*, Metallurgiya, Moscow, (1977), p. 217 (in Russian)
11. D. Čizikov, H. S. Šavkov, *Russ. J. Appl. Chem.* (1936) 31
12. N. S. Harmed, B. B. Owen, *The Physical Chemistry of Electrolytic Solutions*, Rheinold, New York, 1950, p. 165
13. , *Integrated Pollution Prevention and Control (IPCC), Reference Document on the Best Available Techniques in the Non-Ferrous Metals Industries*, European Commission, Brussels, Belgium 2001, p. 338.
14. D. Stanojević, D. Sinadinović, M. Todorović, N. Vidaković, *Tehnika* **8–9** (1994) 11 (in Serbian)
15. D. Stanojević, M. Todorović, in *Proceedings of of the XIX October Meeting on Mining and Metallurgy, Book of papers*, Donji Milanovac, (1997), p. 831 (in Serbian)
16. D. Stanojević, M. Todorović, in *Proceedings of the 1st International Conference of the Chemical Societies of South-East European Countries, Book of Abstracts Vol. II*, Thessaloniki, Greece, 1998, PO 729
17. J. Bjerrum, G. Schwarzenbach, L. G. Sillen, *Stability constants, Part II: Inorganic ligands, No. 7*, The Chemical Society, London, 1958
18. C. F. Hamsdorf, in *Proceedings Electrolytic Zinc Co.*, Risdon, Tasmania, (1961), p. 19
19. Carlo Erba Reagents Catalogue, 2004, p. 212
20. D. Stanojević, B. Nikolić, M. Todorović, *Hydrometallurgy* **54** (2000) 151
21. D. Stanojević, B. Krstić, in *Proceedings of the 1st International Conference of the Chemical Societies of the South-East European Countries, Book of Abstracts Vol. II*, Halkidiki, Greece, (1998), PO 730.

Errata

1. Issue No. 4 (2008), Vol. **73**, page 396:
 - Column “Source” of the Table II should read:
26
26
17
18
27
27
27
28
28
28
29
30
30
31
32
16
16
33
27
2. Issue No. 4 (2008), Vol. **73**, page 397:
 - Scheme 1 caption should read:
Catalytic cycle of chymotrypsin, drawn according to Fray³⁵ and Cleland.⁸